UNIVERSITEIT VAN PRETORIA
UNIVERSITY OF PRETORIA
YUNIBESITHI YA PRETORIA

Solid-phase reactors in sequential injection systems

by

Eliazer Bobby Naidoo

Submitted in partial fulfilment of the requirements for the degree

PHILOSOPHIAE DOCTOR

in the Faculty of Natural & Agricultural Sciences

University of Pretoria

Pretoria

July 2001

Solid-Phase reactors in sequential injection systems

by

Eliazer Bobby Naidoo

Promoter : Professor Jacobus F. van Staden

Department of Chemistry

University of Pretoria

Degree : Philosophiae Doctor

SYNOPSIS

The increasing number of journals and reviews published on the development of process analysers signals the importance thereof in the various fields that require analytical measurement to be performed. Analysis need to be done faster, more precise, accurate and economical. Hence the introduction of solid-phase reactors in flow systems.

The use of a solid-phase reactor incorporated into the sequential injection analysis (SIA) manifold is an improvement on the homogeneous methods applied. This represents an achievement for on-line determination of different substances in clinical, pharmaceutical,

industrial or agricultural fields. Solid-phase reactors has an advantage over homogeneous methods, particularly if the reagent is expensive, only slightly soluble or only available in the solid form. Reagent consumption is greatly decreased and the system is simplified with fewer junctions for mixing of reagent, sample and carrier stream.

The aim of this research was to investigate the application of the SIA technique as a process analyser, by incorporating super serpentine and solid -phase reactors in its manifold.

Super serpentine reactors were investigated for their sensitivity and precision. The solid-phase reactors were used for the determination of manganese, iron, nitrate and nitrite as well as chromium in industrial effluents, natural waters and pharmaceutical products.

For all these determinations, SIA manifold with a single detector was used. The usefulness, cost-effectiveness and advantages of the solid-phase reactor incorporated into the SIA-manifold over the homogeneous system and the flow injection analysis (FIA) system is highlighted during the course of this study.

Vastetoestandreaktore in sekwensiële-inspuitsisteme

deur

Eliazer Bobby Naidoo

Promotor: Proffesor Jacobus F. van Staden

Departement Chemie

Universiteit van Pretoria

Graad: Philosophiae Doctor

SAMEVATTING

Die toenemende aantal joernaal- en oorsigartikelpublikasies rakende die ontwikkeling van prosesanaliseerders toon die belangrikheid daarvan in die verskeie velde wat vereis dat analitiese meetings uitgevoer moet word. Analises moet vinniger, meer presies, akkuraat en ekonomies uitgevoer word. Dit lei tot inskakeling van vastetoestandreaktore in vloeisisteme.

Die gebruik van 'n vastetoestandreaktor, in 'n sekwensiële-inspuitanalise (SIA) reaksiespoel, is 'n verbetering op die homogene metodes . Dit verteenwoordig 'n doelwit

vir aanlyn bepalings van verskillende stowwe in die kliniese, farmaseutiese, industriële en landbou rigtings. Vastetoestandreaktore het 'n voordeel bo homogene metodes, veral indien die reagense duur is, slegs gedeeltelik oplosbaar is of indien dit alleenlik in die vaste toestand beskikbaar is. Reagens verbruik is grootliks verminder en die sisteem is, deur van minder koppelings vir die vermenging van die reagens-, monster- en draerstroom gebruik te maak.

Die doel van hierdie navorsing was om die toepassing van die SIA- tegniek, as 'n prosesanaliseerder, te ondersoek deur superkronkel- en vastetoestandreaktore in die reaksiespoel te inkorporeer.

Superkronkelreaktore is vir sensitiwiteit en presisie ondersoek. Die vastetoestandreaktore is vir die bepaling van mangaan, yster, nitraat, nitriet en chroom in industriële uitvloeisels, natuurlike water en farmaseutiese produkte aangewend.

'n SIA- reaksiespoel, met 'n enkele detektor, was vir al hierdie bepalings gebruik. Die bruikbaarheid, koste-effektiwiteit en voordele van die vastetoestandreaktor in die SIA-reaksiespoel geïnkorporeer, bo die homogene- en vloei-inspuitanalise (VIA) sisteme, word deur die loop van hierdie studie uitgelig.

Acknowledgement

To **GOD** our **Creator** who knows the destiny of every living being on this earth. It is through **His Grace** and **Love** that I am what I am today, tomorrow and forever.

To my supervisor **Prof J. F. van Staden**, thank you for your guidance and mentorship. I have learned a lot from you, I have acquired much from your supevision and I will always remember you.

To **Dr Raluca Stefan**, you have always been there to help with a smile. You always put me first, then your work later whenever there was some kind of help I needed. Thank you.

To my wife, **Christinah**, daughters, **Maureen, Valentine, Pearl** and **Elaine** your patience during my absence and your understanding and support were the only things that kept me going to the fulfilment of my dream. **Elaine**, my girl your eagerness to always ask if I needed any help with typing was of great help. Thank you and I dedicate this **Thesis** especially to you.

To the group I found working with **Prof van Staden** , i.e **Adele, Elrisa, Hanneli, Mack, Neels** and **Vusi**, your acceptance of me and assistance to familiarise me with the environment under which I was going to find myself working, is appreciated. To those who were always ready to help when I needed any help, thank you.

To the **University of the North** and the **Department of Chemistry**, I thank you for having allowed me to further my studies.

Finally I would like to thank, the **National Research Foundation** and the **Irish Government Scholarship** for financial assistance. Without your finance I would not have been able to sustain myself while at the University of Pretoria.

Table of contents

CHAPTER 1

Sequential Injection Analysis (SIA)

From homogeneous to heterogeneous system

1.1 Introduction

The need for process analysers that are able to process large amounts of samples continuously and automatically and deliver accurate and precise results with regard to sample contents are ever growing. Sequential injection analysis (SIA) as a process analyser satisfy these requirements and its popularity has never been better, since its introduction in 1990 [1,2].

Effective cost control is also an important aspect that demanded serious attention. It does not only affect efficient management of industrial, agricultural, clinical and pharmaceutical processes, but it forms the cornerstone in the provision of high quality value-added products in a highly competitive world where clean and sustainable environment must be maintained [3]. These needs triggered the decision to develop automated systems capable of fulfilling the set requirements of real time monitoring and control of process on an analytical base.

The advantages of SIA were exploited by several laboratories and research groups [4-11]. Several reasons can be given for the employment of flow and sequential injection (SI) systems as process analysers. These reasons include: reduction in cost (personnel, equipment and

following aspects must always be highlighted:(i) the components it was constructed of, (ii) the specific manifold dimensions, as well as (iii) the device sequence or method construction (See addendum A).

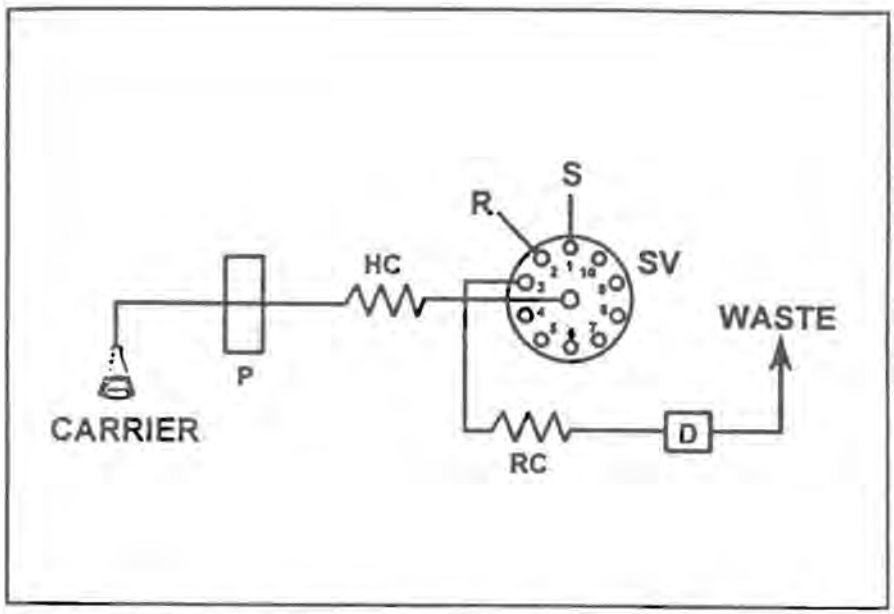

Fig. 1.1 A schematic flow diagram of a typical SIA system. P - pump, HC - holding coil, RC -reaction coil, S - sample, R - reagent, SV - selection valve, D - detector.

There are presently two draw backs of SI to be mentioned. Firstly, since aspirations of the wash solution and sequencing of the zones in the holding coil take some time (typically 30 seconds) the sampling frequency of the SI system is presently half that of a conventional flow injection (FI) systems where filling of the injection valve is a matter of a few seconds. Secondly, SIA requires specialized software, since the sequencing, injection and data collection are entirely computer driven. The mentioned draw backs are however, not an obstacle in using the SIA technique [4].

Automatic methods of analysis have been especially influential in clinical chemistry. Since

for hospitals to obtain a large number of analytical data as quickly and inexpensively as possible. The situation is much the same in most industries where quality control laboratories have become much more important than they were a few decades ago.

Most of the process control systems currently used are based on physical measurements such as flow rate, pressure, electrical resistance, etc. While this has resulted in processes which are operated under statistical control, verification of the process performance can only really be achieved by chemical analysis, usually in a remote plant laboratory. This approach is seen as unacceptable in the design of quality management systems for the production process. In such systems the emphasis is on quality assurance during the process rather than after-the-fact.

Process analysis brings the process controller a step closer to ensuring excellent control of the plant and real time quality assurance. At this stage, lengthy development times, the cost of these analysers and their maintenance requirements mean that only a few critical streams are monitored. The demands in this field are dictated by the large number of samples to be analysed, especially in on-line control of automized manufacturing processes and the quality now required in manufactured products. It is therefore necessary to control not only the raw products, but also the intermediate and end products.

Sequential injection systems have been proven to be suitable as on-line process analyser for most single component [9,10,23] and multi-component analysis [27]. Studies revealed that reduced numbers of samples can be used when applying SIA systems as process analysers, provided a correct regression model is used [23]. The flow systems already adapted to SIA systems involved very simple methods and operations in a homogeneous medium.

systems involved very simple methods and operations in a homogeneous medium.

However, the need for analysis when the reagent is expensive, only slightly soluble or only available in the solid form, has necessitated the introduction of solid-phase reactors (enzymatic, immuno-assay, ion exchange or redox) into the SIA manifold.

1.2 Solid-phase reactors in flow systems

Solid-phase reactors can be classified into two distinct groups, namely, reactors in which a chemical reaction takes place to derivatise the analyte, and reactors in which no derivatisation reaction takes place. The first group includes enzyme reactors while the second group consists mostly of reactors used for pre-concentration.

The introduction of solid-phase reactors in flow systems represents a high achievement for on-line determination of different substances [28,29]. These type of heterogeneous reactions have been converted for use in FI systems with some success [30,31]. It has enhanced such basic analytical parameter such as sensitivity and selectivity. Fig.1.2 illustrates the most common solid-phase reactor incorporated in a FIA manifold.

The use of reagents, particularly enzymes, in the solid-phase has been known from the early part of the 20th century. These enzymes were immobilized on a variety of support materials for a number of reasons [32] and offered a greater degree of control over the relevant reactions.

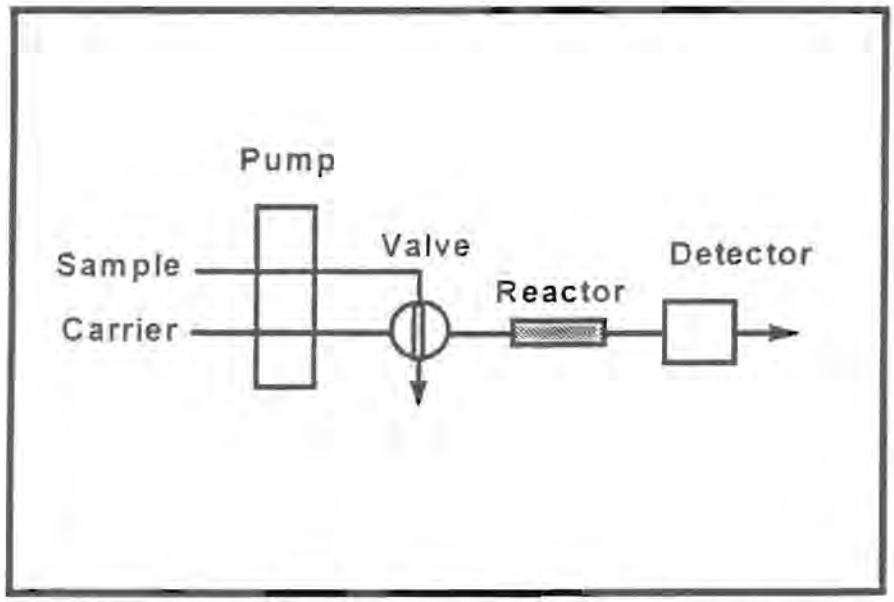

Fig. 1.2 Diagram of the most common location for a solid-phase reactor.

In addition to the excellent analytical features already available with normal FIA systems, systems which incorporate a solid-phase reactor offer further advantages with respect to miniaturisation, simplification and cost reduction. The different types of immobilisation techniques for solid reagents, the location of the reactors in the flow system, along with the various shapes and types of reactors used and its various applications is fully discussed in Chapter 4.

The introduction of solid-phase reactors in a SIA manifold heralded another dimension in process analysers. Since most of the SIA systems originate from conventional FI methods, likewise the incorporation of solid-phase reactors in a SIA manifold is an improvement on existing FIA methods and a further boost for process analysers. Fig.1.3 illustrates a typical SIA system incorporating a solid-phase reactor.

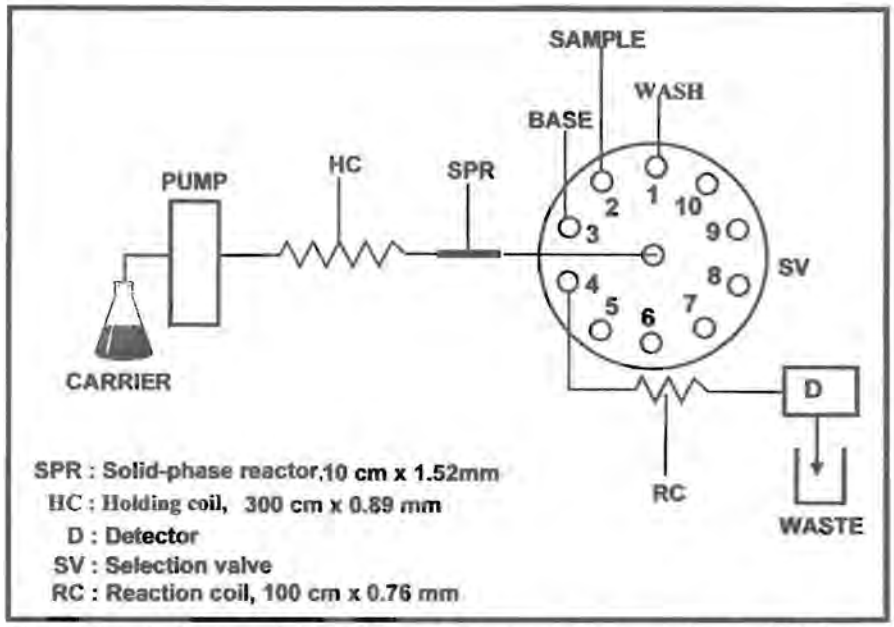

Fig.1.3 A typical sequential injection analysis system incorporating a solid-phase reactor in its manifold.

SIA systems used, incorporating solid-phase reactors in its manifold, include a spectrophotometric method [33] for the determination of lactic acid from industrial inorganics, simultaneous monitoring of glucose, lactic acid and penicillin [34], glucose and penicillin [35], theophylline and caffeine [36] and the separation of radionuclides [37].

1.3 Aim of this study

The study was first devoted at evaluating super Serpentine reactor types for their sensitivity and precision in the SIA system [38]. They are four super Serpentine reactors (I, II, III & IV). A comparative study of these reactors was done.

Due to the need for safe analysis of trace elements, which are toxic at certain concentrations when consumed, cost reduction and robustness, the application of SIA to real samples was considered. The incorporation of a solid-phase reactor (redox reactor) in a SIA manifold was used to enhance the analyses of manganese, iron, nitrate and nitrite as well as chromium in natural, effluent and electroplating waters and pharmaceutical products. The use of solid-phase (redox) reactors in SIA to determine these components were considered since it has not been attempted yet.

Manganese (II) [39] was spectrophotometrically determined in tap water and effluent streams using a redox solid-phase reactor. Manganese (II) from a sample was oxidised by a PbO_2 (solid-phase reactor) embedded in silica gel beads to produce the permanganate ion which is then detected with a UV/VIS spectrophotometer. The reaction is pH dependent.

Total iron as Fe (II) [40] was determined in pharmaceutical products and effluent streams using a solid-phase cadmium reactor incorporated into a SIA system. The reactor reduced the Fe (III) to Fe (II) and was complexed with 1.10 Phenanthroline as Fe $(phen)_3^{2+}$ complex. This was determined with a UV/VIS spectrophotometer.

Oxidised nitrogen (nitrate + nitrite) [41] was determined in natural water as nitrite. The nitrate in water was reduced to nitrite using a cadmium reactor. The nitrite produced was diazotised with sulphanilamide and coupled with ethylene diammonium dichloride to form a highly coloured azo dye which was detected with a UV/VIS spectrophotometer.

Chromium [42] as chromate was determined spectrophotometrically in electroplating and

natural waters. The sample was oxidised with ammonium cerium (IV) sulphate to dichromate/chromate. In a basic medium the redox solid-phase reactor, PbO_2 converted the dichromate to chromate. The chromate was released in excess ammonium hydroxide and was detected using a UV/VIS spectrophotometer.

1.4 References

1. J. Růžička and G. D. Marshall, **Anal. Chim. Acta, 273** (1990) 329.
2. J.Růžička , G. D. Marshall and G. D. Christian, **Anal. Chem., 62** (1990) 1861.
3. J. F. van Staden, **Current Trends in Analytical Chemistry, 1** (1998) 89.
4. T. Gübeli, G. D. Christial and J. Ruzicka, **Anal. Chem., 63** (1991) 2407.
5. J. L. Zable, **Operational Parameters of Sequential Injection Analysis and the Fundamentals of Calculating the Dispersion at the Maximum Zone Overlap,** PhD-Thesis, University of Washington, 1996.
6. G. D. Marshall and J. F. van Staden, **Anal. Instrum., 20** (1992) 79.
7. G. D. Marshall and J. F. van Staden, **Process Control Qual., 3** (1992) 251.
8. G. D. Marshall, **Sequential Injection Analysis,** PhD-Thesis, University of Pretoria, 1994.
9. R. E. Taljaard, **Application of Sequential Injection Analysis as Process Analyzers,** MSc-Thesis, University of Pretoria, 1996.
10. A. Botha, **Sequential Injection Analysis: Evaluation of Operational Parameters and Application to Process Analytical Systems,** MSc-Thesis, University of Pretoria, 1999.
11. A. Cladera, E. Gomez, J. M. Estela and V. Cerda, **Talanta, 43** (1996) 1667.
12. S. D. Chung, G. D. Christian and J. Ruzicka, **Process Control Qual., 3** (1992) 115.
13. E. Gomez, C. Tomas, A. Cladera, J. M. Estela and V. Cerda, **Analyst, 120** (1995) 1181.
14. J. F. van Staden and R. E. Taljaard, **Anal. Chim. Acta, 323** (1996) 75.
15. J. C. Masini, P. J. Baxter, K. R. Detwiler and G. D. Christian, **Analyst, 120** (1995) 1583.
16. E. Rubi, R. Forteza and V. Cerda, **Lab. Robotics. Autom., 8** (1996) 149.

17. J. F. van Staden and R. E. Taljaard, **Anal. Chim. Acta, 331** (1996) 271.

18. J. F. van Staden and H. du Plessis, **Anal. Commun., 34** (1997) 147.

19. J. F. van Staden and R. E. Taljaard, **Anal. Chim. Acta, 344** (1997) 281.

20. A. Ivaska and W. W. Kubiak, **Talanta, 44** (1997) 713.

21. J. Růžička, **Analyst, 119** (1994) 1925.

22. J. Růžička and E. H. Hansen, **Anal. Chim. Acta, 237 (2)** (1990) 329.

23. A. Ruis, M. P. Callao, J. Feere and F. X. Ruis, **Anal. Chim. Acta, 337** (1997) 287.

24. R. E. Taljaard, **Multi-component Determinations using sequential injection analysis.** PhD-Thesis, University of Pretoria, 1999.

25. J. F. van Staden, H. du Plessis and R. E.Taljaard, **Anal. Chim. Acat, 357** (1997) 141.

26. P. Ek, S. Hulden and A. Ivaska, **J. Anal. At. Spectrom., 10** (1995) 121.

27. M. Guzman, C. Pollema, G. D. Christian and J. Růžička, **Talanta, 40** (1993) 81.

28. M. D. Luque de Castro, **Trends in Analytical Chemistry, 11 (4)** (1992) 149.

29. J. Martine-Calatayud and J. V. Garcia Mateo, **Trends in Analytical Chemistry, 12 (10)** (1993) 428.

30. K. Zaitsu, K. Yamagashi and Y. Okhura, **Chem. Pharm. Bull., 36** (1988) 4488.

31. Y. Hayashi, K. Zaitsu and Y. Okhura, **Anal. Chim. Acta, 186** (1986) 131.

32. R. A. Messing, **Immobilized enzymes for industrial reactors, Academic press,** New York, 1975.

33. H. C. Shu, H. Hakanson and B. Mattiason, **Anal. Chim. Acta, 300** (1994) 277.

34. R. W. Min, J. Nielsen and J. Villadsea, **Anal. Chim. Acta, 312** (1995) 149.

35. R. W. Min, J. Nielsen and J. Villadsea, **Anal. Chim. Acta, 320** (1996) 199.

36. B. Dockendorf, D. A. Holman, G. D. Christian and J. Růžička, **Anal. Commun., 35**

(1998) 357.

37. O. B. Egorov, M. J. Ohara and J. W. Grate, **Anal. Chem., 71** (1999) 345.

38. E. B. Naidoo and J. F. van Staden, **Instrum. Sci. & Techn., 29 (2)** (2001) 77.

39. E. B. Naidoo and J. F. van Staden, **Fesenius' J. Anal. Chem., 370 (6)**(2001) 776.

40. J. F. van Staden and E. B. Naidoo, **S.Afr.J.Chem., 53** (2000).

41. E. B. Naidoo and J. F. van Staden, **Waters SA 27 (3)** (2001) 355.

42. E. B. Naidoo and J. F. van Staden, Submitted.

CHAPTER 2

Sequential Injection Analysis (SIA)

2.1 Introduction

It is a decade since the introduction of sequential injection analysis (SIA) as a process analyser. Since its introduction in 1990 [1,2], its growth has exceeded expectations. This signifies recognition of the tremendous versatility of this method originally designed as a mere tool for automation of serial assays [3].

Increasing pressure on the chemical manufacturing industry to provide higher quality products in an economically viable and environmentally acceptable manner, has increased the requirements to maintain strict control of plant conditions throughout the production process. Hence, the use of process control strategies represent a significant shift in the thinking of many process control engineers.

SIA is a technique of flow analysis whose roots can be traced back as far as 1974 [3]. It has introduced a new dimension to flow analysis due to the simplicity of its flow channel, the reduction in both sample and reagent consumption and the efficiency with which the hydrodynamic variables can be controlled. Although SIA is very characteristic of a flow system, especially with regard to the dispersion taking place in the flow conduit, it also has certain inherent characteristics. It is these characteristics that distinguishes SIA from conventional flow

systems, namely the introduction of sample and reagent into the flow conduit as zones as they are propelled towards the detector.

The demand for mechanically simple and robust flow injection methodology has been the driving force behind the development of the sequential injection (SI) technique. The simplicity of the SI manifold and its low need for maintenance makes it an ideal tool in process analysis. As miniaturization and reduction of reagents consumption are also ultimate goals in chemical sensing, it is useful to review the use of combined injection and programmed flow as a central issue in designing chemical sensors and structurally simplified chemical analysers.

Various parameters were assigned to the characteristics of the SIA system and in depth studies were conducted to investigate the result of the stacking of the zones, the influence of the various operational parameters, deformation and dispersions of the zones and subsequent zone penetration [5-10].

Extraction, separation, pre-concentration, dialysis, titrations, dilutions and redox methods were adapted for use in SIA manifolds. Hence, the design of a SI manifold can be considered as the search for optimum dispersion characteristics. Colorimetric, electrochemical and other detectors equipped with a suitable flow-through cells, were also incorporated into these manifolds. A new scope of SIA manifolds were developed for use in both industrial applications as well as in the laboratory. The use of biosensors and the incorporation of solid-phase reactors in SIA manifolds has further enhanced the potential of SIA as a process analyser.

2.2 Historical background

The introduction of SIA in 1990 [1,2] ushered in a new dimension in flow analysis. Although the technique is just a decade old, the number of journals and reviews published bear testimony of its tremendous growth. SIA was born from flow injection analysis (FIA), which can be traced back to 1974 [4]. Hence the discussion that follows will briefly start at FIA after which the development of SIA will flow from it.

FIA is an analytical technique that relies on the injection of a well defined sample zone into moving carrier stream and the subsequent detection of a signal which has been modulated by a combination of physical and chemical interactions. The technique relied on a constant flow rate.

The successful operation of any injection analyser requires that the sample and reagents are brought together, mixed and allowed to react in a perfectly reproducible manner. To obviate the need for frequent re-calibration, it is necessary to maintain reproducible flow conditions for extended periods of operation. This has led to the practice of using unidirectional monotonous flow, because as long as constant flow rate is maintained, the sample may be injected into the system at any time.

The use of an unidirectional monotonous flow rate has been the prevailed practice in FIA, which unlike chromatography does not aim at separation of the analyte components, but rather at their effective chemical conversion into detectable species. Therefore the key issue in FIA is the reproducible dispersion of the injected zone into the carrier stream and timing of the arrival of the reacted zone at the detector. If all critical parameters (reproducible injection, controlled

reaction time and controlled dispersion) are held within certain tolerance levels, the result will be reproducible [11].

The instrumentation needed for an FIA system are a multichannel pump, an injection valve, a flow through detector and a recorder. Save for the last component which was replaced when computers were introduced in laboratories some years later, the basic flow scheme remained essentially unchanged [12]. When FIA research became orientated towards the exploitation of concentration gradients formed by the dispersion process [13], new techniques using stopped flow, reversed flow, sinusoidal flow, reagent injection, sequential injection and single solution calibration were developed.

Use of a flow programme, rather than constant monotonous flow, requires synchronization of sample zone injection with the start of each flow cycle. A system configuration was required which will allow sample zone injection, reagent addition, mixing, measurement, and ejection of the reacted mixture by a combination of forward and reversed flow steps.

While linear flow programming traditionally refers only to the flow pattern employed, i.e. the rate and direction of flow, the inclusion of a mechanism of selecting different streams to be subject to the flow programme may also be added. The group at the University of Washington [14] used these ideas for the basis of an extension of FIA, which was called SIA [15].

The transformation of FIA into SIA stems from the random walk model. By using the random walk model as a basis, it has been postulated that there is no net flow needed for the successful operation of a flow injection system [2]. Růžička *et al.* [1] discussed the consequences of the

latter observation and the role of the random walk model in FIA. It was this discussion that led to defining the principle of SIA. The random walk model suggested that mixing, the fundamental requirement for both FIA and SIA, could take place with no net displacement of sample. The transformation of FIA into SIA signifies recognition of the tremendous versatility of this method originally designed as a mere tool for automation of serial assay [3]. With the introduction of SIA, the basic parameters of flow injection were assumed to be applicable, because the same basic components were used.

Sequential injection is mechanically simpler than flow injection for it uses only a single channel. SI uses a selection valve (rather than an injection), through which precisely measured volumes of sample and reagent solutions are aspirated into a holding coil by means of a pump that is capable of a precisely controlled stop-go-forward-reverse movement [5, 16-18].

A SI manifold must be designed to achieve mixing between reagent and analyte such that the reagent is in sufficient excess at the maximum of the profile to ensure the greatest degree of reaction. Dilution of the formed product zone should, however be minimized so as to avoid an unnecessary loss in sensitivity. The design of a SI manifold can be considered as the search for optimum dispersion characteristics.

A basic sequential injection analysis manifold is shown in Fig. 2.1. Mainly four different liquid drivers were used in SIA. The sinusoidal flow piston pump [6, 17, 19-21] was specially designed for SIA. The flow rate is dependent on the rotation angle, the radius of the pump, the cam and the frequency of the pump. Its repeatability and reproducibility are good, but it is difficult to maintain a constant flow rate during analysis.

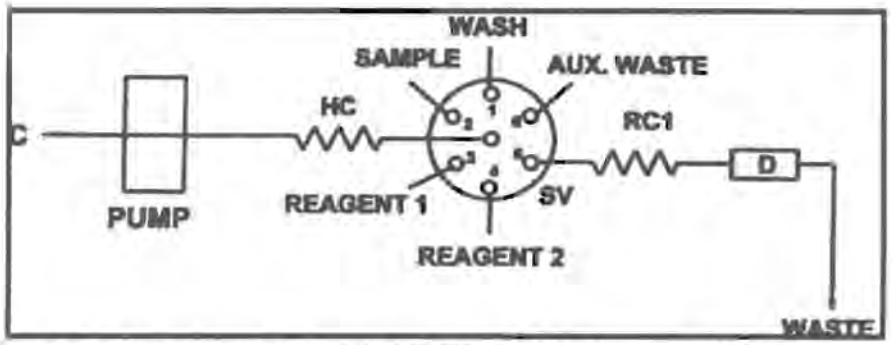

Fig 2.1 A basic sequential injection analysis manifold. C - carrier, HC - holding coil, RC - reaction coil. SV - selection valve and D - detector.

Ivaska and Růžička [22] investigated the performance of peristaltic pumps. These pumps are suitable for SIA applications when used with Neoprene tubing. Automatic burettes that are computer programmable and have variable speed are mainly used by the Spanish group. However a drawback of these liquid drivers is that it is impossible to use flow rates lower than 2 mℓ/min. Finally field-decoupled electro-osmotic pump is described by Liu and Dasgupta [23, 24] as on ideal pumping system for SIA, because the flow direction is readily and reproducibly reversed and the flow rate can be maintained with a high degree of reproducibility.

Optimum exploitation of these flow techniques in automated modes of operation necessitates computer control. Specialized software packages were designed to control both the movement of the apparatus (pumps and valves) and to handle data acquisition and storage. The FlowTEK package (obtainable from MINTEK, Randburg, South Africa) was designed by Marshall and Co-workers [16, 25] and is widely used. The Spanish group uses the program DARRAY, obtainable

from SCIWARE, Palma de Mollorca, Spain [26]. Růžička's group [27] uses a program called FIALab for control and data aquisition.

The advantages of SIA have been discussed in detail by Růžička and Gübeli [19] and in comprehensive reviews and congresses [2, 4-5,14,16,18, 29-30]. A valuable contribution by the group at the University of Washington was the exploitation of new sensor system which broadened the scope of SIA tremendously and opened new horizons in the field of flow analysis.

2.3 Basic principles

The concept of SIA is based on the mixing of a samples zone with a reagent zone in order to produce a measurable response [22]. This necessitates solution handling operations such as sample injection, reagent injection, sample and reagent mixing and detector wash and reconditioning. The SIA system used a selection valve, compared with the injection valve used in FIA. The selection valve is used to aspirate precisely measured volumes of carrier solution, sample solution and reagent solution into a holding coil. The aspiration of the zones is achieved by means of a pump which is capable of a precisely controlled stop-go-forward-reverse-movement [18].

Following the first step of zone sequencing, during which the sample and reagent zones are stacked in the holding coil conduit to each other, the valve is switched to the detector position (Fig. 2.2A). In the next step, the flow is reversed so that the stacked zones are propelled through the valve and the reactor to the detector (Fig. 2.2B). As the central streamline moves at a rate twice the velocity of the mean flow velocity, whereas the elements of fluid more adjacent to the

walls move at lesser rates, the cores of the sequenced zones penetrate each other [31]. During this movement the flow reversal creates a complex region within the analyte which is transformed into a detectable species (Fig. 2.2C). The fundamental requirement for SI to succeed is to achieve maximum zone penetration through a deliberate increase in axial dispersion, obtained by means of the flow reversal and channel design [1,19,32].

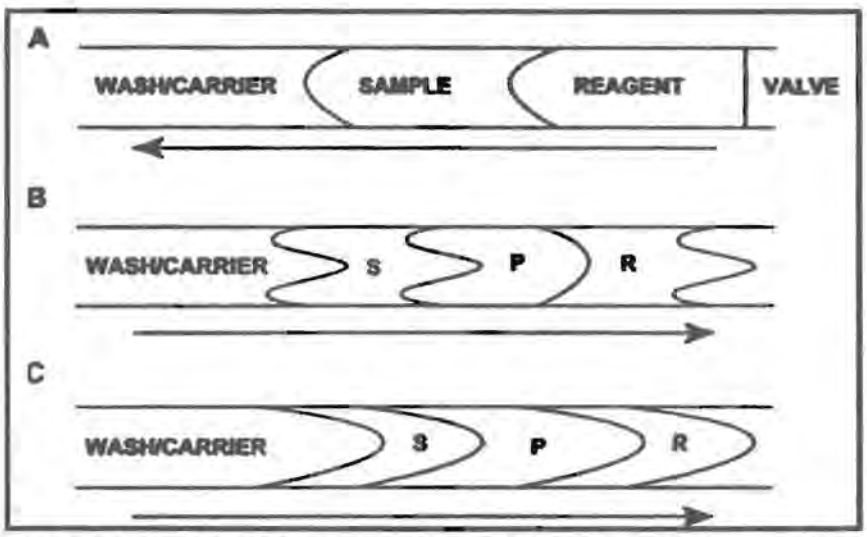

Fig 2.2 Flow profiles of the sequenced (A) and injected zones (B - immediately after flow reversal and C - in reaction coil). S - sample, R - reagent and P - formed product zone.

Reproducible dispersion is the basis for analysis by flow injection methods. Dispersion is the result of all the physical forces acting on the injected zones. It is the process by which the zones transform from homogeneous, geometrically well defined zones at the moment of injection to the final zone that is detected downstream. The dispersion coefficient is the ratio of the detector response of the injected solution in the absence of these forces to that of the solution due to these

forces. Růžička and Hansen [31] defined the conceptually simple and practically useful dispersion coefficient, $D = C^0/C$, where C^0 is the detector response of the undispersed solution zone and C is the detector response of the dispersed element of fluid that yields the analytical readout. Because there is generally a direct relationship between the property used for detection, the magnitude of the transduced signal recorded and the concentration of the sample or its reaction product, the dispersion coefficient can be taken as the height ratio of the signal [16,31]. The random walk model was also used by Růžička and Marshall [1] to describe dispersion in the SIA analyser channel.

Thus, in addition to reproducible timing and sample injection, controlled dispersion is important in flow systems. The purpose of controlling dispersion in a flow system is to optimize the chemical reactions taking place between the sample and reagents. In essence, what has been called "controlled dispersion" is in fact the result of the sample is reproducibly diluted as it travels down the tubing. Dispersion is characterized by the concentration profile adopted by a zone or plug inserted at a given point in the system without stopping the flow.

Two processes are responsible for dispersion in the flow conduit, namely the physical process of material dispersion due to hydrodynamic processes taking place in the flow through system and the chemical process of formation of chemical species.

Although Růžička and Gübeli [19] stated that "for a rational design of the sequential injection analyser, the degree of sample dispersion must be considered as main design guideline", zone penetration (related to dispersion) is found to be the key parameter, the control of which is essential to the successful execution of sequential injection [6]. The importance of zone

penetration can be ascribed to the fact that this influence has a dramatic impact on the surface area over which a concentration gradient exists and therefore over which axial mixing takes place. It follows from the foregoing that, for reagent-based chemistries, a region of mutually inter-dispersed sample reagent zones must be identified, within which D is larger than 2 and where at the same time sufficient excess of reagent is present. Analogous to the definition of resolution, zone penetration is defined as:

$$P = 2W_0/(W_s + W_r) \qquad (2.1)$$

Complete overlap is obtained for $P = 1$, zero overlap for $P = 0$ and for values in between, partial overlap will be obtained. This approach yields useful results although it is difficult to determine the value automatically [17]. An isodispersion point, I_d, is observed in cases where $1 > P > 0$ (Fig. 2.3). At this point the dispersion of the sample and reagents zones are identical and the ratio of sample and reagent concentrations is the same as their ratio prior to injection ($C_s/C_r = C_s^0/C_r^0$).

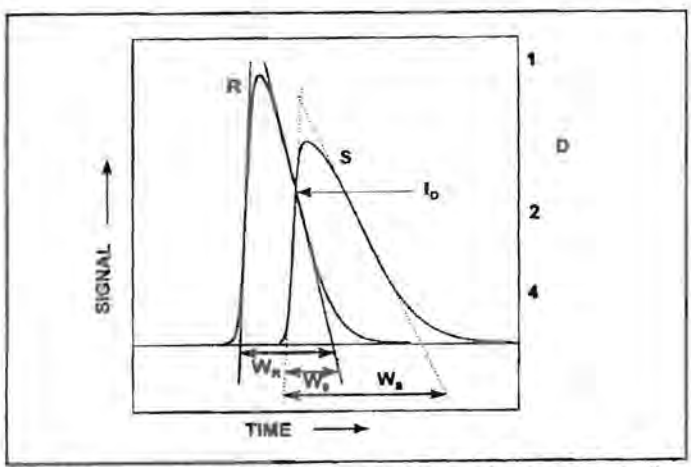

Fig. 2.3 Schematic representation of zone penetration showing the isodispersion point (I_D). R - reagent zone, S - sample zone, D - dispersion coefficient, W_R - baseline width of reagent zone, W_S - baseline width of sample zone and W_0 - baseline of the overlap.

The isodispersion point is independent of concentration, but studies done by van Staden *et al.* [38] illustrate the shift of the isodispersion point due to the difference in concentration gradients when different volume ratios of sample and reagent were employed. These studies also showed that the position of penetration and the sequence of introduction of samples and reagents for different sample and reagent volume ratios in a total constant volume has a major influence on the response of the final peak profile. This is illustrated in Figs. 2.4 and 2.5, where Fig. 2.4 represents the injection order of first the metal followed by the ligand and Fig. 2.5 represents the reversed injection order.

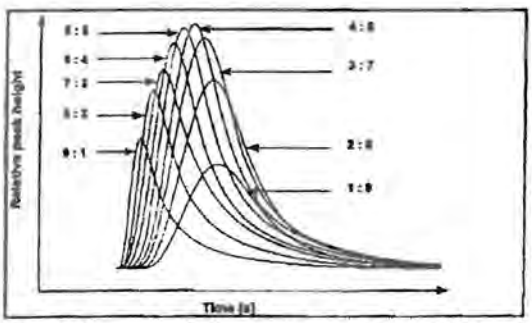

Fig. 2.4 Schematic representation of the influence of different sample : reagent ratios in a total constant volume. The figure represents the injection order of first the metal followed by the ligand.

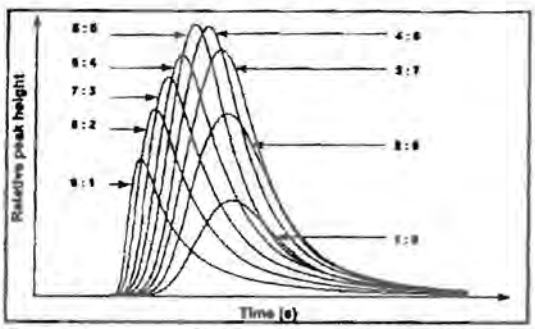

Fig. 2.5 Schematic representation of the influence of different sample : reagent ratios in a total constant volume. The figure represents the injection order of first the ligand followed by the metal (reversed order).

The response of the final peak profile depends largely on the kinetics involved in both the ascending and tailing parts of the sample and reagent zones at the isodispersion point. Zable [11] found mathematical equations to calculate the maximum zone overlap. The larger this number,

the greater the degree of zone penetration. This approach too suffers from certain limitations as it does not indicate the sensitivity of the measurement, because it does not take the concentration of the sample and reagent into account.

2.4 Operational parameters

When applying the SI technique, it is imperative to understand the principles on which it is based in order to do subsequent analysis. The greatest challenge is the theory of flow dynamics, which will lead to optimisation of flow systems based on flow stopping and reversal. Many researchers generally set up a system without regard to the dispersion of the individual components or some of the general rules for optimising the system. There are a number of publications describing different techniques of optimisation [34-37] and standardization [38] as well as systems able to diagnose multivariate responses, with the aim of detecting faulty responses [39,40].

The extent of dispersion that the product peak will undergo is essentially influenced by the operational parameters that govern the SIA flow conduit. Although some would argue that SIA is simply a variation of FIA, there are certain fundamental differences in the use and control of the operational parameters used in SIA.

A number of papers were published that described the most important parameters optimised [6, 9, 11, 16, 17, 41]. Almost without exception the following parameters had been shown to have a marked effect on zone dispersion in an SIA system: the volumetric flow rate, tube diameter length of flow path from injection to detection, sample and reagent volumes, order of sample and reagent injection, flow reversal and to a lesser extent reactor geometry. The use of mixing

chambers in the flow conduit and their influence on dispersion was studied by van Staden and Botha [9, 60]. To evaluate the influence of every parameter, a non-reactive dye was used as sample and reagent zone respectively in a series of experiments

The *volumetric flow rate* includes both the loading and forward flow rates and is also referred to as the combined effect of pump speed and the internal diameter of the pump tubing when using a peristaltic pump [9, 11,16, 60]. In correlation with the Vanderslice expression, $D = k'q$, where q is the flow rate in mℓ/min, the dispersion of the different zones decreases as the flow rate is increased [42]. The dispersion coefficient decreases with increasing flow rate because the residence time decreases, in a non-linear fashion, with increasing flow rate [16]. A linear relationship consists between the pump speed and flow rate; therefore the flow rate can be altered by changing the pump speed [9, 16,17, 70]. At high flow rates a deterioration in sensitivity and reproducibility is experienced due to the higher back-pressure [16,43]. It is preferred that the loading flow rate should be faster than the forward flow rate to ensure higher sample throughput, provided that the pump will allow this [17].

The *length of the tubing* is dictated by the experimental requirements [16]. Longer tubing leads to longer residence times and therefore larger dispersion. Zable [11] stated that the dispersion must be proportional to the square root of the tube length, but experimental data had shown that there was a linear relationship between dispersion and path length. The mixing height (number of plates or tanks) is defined as the average length of tubing for each mixing stage [31].

In SIA the manifold tubing is divided into two parts: the holding coil which is the tubing between the liquid device (pump)and the selection valve and the reaction coil which is the part connecting

the selection valve with the detector. The holding coil primarily acts as a reservoir and should be large enough to prevent the sample and reagents from entering the pump conduit. The reaction coils should not exceed one-third of the volume of the washing solution, thereby ensuring that they are adequately flushed during every experiment [17]. Reaction coils are usually kept as short as possible to avoid excessive dilution of the formed product zone. The length is governed by the physical distance between the valve and the detector [6,19].

A knowledge of the reaction rate is of particular value when adapting a method to sequential injection analysis, because the time spent in the manifold can be too short to ensure complete colour development. Due to the discontinuous nature of SIA, stopped-flow periods can easily be incorporated to enlarge reaction times [44-46]. Van Staden and Taljaard [44] used a stopped-flow period of 80 seconds to ensure adequate formation of indophenol during the determination of ammonia.

Related to the Dean number the *tubing diameter* had a dramatic influence on the dispersion of the different zones [11]. The dispersion is found to be proportional to the fourth root of the coil diameter. Several factors should come to mind when considering the optimum tube diameter. These include the resultant back-pressure in a length of tubing, the vulnerability to blockage and the degree of radial dispersion attainable [16,21]. Wider tubing is usually used for the holding coil, because of its promotion of axial dispersion and, therefore, zone penetration. Narrower tubing is used for the reaction coils to prevent excessive dilution of the former product zone. Wider tubing is used for the uptake tubes to prevent any back-pressure.

Gübeli *et al.* [6] have conducted an in depth study on the effect of *sample and reagent volume*

on zone penetration and sensitivity. Their conclusions can be summarized in three rules:

1. Changing of the sample zone volume is an effective way of changing the sensitivity of measurement. Dilution of concentrated samples is best achieved by reducing the injected sample volume.

2. Injecting at least twice as large reagent zone volume as sample zone volume, while keeping the volume of the sample zone less or equal to 0.5 $S_{1/2}$, allows the optimum conditions for single based chemistries to be met. ($S_{1/2}$ is defined as the sample volume required to yield a dispersion factor of two in the manifold).

3. Two reagent chemistries can be accommodated provided that the sample volume is kept below the $S_{1/2}$ value, so that the sample zone is surrounded by reagent zones and that the concentration of the injected reagents are sufficiently high.

Van Staden *et al.* [33] found that the best sensitivity was obtained when a 1:1 sample to reagent ratio was used. At this ratio, the two zones experienced almost the same axial dispersion and penetration occurred almost at the maximum of the descending sample zone as well as the maximum of the ascending reagent zones. Gübeli *et al.* [6] found that increasing zone volumes at equal volume ratios caused zone overlap to decrease from nearly complete overlap (with small equal volumes) to a partial one (with relatively large equal volumes). While keeping the reagent volume constant, the authors [6] also varied the zone volume ratios by increasing the sample volume from less than the reagent volume to one where the sample volume was in excess of the reagent zone. This also resulted in a decrease in zone overlap.

Optimum sample and reagent zone volumes can be determined by plotting log [1 - (A_{max}/A_0)] versus sample volume ($\mu\ell$), where A_0 is the absorbency corresponding to the case where the element of fluid undergoes no dispersion. The $S_{1/2}$ value can be determined from the slope of the linear relationship. Experimental results gave good correlation with calculated values [9, 60]. $S_{1/2}$ values are, however, influenced by a number of experimental parameters. Cladera *et al.* [7] and Araujo *et al.* [47] showed that the ionic strength or electrolyte concentration of the medium influenced the $S_{1/2}$ value. The flow rate (slower flow rate result in higher $S_{1/2}$ values), the number of flow reversals and the dimensions of the reactor loop also influence the value [7].

A simple and convenient method for the determination of injection volumes in sequential injection analysis is presented by van Staden and Malan [48]. It is based on comparing the dilution of the injected dye with a standard calibration curve. The proposed colourimetric method gave the volume of the whole injection device more accurately than methods where the inner dimensions of the injection device are not precisely known. The colour methods is within the 95% confidence level with an RSD of 0.8%. Sampling strategies in sequential injection analysis were also investigated by Vieira *et al.* [49]. These techniques were exploited using a mono segmented-flow approach.

In a publication of Mas-Torres *et al.* [50], the authors discussed a new approach to sequential injection analysis. This approach involved the use of the sample as carrier stream. Although this technique may render good results, it removes one of the main advantages of sequential injection analysis - the fact that it uses minimized amounts of sample [16].

The importance of the correct order of sample and reagent injection is highlighted in a number

of publications [17, 33, 45, 51-53]. The order which the different of reagents are drawn up are very dependent on the reactions involved. The residence time of a specific zone also depends on its position in the reagent sequence. The zone that is drawn up first reaches the detector last due to the flow reversal. This zones has the longest residence time of all the zone and is therefore more dispersed [11, 16, 17]. The following must be considered: when sensitivity is important, the reagent, at a sufficiently high concentration, should be introduced first and allowed to penetrate the sample zone, which will experience minimal dispersion. If buffering of the sample by the wash solution is required, the order must be reversed. If solubility considerations prevent the reagent concentration from being increased, sandwiching of the sample between two reagent zones is an option to be considered [17].

Since the duration of flow reversal is the most effective in providing mutual zone penetration [6,17], more than one flow reversal was needed in the determination of ammonia, (due to insufficient mixing of the adjacent zones because of their different viscosities). The stack of zones was subjected to three flow reversals before the product zone was propelled to the detector. Multiple flow reversals were also used to better the transfer of ammonia over the membrane in a coupled gas-diffusion-SIA system [54] as well as to improve iron dialysis through the membrane during the determination of iron (III) [4].

Various reactors have been described in the literature on FIA manifolds [31]. Where the reactor consists of a length of tubing, various geometries have been proposed. Three were evaluated to establish the effect of reactor geometry on zone penetration and geometry. Studies done by Taljaard [16] and Marshall and van Staden [17] showed that reactor geometry does not have a marked effect on sensitivity or precision. Straight tubes are, however, preferred in SIA manifolds

due to the better axial dispersion obtained.

It should be noted that only the physical dispersion of all the above mentioned parameters were highlighted. The influence of a chemical reaction on dispersion is not even mentioned. The optimum values for each parameter will to a large extent depend on the specific reaction conditions and do not only depend on maximum sensitivity, but also on the reproducibility of measurements (%RSD). A set of parameters resulting in high sensitivity can be rejected if the relative standard deviation is too high, as shown by van Staden and du Plessis [55] and by Nakano *et al.* [56]. It is however surprising that such good precision is attained in SIA systems, because the reaction takes place at an interface with steep concentration gradient.

2.5 Operational techniques

2.5.1 Simple SIA systems

SIA provides a robust methodology for performing automated wet-chemical analysis. Reagents, samples and wash solutions are selected sequentially using a selection valve and are drawn into a holding coil. The well stacked zones are then propelled through a reaction coil. The reaction products are then expelled through the flow cell of a suitable detector giving rise in the measurable signal. The selection valves used are multi port (up to 20 ports), meaning that single to multi zone SIA techniques may be employed.

Single zone: The analysis of chemical species that can be measured directly, such as those that

have a high molar absorptivity of light at a specific wavelength (e.g. concentrated hexavalent chromium) can be analysed using single zone sequential injection analysis [11]. The technique can also be used for pH determinations or methods where detection is done using non-selective electrodes or chemical sensors. In these types of analysis the sample is the only zone injected.

Double zone: Double zone sequential injection analysis depends on the addition of a single reagent. In this type of analysis, the sample and the reagent solution are the only two zones injected. Reaction stoichiometries of different complexes can easily be determined when using a two zone system [36, 51]. The main advantage of these methods above their FIA counterparts is their tedious and time-consuming process of changing the sample loops for every different ligand: metal ratio, is eliminated. Double zone SIA was also used by others [57-60].

Three zones: In a three zone sequential injection analysis systems, a sample and two reagents are involved. The order in which the different sequences of reagents are drawn up depends very much on the reactions involved. In the determination of ammonia using the indophenol blue method [45] a three zone sequence of sample, phenol and hypochlorite reagents was used. This sequence is in contrast with the manual and flow injection methods [61], where the hypochlorite reagent is first added to the sample. The importance of the correct zone sequence is also highlighted in the determination of phosphate [52], where the sample had to be drawn up first to ensure minimum reaction time between the molybdenum and ascorbic acid reagents. Three zone SIA was also applied by other researchers [62-64].

Multi zones: Although it is stated that three zones were the maximum to ensure effective mixing [4,16,19], Guzman and Compton [65] published an article where six zones were used in the

part of segmented auto analysers, flow injection and sequential injection systems [73]. In this work the influence of various parameters and dialysis efficiency was studied [43].

Dilution: On-line dilution with SIA has been evaluated using a dilution step as part of the timing sequence [16,72,74,75]. The manifold of the SIA system with the dilution coil is more complicated than the system including the dilution step. Control over there magnitude and range of dilution is effected by three volume parameters: sample volume, transfer volume and analysis volume [72].

Mixing chambers: Mixing chambers are often used in SIA when it is necessary to add several reagents serially [32] or when extensive dilution of the analyte is required [76]. The influence of a mixing chamber on dispersion and zone penetration in a SIA manifold has been studied [9,10, 60].

Although mixing chambers have contained undesired properties such as large dead volume and causing hold up effects, it offers some distinct advantages, for example, in the use of mixing liquids with different viscosities [77]. Mixing chambers were essentially used in SIA to dilute highly concentrated samples [72,75,78] or to ensure adequate mixing when three or more zones were involved [32,65,67,79]. Recently, mixing chambers were used to improve the degree of mixing even for cases where only two zones were used [51]. Increased mixing leads to an increase in dispersions [9,60].

Higher volume of mixing chambers is also an important parameter, since larger volumes resulted in larger dispersion, which is not always desirable [9,67,60].

Extraction: Peterson *et al.* [80] described a flow-based extraction method where an aqueous sample and organic solvent were sequentially injected into an extraction coil, mixed and separated due to the differential flow velocities of the aqueous and organic phases. The sequential injection extraction manifolds are much simpler than the ones used for FIA extractions, since no segmenters or phase separations were needed.

Sequential injection extraction (SIE) provides more economical use of reagent and sample solutions as well as simplified manifolds compared to those of flow injection analysis. SIE manifolds do not need phase segmenters and separators which do not only simplify the manifolds, but also exclude extensive dilution and other problems associated with these devices [81]. Despite the use of toxic organic solvents, the role of liquid-liquid extraction SIA in some areas will become indisputable.

2.6 SIA - Application

Since its birth SIA has been used extensively in evaluation of operational parameters (see 2.4), operational techniques (see 2.5) and applications to industrial, clinical agricultural, environment and pharmaceutical products. These applications range from simple to complex method designs, which may involve the incorporation of additional components, such as dialysers, hydride generators, mixing chambers, jet ring cell and currently solid - phase reactors in the SIA manifold.

The group at the University of Washington made a valuable contribution with the exploitation

of new sensor systems which broadened the scope of SIA tremendously and opened new horizons in the field of flow analysis.

First Scudder *et al.* [81] developed a fountain cell in fluorescence microscopy. A chemiluminescence system that combines the simplicity and reproducibility of SIA with the unique radial flow properties of the fountain cell was then successfully employed for the chemiluminescence determination of hydrogen peroxide and glucose [82]. The fountain cell design was further used as basis for a perfusion chamber to perform the characterization of planar concentration gradients in a sequential injection system for cell perfusion studies [83]. The group [15, 84] also innovated and designed a novel jet ring cell which was incorporated into a sequential injection system for automated immuno-assays and for pre-concentration of analytes on sorbents with *in situ* spectroscopic detection. The jet ring cell with a renewable solid support was connected to a sequential injection system to determine glucose amperometrically [85]. A renewable gas sampling interface (liquid droplet) coupled with a SIA analyser was used to determine ammonia [86].

SIA was also applied for the determination of total ammonium nitrogen and free ammonia in a fermentation medium [27], nitrites and nitrates [87-89], D-lactic acid in pork [90], glucose using sensor injection and amperometric detection [91] and cyanide using ion-selective electrodes [92]. Wine [93] and sugar [94] analysis were done using sequential injection (SI)-FTIR spectrometry. Sequential injection manifolds were also used to handle reagents for flourescence microscopic measurements [4].

Coupling of sequential injection analysis with inductively-coupled plasma mass spectrometry as

an analytical tool for trace element detection was used by Al-Swaidan [95]. The technique was applied for the determination of lead, nickel and vanadium at the part per billion level in sample solutions of Saudi Arabian crude oils. Hydride-forming elements were determined by direct current plasma atomic emission spectrometry based on a modified version of the sequential injection technique [96].

SIA was also employed as a sample preparation device, especially for high-performance liquid chromatography [97, 98]. Lukkari *et al.* [97] used solid-phase extraction on Aluminium oxide in a sequential injection system to purify pyrocatechol, protocatechuic acid, pyrogallol and gallic acid in black liquor. Sequential injection systems for the determination of mercury by cold-vapour atomic absorption spectroscopy [99,100] used special gas-liquid separation units for effective analysis.

Application of the SIA technique to anodic stripping voltammetry (ASV) alowed the on-line plating of the mercury film and therefore substantially reduced the generation of mercury waste [101]. Other potentiometric applications include the determination of glycerol and 2.3-butanediol in wine [102]. Primary explosive azides in environmental samples were determined amperometrically using a SIA system [103]. A sequential injection system used in speciation studies employed two detectors in series, namely a potassium ion-selective electrode and a flame emission spectrometer [104].

SIA was also extensively used for the monitoring of bioprocesses [6, 105-107], enzyme activity [108,109] and fermentation processes [110,111]. Immobilized enzyme reactors played a great part in sequential injection analysis [90, 112-116] as well as systems for medical and

pharmaceutical uses [117-123]. Other SIA methods were also used for medical and pharmaceutical uses [124, 125]. Vitamin C was monitored photometrically in a kinetic application involving an iron (II)-iron (III) reaction [126], while morphine was determined with a SIA system employing chemiluminescence detection [127]. Van Staden and McCormack [128] used a SIA system to determine amino acids spectrophotometrically. Chemiluminescence detection was employed in the preliminary analytical evaluation of novel reagents using a SIA system [129]. A method for determining the bromine (Br) number by coulometric flow-injection titrations, using sequential injection with sinusoidal flow is described by Tayler [130]. SIA was even applied to determine 90 Sr in nuclear waste [131].

Iron (II) was separated from a sample matrix by dialysis in an SI system [43]. The dialysed iron was complexed with Tiron and the resulting complex was monitored spectrophotometrically at 667nm. A sample frequency of 8 samples per hour and a detection limit of 45mg/ℓ iron (III) were obtained.

Dialysis was also used in the spectrophotometric determination of L(+)-lactate in wines [132]. In the determination of total ammonium-nitrogen and free ammonia in a fermentation medium, a two channel sequential injection system was used [21]. The streams were propelled by an *Alitea S2-V* two channel piston sinusoidal flow pump equipped with two cam driven parallel syringes. Two electrically actuated multi-position valves, a six port valve on the donor line and an eight port valve on the acceptor line, were used to direct the flow streams. A *Celgard 2400* hydrophobic membrane was used in the combined gas diffusion unit flow cell. Luo *et al.* [133] described the determination of gaseous ammonia using a glass diffusion denuder in an SI system.

Coupling of gas-diffusion separation and sequential injection analysis is applied to determine ammonia in aqueous environmental samples [54]. [The sample and an alkaline solution are sequentially aspirated using an automatic burette and mixed by flow reversal while being propelled to a gas-diffusion unit.]

Van Staden and du Plessis [55] described a sequential injection titration system for the titration of a strong acid with a strong base. The concept is based on the sequential injection of a base titrant, and analyte and a second base titrant zone into a distilled water carrier stream. A titration method without mixing or dilution is described by Holman *et al.*[134]. This method also involves the use of chemical sensing membranes.

In the determination of phosphate, in bio-processes, dilution (when required) was performed in a mixing chamber connected to the selector valve [79]. In the spectrophotometric catalytic determination of iodide in nutrition salts, Lima *et al.* [116] used a SIA system with mixing chamber for handling high concentration solutions.

Barbiturates (phenobarbital, amobarbital, pentobarbital and secobarbital) and serontonin re-uptake inhibitors (SRIs) - venlafaxine, paroxetine, sentraline and norsertraline - were extracted as model acidic and basic compounds from urine into a 1:4 (V:V) mixture.

Nakano *et al.* [56] combined wetting film extraction with colorimetry to determine nanogram amounts of molybdenum (VI). Using a very simple manifold a highly sensitive sequential injection system was developed. Molybdenum (which reacted with thiocyanate) was extracted in the first step into a toluene film as an ion paired complex. The thiocyanate ligands were

displaced by 1.5 diphenylcarbazone (DPC) to form intensely coloured product which was measured at 540 nm. Wetting film extraction was also used in the photometric determination of vanadium (IV) and vanadium (V) [136] and chromium (VI) and chromium (III) in water [136].

Grate and Taylor [137] described an on-line soil extraction procedure employing SIA. On-line extraction was performed with the soil placed in an open-ended column attached to the sample line.

Rubi *et al.* [138,139] described a sequential injection assembly for the determination of iron in natural waters. Iron was pre-concentrated on a micro-column packed with a chelating resin (chelex 100) that was inserted into the manifold. The SIA system offers automatic pre-concentration, elution, detection and data acquisition. Using a simple sequential injection method, ammonia was determined with conductometric detection [140]. The ammonia permeated through a gas permeable membrane and was collected (pre-concentrated) in a static acceptor stream.

In the determination of 90Sr, the 90Sr was separated from other radionuclides using a sorbent micro-column containing a resin that selectively binds 90Sr as a crown ether under acidic conditions [131]. The isolated 90Sr was then detected on-line with a flow through liquid scintillation counter.

In a SIA process control application, a mixing chamber connected to a fibre optic detector has proven to be successful for the determination of total biomass [27,14]. This mixing chamber or cell was used both as a dilution chamber and detection cell. In the simultaneous determination

of cobalt and nickel, a mixing chamber with a volume of 500 mℓ was used to ensure adequate mixing of the reagents before splitting the product zone in two [67]. A sequential injection analysis was developed for the spectrophotometric determination of thiocynate [143].

Taljaard [142] developed a sequential injection analyser to monitor iron and sulphate concentration in aqueous solutions and an sequential injection extraction system for the simultaneous determination of mercury (II) and cobalt (II) ; cadmium (II) and mercury (II) as well as the thiozone metals (lead (II) , copper (II) , zinc (II) , cobalt (II) , cadmium (II) , iron (II) and mercury (II)) in aqueous and soil samples.

A method for the resolution of binary mixtures of cobalt and nickel at low levels was performed by employing coupled on-line complex formation and ligand substitution reactions in a sequential injection analyser [67, 142].

The use of amperometric biosensors based on modified graphite paste has been used as detectors in the SIA. The enantioselective analysis of chiral drugs needs reliable methods, hence an automated system for the enantiopurity test of S-Captopril based on the concept of SIA with an amperometric biosensor as detector was developed [143]. A SIA method for the simultaneous determination of S- and R- captopril is proposed, an amperometric, enantioselective membrane electrode based on maltodextrin for the assay of S-captopril and an amperometric biosensor for the assay of captopril was developed [144]. Through using electrochemical sensors and biosensors, the reliability of the enantiomers assay is improved. The use of SIA has led to a reduction in reagents which are very expensive.

The use of solid-phase reactor incorporated into the SIA manifold is one of the areas in which very little has been done. Lukkari *et al.*[97] incorporated a solid - phase (Aluminium oxide) in a sequential injection system to purify pyrocatechol, protacatechuic acid, pyrogallol and gallic acid in black liquor. Shu *et al.* [145] developed a spectrophotometric method for the determination of lactic acid from industrial inorganics. A method for the simultaneous monitoring of glucose, lactic acid and penicillin [146] by SIA with glucose oxidase or lactate oxidase immobilised onto nylon tubing was developed. The online monitoring of glucose and penicillin [147] with immobilised glucose oxidase and penicillinase on a piece of nylon tubing from industrial organics was accomplished spectrophotometrically. Theophylline and caffeine [148] using a microcolumn packed with Micro High Q anion exchange beads were determined spectrophotometrically. The separation of radionuclides [149] using Sr-resin, TRU-resin and TEVA resin beads as slurry packed into a microcolumn was developed.

2.7 Conclusion

Sequential injection analysis introduced a new approach in conducting analysis by the sequencing of the sample and reagent zones in the flow conduit. Since, its introduction into the analytical field , it is evident from the amount of work done, that by careful manipulation of the system parameters, successful analyses can be conducted with SIA by controlling the degree of zone penetration and dispersion.

Sequential injection analysis has reached the point where a manifold that does not need changing can be designed and adapted for multi-reagent techniques and multi-detection systems without the need of reconfiguring the manifold. Different sample handling techniques were successfully

adapted to SIA with the incorporation of different components within the manifold to perform certain function.

The advantages of SIA over conventional FIA , is its more cost effectiveness in the use of reagents and samples, its versatility, robustness, flexibility for applying stopped-flow and reversed flow operations and the use of multiport selection valve. However, the sample throughput frequency of an SIA system is normally less than that of the conventional FIA system.

Further developments in SIA, involves the incorporation of solid - phase reactors in the SIA manifold, the use of biosensors as well as using versatile controlling software to manipulate sample and reagents in novel ways to achieve desired sample handling procedures.

SIA, surely has a very useful and bright future lying ahead if properly explored, especially with the use of biosensors and the incorporation of solid - phase reactors in the SIA manifold which is gradually gaining momentum. This, however, does not mean that SIA will replace FIA.

2.8 References

1. J. Růžička and G. D. Marshall, **Anal. Chim. Acta, 237** (1990) 329.
2. J. Růžička, G. D. Marshall and G. D. Christian, **Anal. Chem., 62** (1990) 1861.
3. J. Růžička, **Anal. Sci., 7** (1991) 635.
4. J. Růžička, **Analyst, 119** (1994) 1925.
5. G. D. Marshall, **Sequential-Injection Analysis,** PhD-Thesis, University of Pretoria, 1994.
6. T. Gübeli, G. D. Christian and J. Růžička, **Anal. Chem., 63** (1991) 2407.
7. A. Cladera, E. Gómez, J. M. Estela, and V. Cerdà, **Talanta, 43** (1996) 1667.
8. J. F. van Staden, H. du Plessis, S. M. Linsky, R. E. Taljaard and B. Kremer, **Anal. Chim. Acta, 354** (1997) 59.
9. J. F. van Staden and A. Botha, **S. Afr. Jour. Chem., 51** (1998) 100.
10. T. McCormack and J. F. van Staden, **Anal. Chim. Acta, 367** (1-3) (1998) 111.
11. J. L. Zable, **Operational Parameters of Sequential Injection Analysis and the Fundamentals of Calculating the Dispersion at the Maximum Zone Overlap,** PhD-Thesis, University of Washington, 1996.
12. J. Růžička and E. H. Hansen, **Trends Anal. Chem., 17** (1998) 69.
13. J. Růžička, **Anal. Chem., 55** (1983) 1040A.
14. G. D. Christian, **Biol. Prospect., 8** (1993) 7.
15. J. Růžička, C. H. Pollema and K. M. Schudder, **Anal. Chem., 65** (1993) 3566.
16. R. E. Taljaard, **Application of Sequential Injection Analysis as Process Analyzers,** MSc-Thesis, University of Pretoria, 1996.

17. G. D. Marshal and J. F. van Staden, **Process Control and Quality, 3** (1992) 251.

18. J. Růžička, **Anal. Chim. Acta, 261** (1992) 3.

19. J. Růžička and T. Gübeli, **Anal. Chem., 63** (1991) 1680.

20. G. D. Christian and J. Růžička, **Anal. Chim. Acta, 261** (1992) 11.

21. I. Lukkari, J. Růžička and G. D. Christian, **Fresenius' J. Anal. Chem., 346** (1993) 813.

22. A. Ivaska and J. Růžička, **Analyst, 118** (1993) 885.

23. S. Liu and P. K. Dasgupta, **Talanta, 41** (1994) 1903.

24. S. Liu and P. K. Dasgupta, **Anal. Chim. Acta, 308** (1995) 281.

25. G. D. Marshall and J. F. van Staden, **Anal. Instrum., 20** (1992) 79.

26. A. Cladera, C. Tomàs, E. Gómez, J. M. Estela and V. Cerdà, **Anal. Chim. Acta, 302** (1995) 297.

27. P. J. Baxter, G. D. Christian and J. Růžička, **Analyst, 119** (1994) 1807.

28. D. A. Joelsson and A. Ivaska, **Kemi, 20** (1993) 591.

29. G. D. Christian, **J. Flow Injection Anal., 11** (1994) 2.

30. G. D. Christian, **Analyst, 119** (1994) 2309.

31. J. Růžička and E. H. Hansen, **Flow Injection Analysis,** 2nd ed., Wiley & sons, New York, 1988.

32. M. Guzman, C. Pollema, J. Růžička and G. D. Christian, **Talanta, 40** (1993) 81.

33. J. F. van Staden, H. du Plesis, S. M. Linsky, R. E. Taljaard and B. Kremer, **Anal. Chim. Acta, 354** (1997) 59.

34. J. de Gracia. M. L. M. F. S. Saravia, N. J. Araujo, J. L. F. C. Lima, M. del Valle and M. Poch, **Anal. Chim. Acta, 348** (1997) 143.

35. A. Rius, M. P. Callao, J. Ferre and F. X. Rius, **Anal. Chim. Acta, 337** (1997) 287.

36. F. E. O. Suliman and S. M. Sultan, **Talanta, 43** (1996) 559.

37. A. Rius, M. P. Callao and F. X. Rius, **Anal. Chim. Acta, 316** (1995) 27.

38. F. Sales. M. P. Callao and F. X. Rius, **Chemom. Syst., 38** (1997) 63.

39. I. Ruisanchez, J. Lozano, M. S. Larrechi, F. X. Rius and J. Zupan, **Anal. Chim. Acta, 348** (1997) 113.

40. A. Rius, M. P. Callao and F. X. Rius, **Analyst, 122** (1997) 737.

41. A. Joelsson and A. Ivaska, **Kem. Tidskr., 105** (1993) 20.

42. M. Valcarcel and M. D. Luque de Castro, **Flow Injection Analysis. Principles and Applications,** Horwood, Chichester, 1987.

43. J. F. van Staden, H. du Plessis and R. E. Taljaard, **Anal. Chim. Acta, 357** (1997) 141.

44. J. F. van Staden, R. E. Taljaard, **Anal. Chim. Acta, 344** (1997) 281.

45. C. Zang, Y. Naruzawa and S. Kitahama, **Chem. Lett., 5** (1993) 877.

46. C. Zang, Y. Naruzawa and S. Kitahama, **J. Flow Injection Anal., 10** (1993) 79.

47. A. N. Araujo, J. Gracia, J. F. Lima, M. Poch and M. F. S. Saraiva, **Fresenius' J. Anal. Chem., 357** (1997) 1153.

48. J. F. van Staden and D. Malan, **Anal. Comm., 33** (1996) 339.

49. J. A. Vieira, I. M. Jr. Raimundu, B. Reis, E. A. G. Zagatto and J. L. F. C. Lima, **Anal. Chim. Acta, 366** (1998) 257.

50. F. Mas-Torres, A. Cladera, J. M. Estela and V. Cerdà, **Analyst, 123** (1998) 1541.

51. J. F. van Staden, H. du Plessis and R. E. Taljaard, **Instrum. Sci. &Techn., 27** (1999) 1.

52. J. F. van Staden and R. E. Taljaard, **Mikrochim. Acta, 128** (1998) 297.

53. J. F. van Staden and R. E. Taljaard, **Anal. Chim. Acta, 323** (1996) 75.

54. M. T. Ohms, A. Cerdà, A. Cladera, V. Cerdà and R. Forteza, **Anal. Chim. Acta, 318**

(1996) 251.

55. J. F. van Staden and H. du Plessis, **Anal. Comm., 34** (1997) 174.

56. S. Nakano, Y. Luo, D. Holman, J. Růžička and G. D. Christian, **Microchem. J., 55** (1997) 392.

57. S. M. Sultan and N. I. Desai, **Analyst, 122** (1997) 911.

58. J. F. van Staden and R. E. Taljaard, **Anal. Chim. Acta, 331** (1996) 271.

59. J. F. van Staden and A. Botha, **Talanta, 49** (1999) 1099.

60. A. Botha, **Sequential Injection Analysis: Evaluation of operational Parameters and Application to Process Analytical Systems,** MSc-Thesis, University of Pretoria, 1999.

61. J. J. Pauer, **The Flow-Injection Analysis of Certain Determinants in Surface and Ground Water,** MSc-Thesis, University of Pretoria, 1989.

62. A. Munoz, F. Mas-Torres, J. M. Estela and V. Cerdà, **Anal. Chim. Acta, 350** (1997) 21.

63. J. Nyman and A. Ivaska, **Anal. Chim. Acta, 308** (1995)286.

64. J. Nyman and A. Ivaska, **Pap. Puu, 78** (1996) 513.

65. M. Guzman and B. J. Compton, **Talanta, 40** (1993) 1943.

66. E. Gómez, C. Tomás, A. Cladera, V. J. M. Estela and Cerdà, **Analyst, 120** (1995) 1181.

67. R. E. Taljaard and J. F. van Staden, **Anal. Chim. Acta, 366** (1998) 177.

68. J. M. Estela, A. Cladera, A. Munoz and V. Cerdà, **Int. J. Environ. Anal. Chem., 64** (1996) 205.

69. J. Alpizar, A. Crespi, A. Cladera, R. Forteza and V. Cerdà, **Electroanalysis, 8** (1996) 1051.

70. A. N. Araujo, R. C. C. Costa, J. L. F. C. Lima and B. F. Reis, **Anal. Chim. Acta, 358** (1998) 111.

71. F. Mas-Torres, A. Munoz, J. M. Estela and V. Cerdà, **Analyst, 122**(1997) 1033.

72. A. Baron, M. Guzman, J. Růžička and G. D. Christian, **Analyst, 117** (1992) 1839.

73. J. F. van Staden, **Fresenius' J. Anal. Chem., 352** (1995) 271.

74. J. F. van Staden and R. E. Taljaard, **Fresenius' J. Anal. Chem., 357** (1997) 577.

75. A. N. Araujo, J. L. F. C. Lima, M. L. M. F. S. Saraiva, R. P. Sartini and E. A. G. Zagatto, **J. Flow Injection Anal., 14** (1997) 151.

76. M. Gisin, C. Thommen and K. F. Mansfield, **Anal. Chim. Acta, 179** (1986) 149.

77. H. C. Shu and Y. C. Lin, **Huaxue, 53** (1995) 424.

78. J. C. Masini, P. J. Baxter, K. R. Detwiler and G. D. Christian, **Analyst, 120** (1995) 1583.

79. A. R. Crespi, R. Forteza and V. Cerdà, **Lab. Robotics. Autom., 7** (1995) 245.

80. K. L. Peterson, B. K. Logan, G. D. Christian and J. Růžička, **Anal. Chim. Acta, 337** (1997) 99.

81. I. Facchini, J. J. R. Rothwedder and Pasquine, **J. Autom. Chem., 19** (1997) 33.

82. K. M. Scudder, C. H. Pollema, J. Růžička, **Anal. Chem., 64** (1992) 2657.

83. D. J. Tucker, B. Toivola, C. H. Pollema, J. Růžička and G. D. Christian, **Analyst, 119** (1994) 975.

84. C. H. Pollema and J. Růžička, **Analyst, 118** (1993) 1235.

85. C. H. Pollema and J. Růžička, **Anal. Chem., 66** (1994) 1825.

86. T. Lindfors, I. Lahdesmaki and A. Ivaska, **Anal. Lett., 29** (1996) 2257.

87. S. Liu and P. K. Dasgupta, **Anal. Chem., 67** (1995) 2042.

88. M. T. Ohms, A. Cerdà and V. Cerdà, **Anal. Chim. Acta, 315** (1995) 321.

89. J. F. van Staden and T. A. van der Merwe, **S. Afr. J. Chem., 51** (1998) 109.

90. S. V. Karmarkar, **Am. Environ. Lab., 10** (1998) 6.

91. H. Shu, H. Håkanson and B. Mattiasson, **Anal. Chim. Acta, 283** (1993) 727.

92. M. J. C. Taylor, D. E. Barnes, G. D. Marshall, D. R. Groot and S. J. S. Williams, **Process Control Qual., 3** (1992) 173.

93. R. Schindler, R. Vonach, B. Lendl and R. Kellner, **Fresenius' J. Anal. Chem., 362** (1998) 130.

94. R. Schindler, M. Watkins, R. Vonach B. Lendl, R. Kellner and R. Sara, **Anal. Chem., 70** (1998) 226.

95. H. M. Al-Swaidan, **Talanta, 43** (1996) 1313.

96. P. Ek, S. G. Hulden and A. Ivaska, **J. Anal. Atom. Spectrom., 10** (1995) 121.

97. I. Lukkari, K. Irgum, P. Lindgren and J. Liden, **Process Control Qual., 7** (1995) 185.

98. J. Emneus and G. Marko-Varga, **J. Chromatogr. A, 703** (1995) 191.

99. F. M. B. Mirabo, A. C. Thomas, E. Rubi, R. Forteza and V. Cerdà, **Anal. Chim. Acta, 355** (1997) 203.

100. I. D. Brindle and S. Zheng, **Spectrochim. Acta. Part B, 51** (1996) 1777.

101. A. Ivaska and W. W. Kubiak, **Talanta, 44** (1997) 713.

102. G. C. Luca, B. F. Reis, E. A. G. Zagatto, M. Conceicao, B. S. M. Montenegro, A. N. Araujo and J. L. F. C. Lima, **Anal. Chim. Acta, 366** (1998) 193.

103. R. T. Echols, R. R. James and J. H. Aldstadt, **Analyst, 122** (1997) 315.

104. A. O. S. S. Rangel and I. V. Toth, **Port. Anal. Sci., 12** (1996) 887.

105. P. J. Baxter and G. D. Christian, **Chem. Res., 29** (1996) 515.

106. L. H. Christensen, J. Marcher, U. Schultz, M. Carlson, R. W. Min, J. Nielsen and J. Villaden, **Den. Biotechnol. Bioeng., 52** (1996) 237.

107. E. H. Hansen, B. Willumsen, S. K. Winther and H. Drabøl, **Talanta, 41** (1994) 1881.

108. R. W. Min, M. Carlsen, J. Nielsen and J. Villadsen, **Biotechnol. Tech., 9** (1995) 763.

109. S. C. Chung, G. D. Christian and J. Růžička, **Process Control Qual., 3** (1992) 115.

110. H. C. Shu, H. Håkanson and B. Mattiasson, **Anal. Chim. Acta, 300** (1995) 277.

111. C. Garcia de Maria and A. Townshed, **Anal. Chim. Acta, 261** (1992) 137.

112. M. Hedenfalk and B. Mattiasson, **Anal. Lett., 29** (1996) 1109.

113. X. Liu and E. H. Hansen, **Anal. Chim. Acta, 326** (1996) 1.

114. C. H. Pollema, J. Růžička, G. D. Christian and A. Lernmark, **Anal. Chem., 64** (1992) 1356.

115. N. W. Barnett, S. W. Lewis and D. Tucker, **Fresenius' J. Anal. Chem., 355** (1996) 937.

116. J. L. F. C. Lima, T. I. M. S. Lopes and A. O. S. S. Rangel, **Anal. Chim. Acta, 366** (1998) 187.

117. S. M. Sultan and F. E. O. Suliman, **Analyst, 121** (1996) 617.

118. R. W. Min, J. Nielsen and J. Villadsen, **Anal. Chim. Acta, 320** (1996) 199.

119. G. D. Christian, **J. Pharm. Biomed. Anal., 10** (1992) 769.

120. S. M. Sultan, F. E. O. Suliman and B. B. Saad, **Analyst, 120** (1995) 561.

121. P. J. Baxter, G. D. Christian and J. Růžička, **Anal. Chem., 40** (1994) 455.

122. L. X. Tang and F. J. Rowell, **Anal. Lett., 31** (1998) 891.

123. M. R. Wei, J. Nielsen and J. Villadsen, **Anal. Chim. Acta, 312** (1995) 312.

124. S. Parab, B. J. van Wie, I. Byrnes, E. J. Robles, B. Weyrauch and T. O. Tiffany, **Anal. Chim. Acta, 123** (1998) 157.

125. F. E. O. Suliman and S. M. Sultan, **Microchem. J., 57** (1997) 320.

126. S. M. Sultan and N. I. Desai, **Talanta, 45** (1998) 1061.

127. N. W. Barnett, C. E. Lenehan, S. W. Lewis, D. J. Tucker and K. M. Essery, **Analyst, 123**

(1998) 601.

128. J. F. van Staden and T. McCormack, **Anal. Chim. Acta, 369** (1998) 163.

129. N. W. Barnett, R. Bos, S. W. Russel and R. A. Russel, **Analyst, 123** (1998) 1239.

130. R. H. Taylor, C. Winbo, G. D. Christian and J. Růžička, **Talanta, 39** (1992) 789.

131. J. W. Grate, R. Strebin, J. Janata, O. Egorov and J. Růžička, **Anal. Chem., 68** (1996) 333.

132. A. N. Araujo, J. L. F. C. Lima, M. L. M. F. S. Saraiva and A. E. G. Zagatto, **Am. Jour. Enol. Viticul., 48** (1997) 428.

133. Y. Luo, R. Al-Othman, G. D. Christian and J. Růžička, **Talanta, 42** (1995) 1545.

134. D. A. Holman, G. D. Christian and J. Růžička, **Anal. Chem., 69** (1997) 1763.

135. S. Nakano, Y. Luo, D. A. Holman, J. Růžička and G. D. Christian, **J. Flow Injection Anal., 13** (1996) 148.

136. Y. Luo, S. Nakano, D. A. Holman, J. Růžička and G. D. Christian, **Talanta, 44** (1997) 1563.

137. J. W. Grate and R. H. Taylor, **Field Anal. Chem. Technol., 1** (1996) 39.

138. E. Rubi, M. S. Jimenez, F. B. de Mirabo, R. Forteza and V. Cerdà, **Talanta, 44** (1997) 553.

139. E. Rubi, R. Forteza and V. Cerdà, **Lab. Rob. Autom., 8** (1996) 149.

140. M. T. Ohms, A. Cerdà and V. Cerdà, **Electroanalysis, 8** (1996) 387.

141. J. F. van Staden and A. Botha, **Anal. Chim. Acta, 403** (2000) 279.

142. R. E. Taljaard, **Multicomponent Determinations using Sequential Injection Analysis**, PhD-Thesis, University of Pretoria, 1999.

143. R. I. Stefan, J. F. van Staden and H. Y. Aboul-Enein, **Anal. Chim. Acta, 429** (2000) 1.

144. R. I. Stefan, J. F. van Staden and H. Y. Aboul-Enein, **Talanta,** (2000).

145. H. C. Shu, H. Håkanson and B. Mattiasson, **Anal. Chim. Acta, 300** (1995) 277.

146. R. W. Min, J. Nielsen and J. Villadsen, **Anal. Chim. Acta, 312** (1995) 149.

147. R. W. Min, J. Nielsen and J. Villadsen, **Anal. Chim. Acta, 320** (1996) 199.

148. B. Dockendorf, D. A. Holman, G. D. Christian and J. Růžička, **Anal. Commun., 35** (1998) 357.

149. O. B. Egorov, M. J. Ohara and J. W. Grate, **Anal. Chem., 71** (1999) 345.

CHAPTER 3

Super Serpentine reactors in Sequential Injection Analysis Systems

3.1. Introduction

Sequential injection analysis (SIA) is well known for its use as an analytical technique, having the advantage of reduced sample and reagent consumption compared to flow injection analysis (FIA). An important aspect that needs critical attention in the optimization of this system is the dispersion which could have a direct effect on zone penetration that takes place within the SIA conduit.

Reactors provide an extensive range of control of dispersion for the development and application of FIA/SIA methodologies. Control of dispersion is key in both the development and optimization of its analytical performance.

There are various reactors that have been used in SIA , straight tubes, helically coiled tubes, knotted tubes, mixing chambers, solid phases, single bead string reactors and Serpentine 8. Solid phase reactors will be discussed in full in chapter 4 and the other reactors will be briefly discussed in this chapter. However, this chapter will mainly focus on super Serpentine reactors, where the influence or effect of reactor type and length will be investigated on sensitivity and precision. Dispersion and zone overlapping will be paramount in this investigation.

3.2 Dispersion

An important cornerstone of the family of flow systems, in addition to reproducible timing and sample injection, is the concept of controlled dispersion. The purpose of controlling dispersion in a flow system is to optimize the chemical reactions taking place between the sample and reagents. In essence, what is called "controlled dispersion" is in fact the recognition that the sample is reproducibly diluted as it travels down the tubing. Dispersion is characterized by the concentration profile adopted by a zone or plug inserted at a given point in the system without stopping the flow.

Dispersion is the result of all physical forces acting on the injected sample zone. It is the process by which the sample zone transforms from a homogeneous geometrically well defined zone at the moment of injection, to the final zone that is detected down stream. Two processes are responsible for dispersion in the flow conduit, namely the physical process of material dispersion due to hydrodynamic processes taking place in the flow-through system and the chemical process of formation of chemical species. Dispersion of the sample is the product of three processes: laminar flow, secondary flow and molecular diffusion which results from the transportation of the sample.

3.2.1 Transport

The transport of matter along the tubes of a flow system is said to take place essentially by laminar flow [1] and not as a result of turbulent flow as thought earlier [2]. There are two

mechanism that contributes to dispersion of the injected sample, namely convective transport and diffusional transport [3].

(i) *Convective* transport occurs under laminar flow conditions. It yields a parabolic velocity profile with sample molecules at the tube walls having zero linear velocity and those at the centre of the tube having twice the average velocity. Fig 3.1 illustrates the two types of convective transport, namely turbulent and laminar flow. Laminar flow is also referred to as the axial dispersion and it is the result of viscous shear forces near the tube wall.

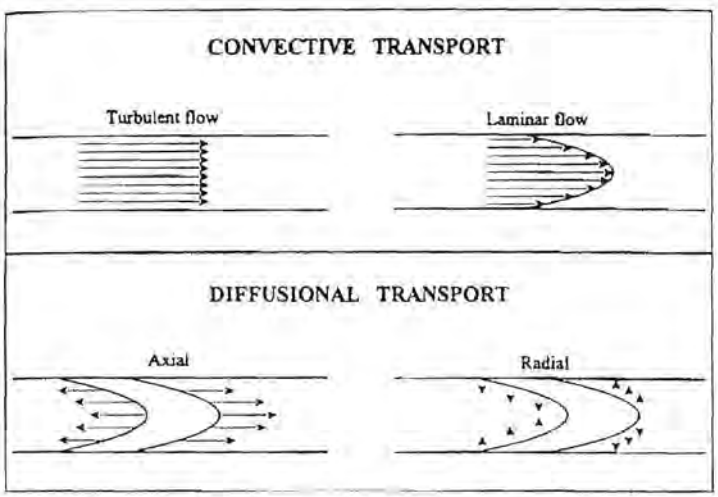

Fig. 3.1 General types of transport in closed tubes

(ii) *Diffusional* transport gives rise to axial and radial diffusion (Fig. 3.1) due to the presence of concentration gradient at the leading and trailing edges of the injected sample zone. It contributes insignificantly to the overall dispersion. Radial diffusion results from concentration differences perpendicular to the overall dispersion. It tends to balance concentrations in such a manner that the molecules located at the tube walls tend to move to the centre, whereas those

at the centre travel outwards. Indeed this motion slows down convective transport, thus hindering progressive dilution of the zone in the carrier stream.

3.2.2 Theoretical models

First of all, it is salutary to explain the difficulties involved in the theoretical predictions of the behaviour of the injected sample or reagent plug in practical systems. It is not an easy task to define the contributions of the elements such as the injection operation, connectors or geometry of the flow cell to the dispersion. All relations are therefore empirical in nature, nevertheless, several models have been developed for laminar conditions, to define the theoretical principles and derive mathematical expressions accounting for the physical behaviour of the injected plug. A number of these models are described in the following paragraphs. Table 3.1 gives the list of symbols that will be used in the discussion.

TABLE 3.1 List of symbols

Name	Symbol	Name	Symbol
Concentration (M)	C	Partial tube radius (mm)	r
Injected volume (mℓ)	V_i	Partial tube length (cm)	l
Initial concentration	C_p	Flow rate (mℓ/min)	q
Concentration at signal peak maximum	C_{max}	Linear velocity (cm/sec)	u
Molecular diffusion coefficient (cm^2/sec)	D	Maximum linear velocity (cm/sec)	u_o
Overall tube length (cm)	L	Mean residence time (sec)	$\bar{t}$
Tube diameter (mm)	d	Dispersion coefficient	**D**

Volume of system (mℓ)	V_r	Baseline-to-baseline time (sec)	Δt
Travel time (sec)	t_a	Vanderslice's accommodation factor	f
Tube radius (mm)	R	Residence time (sec)	T

3.2.2.1 Taylor' models

This model only holds for low flow rates and very long reactors, which help to compensate for radial concentration changes and favour the prevalence of diffusion phenomena. Taylor's model [3] is applicable to a Gaussian distribution defined by $C = f(t)$ in a form which depends on the chosen parameters, namely:

$$C = \frac{m}{4r^2\pi Dt} \exp\left[\frac{-(x - L)^2}{4Dt}\right]$$

and

$$C = \frac{C_0 V_i}{q\sigma(2\pi)^{1/2}} \exp \frac{(t - \bar{t}_r)^2}{2\sigma^2}$$

where m is the injected solute mass ($m = C_o V_i$), σ is the parameter corresponding to the standard deviation characteristic of a Gaussian distribution and x is the axial distance from the injection point. This model is only applicable if the injected volume is practically negligible compared with the reactor volume, thus $V_i \ll V_r$.

3.2.2.2 Tanks-in-series model

This model is analogous to the description of liquid chromatography in terms of theoretical plates. It relies on the assumption that the fluid flow passes sequentially through a large number (N) of mini chambers in which stirring is perfect (instantaneous mixing). The mathematical expression derived from this model [2] is:

$$C = \frac{1}{(\bar{t}_r)_N} \left[\frac{t}{(\bar{t}_r)_N}\right]^{N-1} \frac{1}{(N-1)!} \exp\left[\frac{-t}{(t_r)_N}\right]$$

$(\bar{t}_r)_N$ being the mean residence time of an element of fluid in a given tank. The larger N, the more Gaussian the profiles of the $C = f(t)$ curves become. Under this conditions, the variance is given by:

$$\sigma^2 = N(\bar{t}_r)_N^2 = \frac{(\bar{t}_r)^2}{N}$$

since the overall mean residence time is $\bar{t}_r = N(\bar{t}_r)_N$. The suitability of this model is rather questionable for small N values, i.e for reactors that are not very long.

3.2.2.3 Mixing chamber model

Pungor *et al.* [4] developed a mathematical model to describe the dispersion when there is a mixing mini chamber positioned close to or in the reactor itself. The concentration of a substance in the mixing chamber can be described as a function of time by:

$$\frac{d\Delta C_t}{dt} = \frac{V}{W}\left[\Delta(C_s)_t - \Delta C_t\right]$$

where t is the time (sec) from the moment of injection, $\Delta C_t = C_t - C_o$; C_t is the actual analyte concentration in the carrier stream on entry to the mixing chamber, C_o is the analyte concentration before injection, V is the flow rate (mℓ/min) and W is the volume of the mixing chamber.

Mixing chambers are often used in SIA when it is necessary to add several reagents serially [5] or when extensive dilution of the analyte is required [6]. The influence of a mixing chamber on dispersion and zone penetration in an SIA manifold has been studied [7, 8].

3.2.2.4 General model

The expression which takes place strictly into account both convective and diffusional transport and therefore best describes the overall physical dispersion phenomena is:

$$\frac{\delta C}{\delta t} = D\left[\frac{\delta^2 C}{\delta l^2} + \frac{\delta^2 C}{\delta r^2} + \frac{1\delta C}{r\delta r}\right] - u_0\left(1 - \frac{r^2}{R^2}\right)\left(\frac{\delta C}{\delta l}\right)$$

This expression takes into account axial and radial concentration gradients, as well as flow profiles under laminar flow regime. The left-hand side corresponds to diffusional transport, the

first term within the brackets accounting for axial diffusion (dependence of C on l) and the other two for radial diffusion (dependence of C on r). The first term on the right -hand side corresponds to build-up of matter, which only occurs in a non-safety regime, and the second term accounts for the contribution from convective transport for which the velocity profile is parabolic in shape and given by:

$$u = u_0(1 - \frac{r^2}{R^2})$$

The molecules at the tube walls ($r = R$) have zero velocity ($u = 0$), whereas those at the centre ($r = 0$) have the maximum velocity ($u = u_0$).

3.2.3 Practical definition of dispersion

The dispersion or dilution at the detector, of a sample injected into the flow, is given by the position and shape of the analyte signal band. Therefore, in practice it is the parameters characterizing the transient signal which are chosen to define the dispersion. An FIA peak is characterized, at least qualitatively, by:

a) its position, as defined by the travel time, t_{av}

b) its bandwidth, characterized by the baseline-to-baseline time, Δt, and

c) the co-ordinate of the band maximum (T, C_{max}).

Bearing in mind the general theoretical considerations and the description of the different models used to define dispersion, it is easy to understand the difficulty involved in relating them

to the experimental observations in a straightforward way.

3.2.3.1 Růžička's dispersion coefficient

This is the earliest parameter used to characterize passage of the sample through the system. The dispersion coefficient at the peak maximum (**D**) is defined as the ratio between C_0, the concentration of the dye injected into the system as it passes through the detector in an FIA system and when at maximum, C_{max} [3, 9], i.e.

$$D_{max} = \frac{C_o}{C_{max}}$$

The dispersion coefficient is useful in that it allows comparisons of different manifolds [9]. Furthermore, it provides a means to verify and monitor the degree of sample dilution resulting from any changes made to the manifold during method development. It is important to note that the definition of the dispersion coefficient considers only physical process of dispersion and not the ensuing chemical reactions.

3.2.4 Influence of various factors on the dispersion

The parameters that influences the amount of dispersion to be achieved in a flow conduit has been studied for both FIA [3, 11] and SIA [7, 12, 13]. These parameters essentially affects the sensitivity of the measured signal and the success of the reaction between the sample and reagent components. The effect of these parameters on dispersion in both FIA and SIA are very

similar as will follow clearly from the following discussion. The effect of the physical parameters on dispersion is usually investigated by injecting (FIA) or aspirating (SIA) a well-defined volume of a dye solution into a colourless carrier stream and evaluating the resulting signal of the dispersed dye zone, which is an indication of the amount of dispersion the sample has undergone.

It is clear that the analyst has complete control over the amount of sample dispersion or dilution that occurs as the sample passes through the manifold. This control originates from the way in which the manifold is designed. In the discussion below the factors that influences sample dispersion in the flow conduit are discussed. The experimental parameters have been classified according to whether they are representative of the sample, geometry of the system or hydrodynamic working conditions.

3.2.4.1 Sample volume

The introduction of increasing volumes of dye into an FIA system revealed the following information [3]:

a) the travel time is independent on the injected sample volume,
b) the residence time, and hence t', increases with the injected volume,
c) the baseline-to-baseline time also increases with the injected volume and
d) the dispersion coefficient decreases with increasing sample volume.

According to Růžička, **D** and V_i are inversely proportional to each other, i.e.

$$D = \frac{k}{V_i}$$

Růžička *et al.* [10] formulated the following rule to define the behaviour of different sample volumes in the flow conduit:

"**Rule 1.** Changing the injected sample volume is a powerful way to change dispersion. An increase in peak height and in sensitivity of measurement is achieved by increasing the volume of the injected sample solution. Conversely, dilution of overly concentrated sample material is best achieved by reducing the injected sample."

A similar conclusion was drawn from the dispersion experiments in an SIA system [7, 13], especially with regard to increased sensitivity, and decreased dispersion, with increasing sample volumes. It was also stated that the increase in sensitivity of the measurement will be possible only when sufficient reagent in excess is available in the element of fluid situated at the peak maximum [13].

3.2.4.2 Hydrodynamic factors

The flow rate *(q)* was related to the travel and baseline-to-baseline times through the following equations [3]:

$$t_a = \frac{k}{q^{1.025}}$$

and

$$\Delta t = \frac{k'}{q^{0.64}}$$

where the constants k and k' include, among other parameters, the accommodation factor, f, which is independent of the flow rate. As can be seen, t_a and Δt, and hence the dispersion, should decrease with increasing flow rate. Valcárcel *et al.* [3] indicated that the dispersion coefficient does indeed decrease with increasing flow rate contrary to Růžička *et al.* [11] who stated that:

"Rule 3. The dispersion of the sample zone increases with the square root of the distance travelled through the tubular conduit and decreases with decreasing flow rate. Thus, if the dispersion is to be reduced and the residence time is to be increased, the tube dimensions should be minimized and the pumping rate should be decreased..."

The increase in sensitivity with increasing flow rates has been demonstrated for SIA [7], thus confirming that which had been observed by Valcárcel *et al.* [3]. They stated further that the decrease in the dispersion coefficient with increasing flow rate, occurs in a non-linear fashion, except for large L and q values, in which case a slight increase in **D** with increase in q is observed.

3.2.4.3 Geometric factors

This section deals with the influence of the reactor shape (open, coiled, packed) its dimensions and the presence of a mixing chamber on the dispersion in a flow system. The function of these reactors is to increase the intensity of radial mixing, by which the parabolic velocity profile in the axial direction is reduced when the sample zone is injected into a laminar flow carrier stream [11]. Thus, the reagent becomes more readily mixed with the sample and the axial dispersion of the sample zone is reduced.

Relaxation of the laminar profile in the radial direction is best achieved by creating a local turbulence whereby the direction of flow is suddenly changed. This causes the elements of fluid that are falling behind because they are close to the walls of the channel to be moved into the rapidly advancing central streamline. The elements of fluid that have been advanced in an axial direction because they are close to the central streamline are repositioned closer to the tube wall. The more frequently this process is repeated, the more symmetrical the concentration gradient within the dispersed sample zone will be, and the peak shape will change from an asymmetric to a symmetric (Gaussian) one.

3.2.4.3.1 Straight tubes

Straight tubes represent the simplest situation. The influence of the reactor length, L, on t_a and Δt is predicted by the Vanderslice's expression[3]:

$$t_a = k L^{1.025}$$

and

$$\Delta t = k' L^{0.64}$$

It is evident from these expressions that an increase in reactor length is accompanied by an increase in t_a and Δt . The dispersion coefficient also increases with increasing reactor length, which is consistent with Růžička's expression,

$$\boldsymbol{D} = K L^{1/2}$$

The influence of the reactor diameter (R = d/2), is in agreement with Vanderslice's prediction [1], and it is evident that t_a and Δt are directly related to the diameter.

$$t_a = k d^2$$

and

$$\Delta t = k' d^2$$

The residence time and the dispersion coefficient both increased, with increasing tube diameter [3]. In SIA however, the tube internal diameter has been shown to have a more pronounced effect on the dispersion obtained than the length thereof [7, 14, 15].

3.2.4.3.2 Coils

When the reactor tube is coiled helically, the centrifugal force originating from the circulation of a fluid through the tube results in a radial-type flow as illustrated in Fig. 3.2. At low flow rates, the centrifugal force is not very great and the velocity profile is practically parabolic. At high flow rates the profile is completely different since molecules at the tube walls travel at a higher velocity than those at the centre of the tube.

Both situations result in a split circulation, symmetrical with respect to the ideal central plane of the tube. This circulation, especially fast at high flow rates, has been termed "secondary flow" [3]. It has the same effect as radial diffusion, thus tending to decrease the dilution or dispersion of the injected sample, a feature of great importance. It is observed that the smaller the coil diameter, the smaller the dispersion [3].

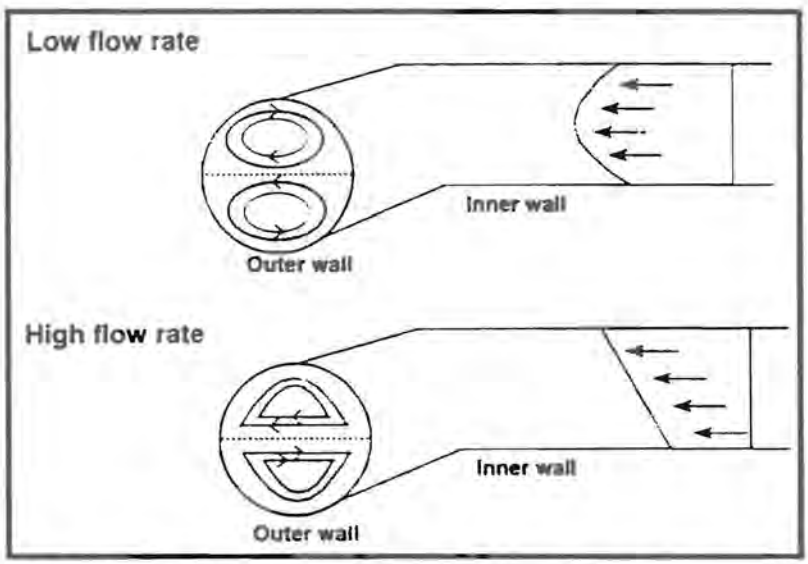

Fig. 3.2 Fluid dynamics corresponding to various in flow rate.

A coiled tube is the most frequently used reactor geometry, since it can conveniently accommodate any length of tubing in an experimental setup and also because secondary flow within the coiled tubing promotes mixing in the radial direction. The tighter the coiling of the tube is, the more pronounced this effect will be.

3.2.4.3.3 Knotted reactors

This type of reactor is also known as a three dimensionally disoriented (3-D) reactor. It is formed when a length of flexible tubing is knotted from end to end, resulting in a drastic decrease of dispersion. This may be due to the intensification of the dispersion-reducing effect introduced by coiling, since in effect the knots are very tight coils. The chaotic movement of the carrier stream through a spatially disoriented path promotes radial dispersion. The Serpentine 8 and super Serpentine reactors falls in this category. The Serpentine 8 reactor provides less axial dispersion and more radial dispersion compared to coiled reactors which are used when larger dilutions are required providing largely axial dispersion with minimal radial dispersion. It is intended for methodologies where less dilution, greater sensitivity, and higher sample throughput is desired. A single reactor may be wound on the frame as two separate reactors on the same frame. The reactor is easy to wind and knit to any length. The super Serpentine reactors will be discussed in detail later in this chapter.

3.2.4.3.4 Normal packed tubes

The behaviour of packed reactors is a well known in chromatography . The ratio, τ = tube diameter : particle diameter is a useful parameter to describe dispersion. For τ between 5 and

50 the axial dispersion is directly related to the particle size, the smaller the particle diameter, the smaller the dispersion. A major drawback though of this type of reactor results from the hydrodynamic resistance of the system, requiring high pressures and hence a technical sophistication.

3.2.4.3.5 Single bead string reactor

The single bead string reactor (SBSR) consists of ordinary Teflon tubes packed with tiny glass beads having diameters that are 60 - 80% of that of the tube. The chief effect of the beads is to increase radial dispersion, which reduces dilution of sample in the flow line, and therefore decreases dispersion [3]. This reactor provides several advantages, e.g. a significantly high sampling rate and dispersion that is approximately one -tenth of that corresponding to open tubes with the same dimensions. It does though also have certain disadvantages namely that small air bubbles and solid particles tend to be trapped in the SBSR, which may increase carry-over and flow resistance.

3.2.4.3.6 Mixing chamber

A mixing chamber with a magnetic stirrer is sought to achieve homogeneous mixing of sample and reagent. It has been shown that the mixing chamber contributes considerably to increasing dispersion zones both in FIA [11] and SIA [7, 8, 15] when introduced in the flow conduit. Růžička *et al.* [11] drew following conclusion regarding the use of a mixing chamber:

"Rule 4. Any continuous flow system that includes a mixing chamber generates larger

dispersion and yields a lower meuasurement sensitivity than a corresponding channel without a mixing chamber. A system with mixing chamber will also have a lower sampling frequency, unless the pumping rates are increased, which, in turn, requires large sample and reagent volumes."

The use of a mixing chamber is justified for the following reasons: first, substantial variations of injected volume, hold-up volume of the chamber and flow rate do not adversely affect the precision over a large dynamic range of dispersion coefficients (D up to 2000) [11]. The sample conditioning (density, viscosity, ionic strength, buffer capacity, etc.) is very efficient, because active stirring provides better compensation of matrix effects than the confluence technique commonly used with tubular reactors.

3.3 Super Serpentine reactors

3.3.1 Introduction

The super Serpentine reactor has four stitch patterns, hence super Serpentine I, super Serpentine II, super Serpentine III and super Serpentine IV (Figs. 3.3 -3.6). The stitch patterns have been designed (Global FIA) for optimum radial dispersion with minimal axial dispersion. It is intended for applications, such as trace analysis where high sensitivity and high sample throughput is desired. It provides the most narrow and highest peaks compared to Serpentine 8 reactors. It can be custom made to any length [17]. Marshall and van Staden [12] investigated the influence of pump speed, tubing diameter, reactor tube geometry and order of reagent and

sample zone injection on dispersion in the SIA manifold. Although Marshall and van Staden [12] studied the influence of the holding coil and reactor length have on dispersion, it was van Staden and Botha [7, 15] who made an in depth study thereof by also including their internal diameters. They [7, 15] also included flow rate, sample and reagent zone volumes. Gübeli *et al.* [13] also carried out studies on the effect of certain operational parameters on the dispersion in a SIA conduit. Van Staden and McCormack also investigated SBSR [16] as well as mixing chambers [8] for sensitivity and precision.

The objective of this study was to investigate the effect or influence reactor type and lengths have on sensitivity and precision [17]. Hence six reactors, straight tubes, helically coiled tubes, super Serpentines I, II, II and IV were investigated and their peaks overlayed for comparative studies. A Tiron-iron(III) complex solution was used. The dispersion profiles obtained were key to the results that follow in this Chapter.

3.3.2 Experimental

In this section the reagents and reactor preparations, instrumentation as well as procedure will be discussed.

3.3.2.1 Reagents and solutions

All reagents were prepared from analytical reagent grade unless specified otherwise. All aqueous solutions were prepared using de-ionised water from a Modulab system (Continental Water System, San Antonio, Texas).

3.3.2.1.1 Stock Iron(III) solution

A 7.2340 g of iron (III) nitrate [$Fe(NO_3)_3.9H_2O$] was dissolved in 0.01 mol/ℓ of perchloric acid. and made up to a litre. Working standards were prepared by suitable dilution of the stock solution with 0.01 mol/ℓ perchloric acid solution.

3.3.2.1.2 Perchloric acid solution

A 0.01 mol/ℓ perchloric acid solution was prepared by diluting 4.4 m ℓ of $HClO_4$ (Merck, GPR 70%) to 5 ℓ with double deionised water. The 0.01 mol/ℓ perchloric acid solution was also used as carrier.

3.3.2.1.3 Tiron solution

A 0.1 mol/ℓ Tiron (4,5-dihydroxy-1,3-benzene disulfonic acid) stock solution was prepared by dissolving 3.3120 g of Tiron in 100 mℓof a 0.01 mol/ℓ perchloric acid solution. A 0.025 mol/ℓ Tiron solution was prepared by suitable dilution of the stock solution with 0.01 mol/ℓ perchloric acid solution.

3.3.2.2 Reactor preparation

The super Serpentine reactors were made in house from FEP tubing obtained from Global FIA. The platens on which the tubings were knitted were purchased from a local electronic shop (Pretoria, South Africa). The super Serpentine I stitch pattern is similar to a knotted membrane

reactor with "all overhand knots". Each repetitive stitch is horizontally joined.

Fig. 3.3 A diagram of a super Serpentine I stitch pattern

Super Serpentine II is similar to a knotted membrane reactor with alternating "overhand and underhand knots". Each repetitive stitch pattern is diagonally joined.

Fig. 3.4 A diagram of a super Serpentine II Stitch pattern

Super Serpentine III and IV do not really have a knotted reactor, however their unit stitch patterns are twice the size of the unit stitch pattern of super Serpentine II. They have knotted reactors with alternating outer and underhand knots.

To form a single unit stitch pattern of super Serpentine III, two units of super Serpentine II were horizontally joined. To form a single unit stitch pattern of super Serpentine IV, two units stitch pattern of super Serpentine III were diagonally joined.

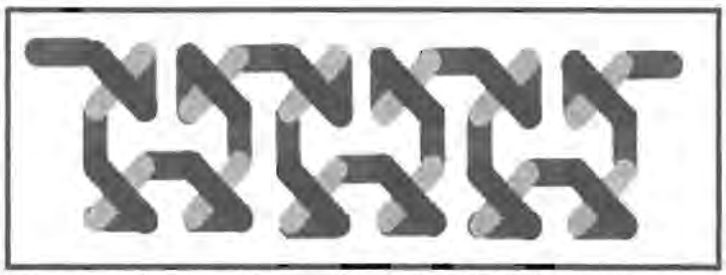

Fig. 3.5 A diagram of a super Serpentine III stitch pattern

To build a specific length of super Serpentine III, each stitch pattern unit of super Serpentine III was repetitively joined from inside to the outside alternately. To build a specific length of super Serpentine IV, each stitch pattern unit of super Serpentine IV was repetitively joined from outside.

Fig. 3.6 A diagram of a super Serpentine IV stitch pattern

3.3.2.3 Instrumentation

The sequential injection system depicted in Fig. 3.7A was constructed from the following components: A Gilson minipuls peristaltic pump (Model M 312, Gilson, Villiers-le-bel, France); a 10-port electrically actuated selection valve (Mode ECSDIOP; Valco Instrument, Houston,

Texas); and a Unicam 8625 UV/VIS spectrometer equipped with a 10 mm Hellma-type (Hellma GmbH and Co., Mülheim/Baden, Germany) flow-through cell (volume 80 $\mu\ell$) for absorbance measurements. The absorbance of the Tiron-iron (III) complex was measured at 667 nm.

The holding coil was of 3.0 m x 0.76 mm internal diameter coiled Tygon tubing. The reactors were: a straight tube, a coiled tube and super Serpentine I, II, III, and IV of various length (50 cm; 60 cm; 80 cm and 90 cm) constructed from a 0.76 mm inner diameter FEP tubing.

Computer aided flow analysis was carried out using a general purpose analogue and a digital input/output PC30-B interface board (Eagle Electric, Cape Town, South Africa) and a FlowTEK [17] software package (obtainable from Mintek) for computer-aided flow analysis was used throughout for device control and data acquisition.

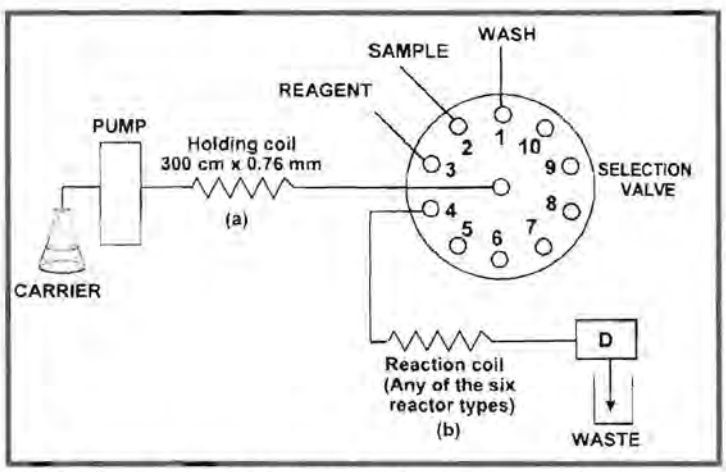

Fig. 3.7A A sequential injection analyses system used.

3.3.2.4 Procedure

Six reactor types were used in the SIA system. The carrier stream was a 0.01 mol/ℓ perchloric acid. The sample solution was iron (III) and the reagent Tiron. The concentration of both sample and reagent were kept constant during the whole process. The sample/reagent volume ratio was 1:1.25.

The experimental work was carried out by first drawing the wash solution (deionised water) followed by the sample solution [iron(III)] and then, the reagent solution (Tiron). These were flushed to the detector by the carrier (0.01 mol/mol/ℓ perchloric acid). The iron (III)-Tiron complex was detected at 667 nm using a UV/VIS spectrometer. This wave length was the maximum obtained when the solution was scanned between 100 and 1100 nm. The device sequence is shown in Fig. 3.7B and Table 3.2.

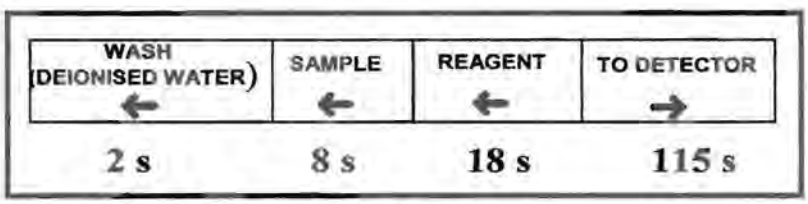

Fig. 3.7B A device sequence for one cycle.

The experiments were performed with the reactors incorporated in one of the two positions in the SI manifold shown in Fig. 3.7A. The two positions were: (a) between the selection valve and the pump, replacing the normal holding coil and (b) before the detector, replacing the normal

reaction coil between the valve and the detector. In position (a) the sample and reagent zones were stacked into the reactor as is the case with the normal holding coil. In position (b) the selection valve is switched to the detector and due to flow reversal the stack of zones from the holding coil mutually disperse and penetrate on their way to the detector. Four different flow rates were investigated (0.6; 1.2; 2.2 and 4.2 mℓ/min)

TABLE 3.2 Device sequence for one cycle

Time (s)	Pump	Valve	Description
0	Off	Position 1	Pump off. Select wash solution.
1	Reverse		Draw up wash solution.
3	Off		Pump stop.
4	Off	Position 2	Select sample stream.
5	Reverse		Draw up sample.
13	Off		Pump stop.
14	Off	Position 3	Select reagent stream. Valve
15	Reverse		Draw up reagent.
33	Off		Pump stop
34	Off	Position 4	Select detector line.
35	Forward		Pump all zones to detector.
150	Off	Position 1	Valve return home

3.3.3 Results and discussion

When studying sensitivity in SIA, the degree of sensitivity can easily be approximated by using the response which manifest itself in peak heights. It is known from FIA that the degree of

dispersion that occurs in an FIA flow conduit is equal to the inverse of the peak height. This means that the longer the peak height the smaller the resultant dispersion. Since SIA is seen as an extension of FIA, the same conclusion regarding the relationship between peak height and dispersion can be applied. Thus, by studying the resultant peak heights obtained, it becomes possible to make certain conclusions regarding sensitivity. The precision of the results was measured by determining the relative standard deviation of ten measurements at a given concentration of the iron (III)-Tiron complex.

The response and precision were studied as a function of length and reactor type using an iron (III)-Tiron complex. The results were the mean of 10 measurements. An investigation showed that no significant difference in the response was obtained for the different type of reactors when incorporated into position (a) between the selection valve and the pump. The results, however, showed that the reactor type had an influence on sensitivity when placed before the detector.

3.3.3.1 Influence of reactor type on ***sensitivity and precision***

Figs. 3.8A - 3.11D show the overlay of peaks that was investigated for sensitivity and precision. When each reactor type was considered separately, there was a general decrease insensitivity with increase in flow rate. The high response obtained at the highest flow rates corresponded to sharp peaks. This confirmed work already done [6, 11, 14]. However, when the six reactor types were compared to one another(overlay of peaks) for a given reactor length there was no definite pattern with the change in sensitivity with increase in flow rate. The reactor that gave the best response at the lowest flow rate (compared to other types of the same length), did not necessarily maintain that as flow rate increased. The behaviour of the different types of reactors

was first grouped according to reactor length and the observation accordingly discussed below for each reactor length.

3.3.3.1.1 50 cm reactors (Figs. 3.8A- 3.8D)

Figs. 3.8A to 3.8D shows the overlay of peaks for 50 cm reactors at flow rates of 0.6, 1.2, 2.2 and 4.2 mℓ/min respectively. The results show clearly that for the lower flow rates (0.6 mℓ/min, Fig. 3.8A; 1.2 mℓ/min, Fig. 3.8B) super Serpentine IV reactor gave the best response.

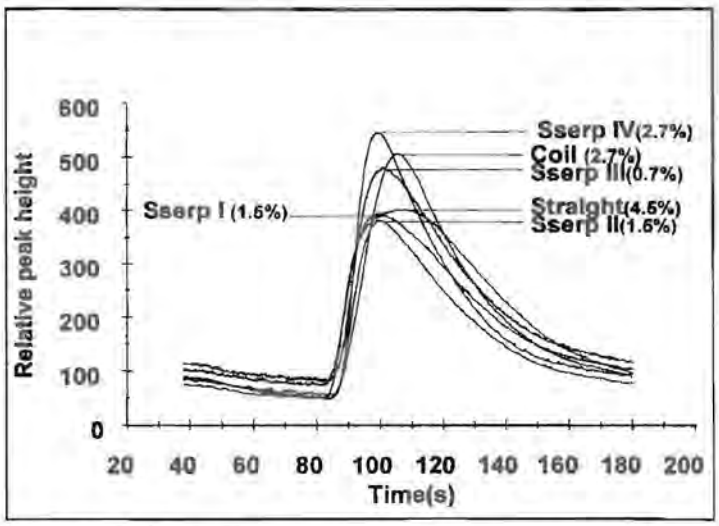

Fig. 3.8A Influence of 50 cm reactor types on response and precision at 0.6 mℓ/min

However, at 0.6 mℓ/min (Fig. 3.8A) super Serpentine III gave the best precision. When the flow rate was increased to 1.2 mℓ/min the precision of all reactors improved (Fig. 3.8B), with super Serpentine I giving the best precision.

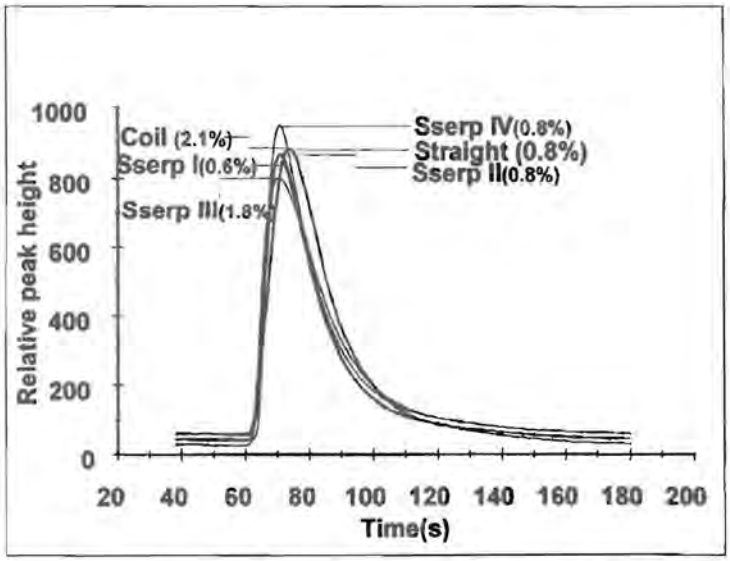

Fig. 3.8B Influence of 50 cm reactor types on response and precision at 1.2 mℓ/min

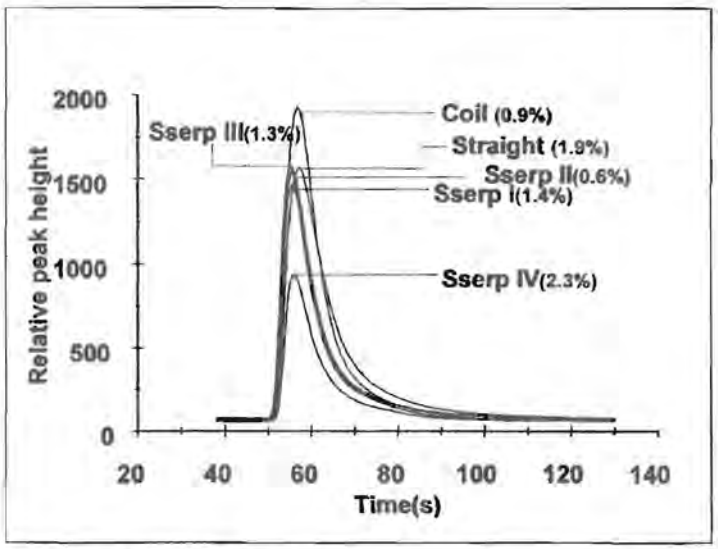

Fig. 3.8C Influence of 50 cm reactor types on response and precision at 2.2 mℓ/min.

At a flow rate of 2.2 mℓ/min (Fig. 3.8C) and 4.2 mℓ/min (Fig. 3.8D), it was the coiled tube reactor that gave the best response. It was, however, super Serpentine II (Fig. 3.8C) and super Serpentine III (Fig. 3.8D) that gave the best precision respectively. From these observations it is clear that super Serpentine III was on average the best reactor for this length. However, super Serpentine IV emerged the best at a flow rate of 1.2 mℓ/min in both precision and response.

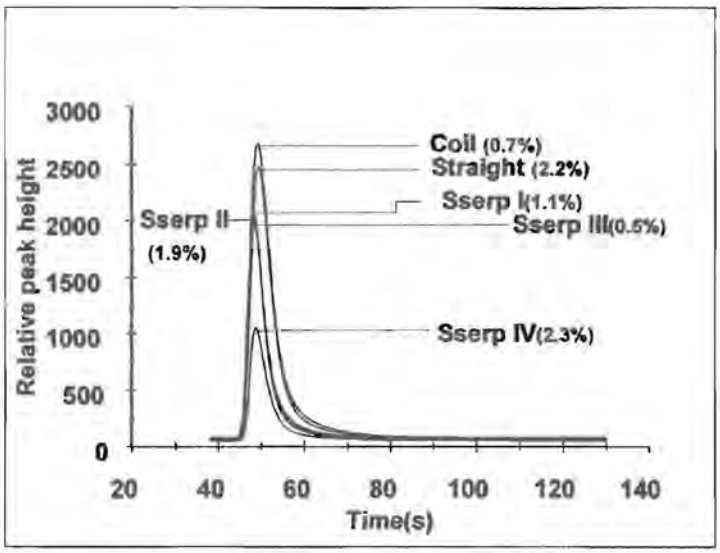

Fig.3.8D Influence of 50 cm reactor type on response and precision at 4.2 mℓ/min.

3.3.3.1.2 60 cm reactors (Figs. 3.9A-3.9D)

Figs. 3.9A to 3.9D shows the overlay of peaks for 60 cm reactors at flow rates 0.6, 1.2, 2.2 and 4.2 mℓ/min respectively. It is clear from the results obtained (Figs. 3.9A- 3.9D) that super Serpentine IV is by far the most reliable reactor with the best precision for the 60 cm reactor at flow rates between 0.6 and 4.2 mℓ/min. At flow rates of 0.6 and 1.2 mℓ/min, super Serpentine II

gave the best response, but a bad precision. On the other hand, super Serpentine IV gave a better precision (Figs. 3.9A and 3.9B).

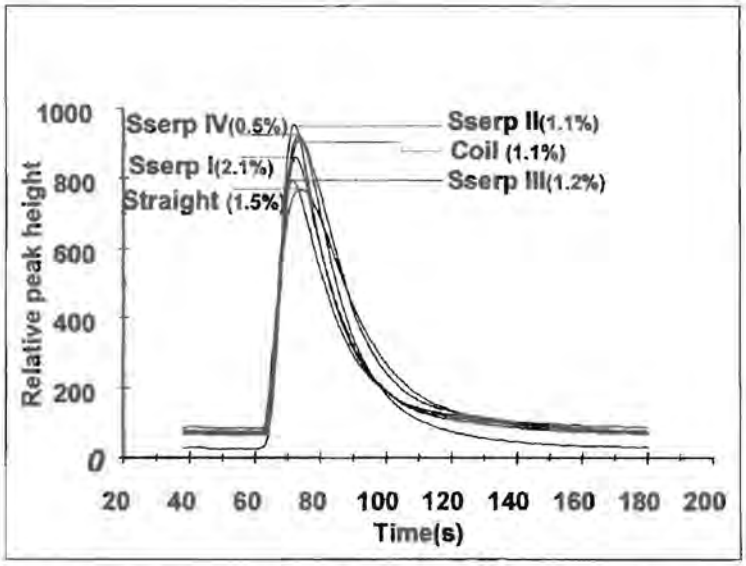

Fig. 3.9A Influence of 60 cm reactor types on response and precision at 0.6 mℓ/min.

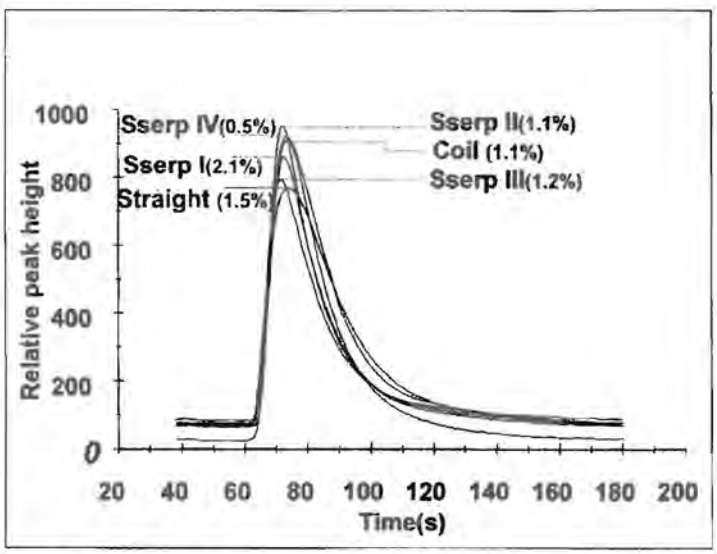

Fig. 3.9B Influence of 60 cm reactor types on response and precision at 1.2 mℓ/min.

At a flow rate of 2.2 mℓ/min, the coiled tube reactor gave the best response. However, it was super Serpentine IV with the second best response that gave the best precision (Fig. 3.9C).

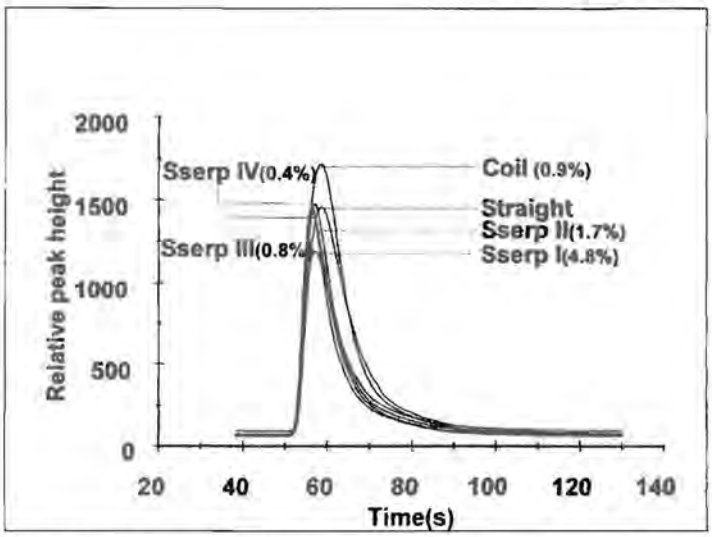

Fig. 3.9C Influence of 60 cm reactor types on response and precision at 2.2 mℓ/min.

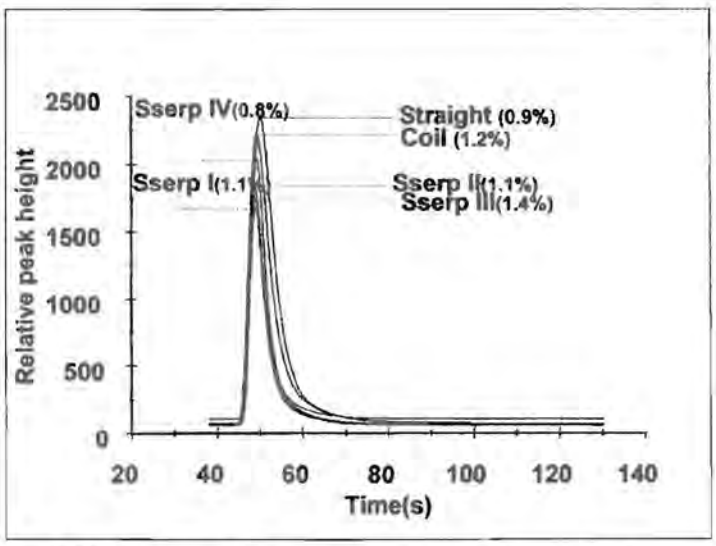

Fig. 3.9D Influence of 60 cm reactor types on response and precision at 4.2 mℓ/min.

When the flow rate was increased to 4.2 mℓ/min, the best response came from the straight tube reactor and the best precision from super Serpentine IV (Fig. 3.9D).

3.3.3.1.3 80 cm reactor (Figs. 3.10A-3.10D)

Figs.3.10A to 3.10D shows the overlay of peaks for 80 cm reactors at flow rates 0.6, 1.2, 2.2 and 4.2 mℓ/min respectively. Super Serpentine IV gave the best response at a flow rate of 0.6 mℓ/min. However, the percent relative standard deviation (%RSD) for all the reactors at this flow rate was above 0.9% (Fig. 3.10A).

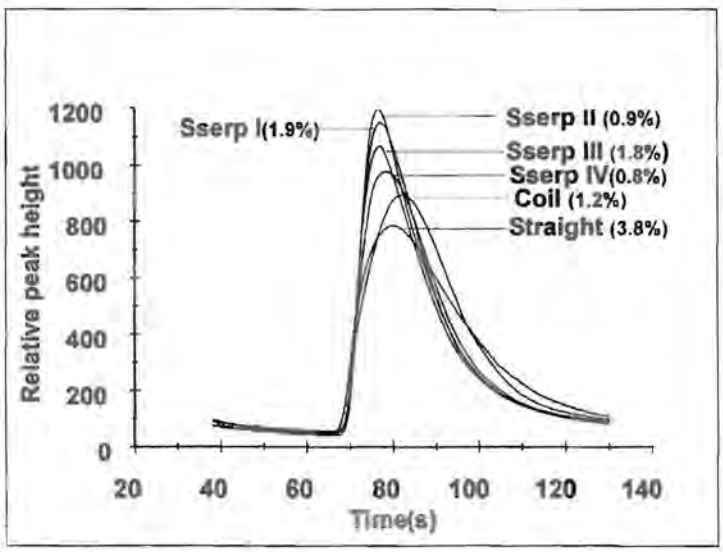

Fig. 3.10A Influence of 80 cm reactor types on response and precision at 1.2 mℓ/min.

When the flow rate was increased to 1.2 mℓ/min, super Serpentine II gave the best response (Fig. 3.10B). When the flow rate was increased to 2.2 mℓ/min, the coiled tube reactor gave the best response (Fig. 3.10C). At a flow rate of 4.2 mℓ/min, the straight tube reactor gave the best

response and super Serpentine III gave the best precision (Fig. 3.10D).

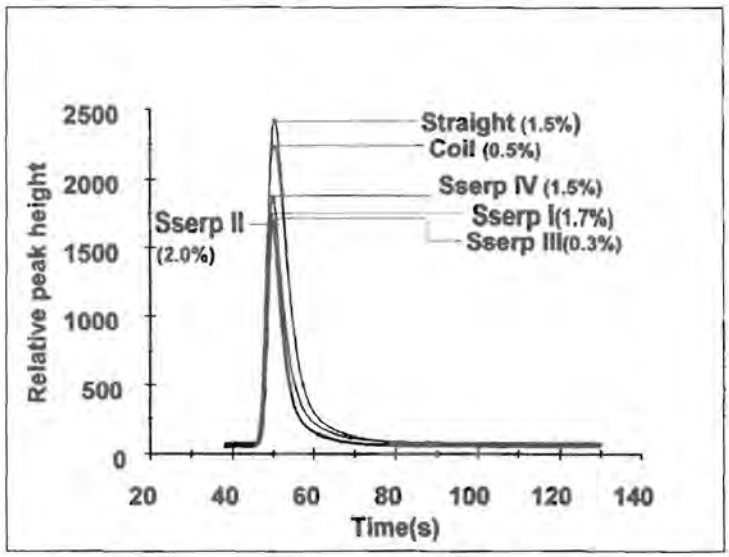

Fig. 3.10B Influence of 80 cm reactor types on response and precision at 1.2 mℓ/min.

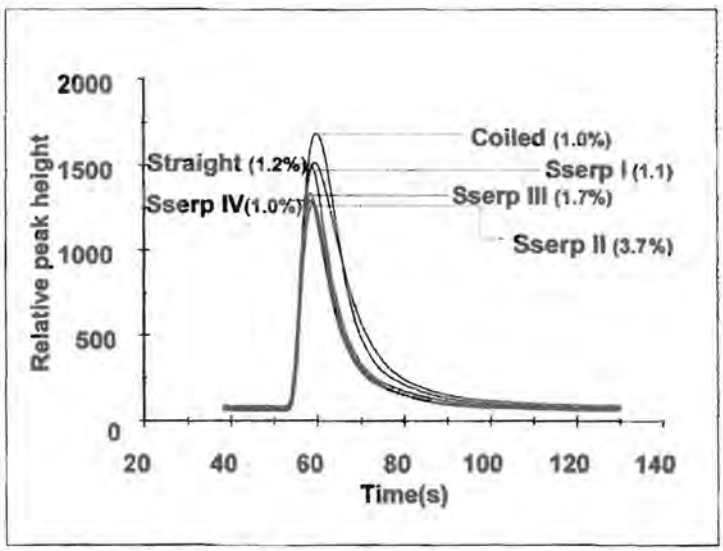

Fig. 3.10C Influence of 80 cm reactor types on response and precision at 2.2 mℓ/min.

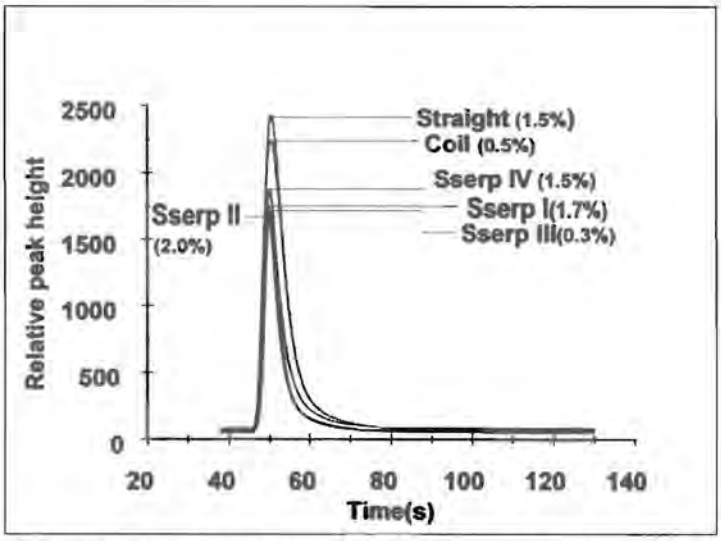

Fig. 3.10D Influence of 80 cm reactor on response and precision at 4.2 mℓ/min.

3.3.3.1.4 90 cm reactor (Figs. 3.11A -3.11D)

Figs. 3.11A to 3.11D shows the overlay of peaks for 90 cm reactors at flow rates 0.6, 1.2, 2.2 and 4.2 mℓ/min respectively. At a flow rate of 0.6 mℓ/min, super Serpentine III gave the best response and super Serpentine I gave the best precision (Fig3.11A). When the flow rate was increased to 1.2 mℓ/min super Serpentine II gave the best response and the coiled tube reactor the best precision (Fig. 3.11B).

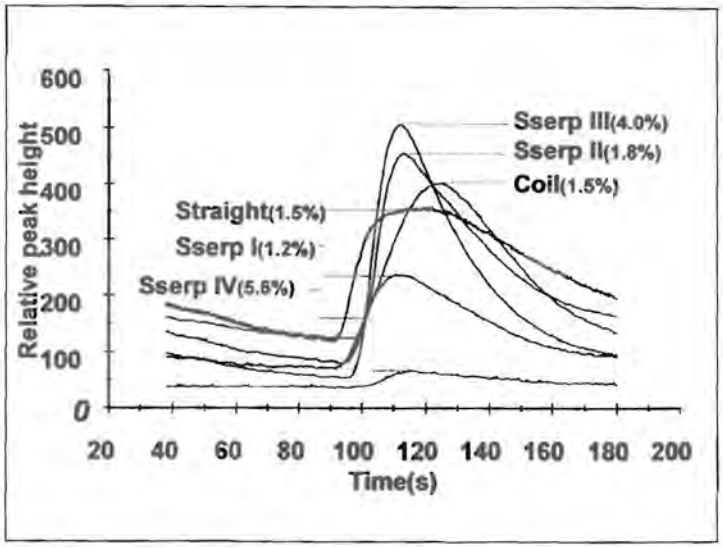

Fig. 3.11A Influence of 90 cm reactor types on response and precision at5 0.6 mℓ/min.

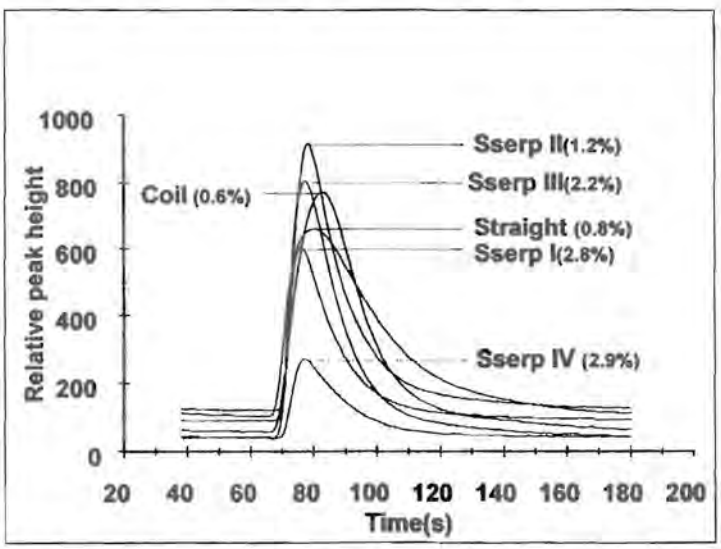

Fig. 3.11B Influence of 90 cm reactor types on response and precision at 1.2 mℓ/min.

At a flow rate of 2.2 mℓ/min the coiled tube reactor gave the best response, while super Serpentine

I gave the best precision (Fig 3.11C). When the flow rate was increased to 4.2 mℓ/min the straight tube reactor gave the best response (Fig. 3.11D).

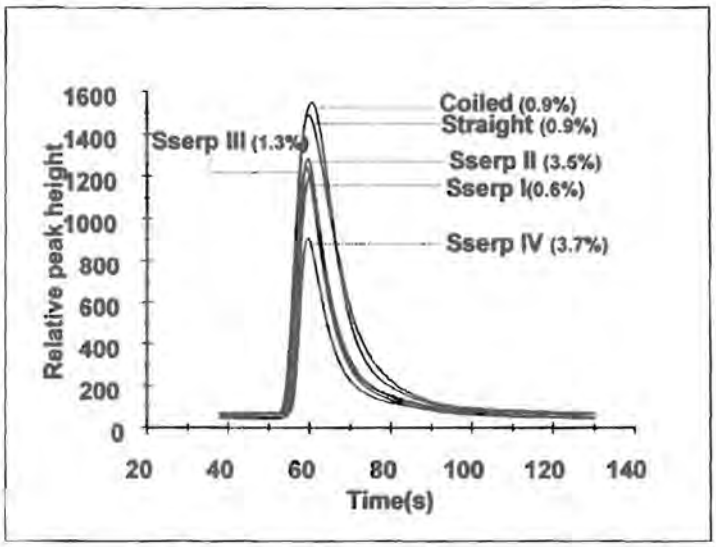

Fig. 3.11C Influence of 90 cm reactors on response and precision at 2.2 mℓ/min.

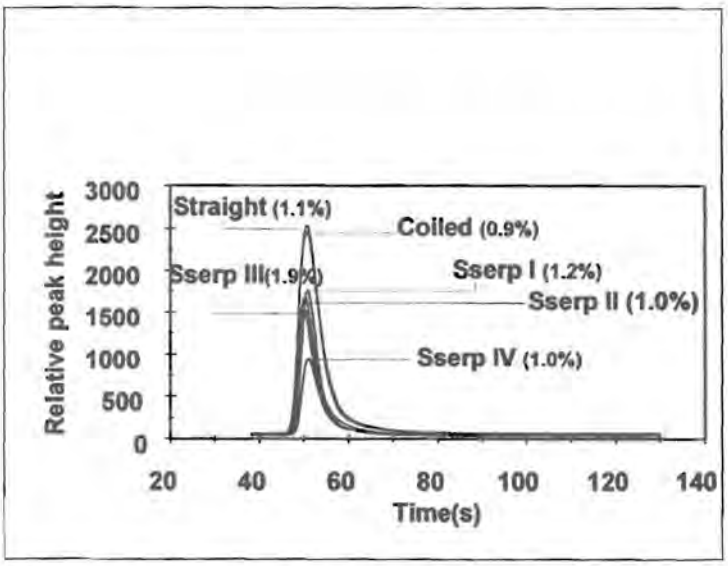

Fig. 3.11D Influence of 90 cm reactor types on response and precision at 4.2 mℓ/min.

Despite all these, the precision shown by super Serpentines was very good except for super Serpentine III where %RSD was close to 2%.

3.4 Conclusion

When the six reactor types of the same lengths were compared by overlaying their peaks, no consistency was observed with increase in the flow rate. The response from each reactor type also differed at different flow rates. However, some reactors did show some consistency just for two consecutive flow rates. The reactor with the highest response did not necessarily give the best precision.

Furthermore, when overlaying peaks of each super Serpentine of different lengths at a given flow rate, there was no clear correlation between the response obtained and the reactor length. Similar observations were made with the precision.

The overlayed peaks revealed that the longest super Serpentine reactors gave the highest response at the lowest flow rate. The shortest super Serpentine reactors gave the highest response at the highest flow rates with a relatively good precision.

From all these, it may be said that the choice of a suitable super Serpentine reactor for the development of method for trace analysis is important. A specific reactor has to be defined with regard to length and flow rate at the same time. Super Serpentine reactors were intended for applications such as trace analysis where high sensitivity and /or high throughput is desired

(Global FIA). Thus one has to know the type of trace analyte intended, throughput, sensitivity and precision so desired to effectively accomplish the analysis. Hence the simultaneous choice of reactor type and length plays an important role with regard to sensitivity and precision and hence dispersion. The sensitivity and precision obtained for the various super Serpentines may with proper choice of the reactor accomplish this objective.

3.5 References

1. J. Růžička and E. H. Hansen and E. A. Zagato, **Anal. Chim. Acta, 88** (1977) 1.
2. J. Růžička and E. H. Hansen, **Anal. Chim. Acta, 99** (1998) 37.
3. M. Valcàrcel and M. D. Luque de Castro, **Flow Injection Analysis: Principles and Application**, Horwood,Chichester, 1987.
4. E. Pungor, Z. Fehèr, G. Nagy, Tóth, G. Horvaiand M. Gratzi, **Anal. Chim. Acta**, 109 (1979)1.
5. M. Guzman, C. Pollema, J. Růžička and G.D. Christian, **Talanta, 40** (1993) 81.
6. M. Gisin, C. Thommen and K. F. Mansfield, **Anal. Chim. Acta, 179** (1986) 149.
7. J. F. van Staden and A. Botha, **S. Afr. J. Chem., 51 (2)** (1998) 100.
8. T. McCormack and. F. van Staden, **Anal. Chim. Acta, 367(1-3)** (1998) 111.
9. G. E. Pacey, **Handb. Chem. Biol. Sens.**, (1996) 515.
10. B. Karlberg and G. Pacey, **Flow Injection Analysis: A practical guide**, Elsevier, Amsterdam, 1989.
11. J. Růžička and E. H. Hansen, **Flow Injection Analysis, 2nd ed.**, Wiley & Sons, New York, 1988.
12. G. D. Marshall and J. F. van Staden, **Process Control and quality, 3 (1-40** (1992) 251.
13. T. Gübeli, G. D. Christian and J. Růžička, **Anal.Chem., 63 (21)** (1991) 240.
14. R. E. Taljaard, **Applications of Sequential Injection Analysis as Process Analyzer**. M.Sc-Thesis , University of Pretoria, 1996.
15. A. Botha, **Sequential Injection Analysis: Evaluation of Operational Parameters and Application to Process Analytical Systems**, M.Sc-Thesis, University of Pretoria,1999.
16. J. F. van Staden and T. McCormack, **Instrum. Sci. & Technol., 27 (3)** (1999)107.

17. G. D. Marshall and J. F. van Staden, **Anal. Instrum., 20** (1992) 79.

18. J. F. Van Staden and E. B. Naidoo , **Instrum. Sci. & Techn., 29 (2)** (2001) 77.

CHAPTER 4

Solid-phase reactors

4.1 Introduction

The introduction of solid-phase reactors in flow systems represents a high achievement for on-line determination of different substances [1,2]. The development of the system in flow injection analysis (FIA) and lately in sequential injection analysis (SIA) has revolutionalised flow systems.

There are various types of solid-phase reactors which have been developed. The type dictates the purpose for which it is intended. The solid-phase reactors developed to date are enzymatic, immuno-assay, ion-exchange, redox, absorbent extractors or reagent releasers. In all these the concept of immobilization still leads.

The use of reagents, particularly enzymes in the solid-phase has been known from the early part of the 20th century. These enzymes where immobilized on a variety of support materials for a number of reasons [3].

The use of these immobilized reagents thus offered a greater degree of control over the relevant reactions. These type of heterogeneous reactions have been converted for use in FIA with some success [4,5]. In addition to the excellent analytical features already available with the incorporation of solid-phase reactors in FIA, further advantages with respect to miniaturization, sample reduction, efficiency and cost reduction can be expected from SIA.

Different types of immobilization techniques for solid-phase reactors are described in this Chapter, along with the shapes and designs of reactors used, the location of the reactor in the system manifold in both FIA and SIA are given. The various applications are also given for both FIA and SIA.

The FIA methodology using a solid-phase reactor has advanced remarkably and its adaptation to SIA is already gaining momentum and is expected to enhance and improve this technique to such an extent that almost any analyte can be determined, especially with regard to the most expensive, slightly soluble and insoluble ones.

4.2 Reactor types and preparation

The approach in the preparation of solid-phase reactors is dictated by its nature and the analytical purpose of its immobilization. There are various ways in which these reactors can be designed and hence, the name for each reactor is related to the type of material it is made of. Solid-phase reactors can be classified into two distinct groups, namely reactors in which a chemical reaction takes place to derivatise the analyte and reactors in which no derivatising reaction takes place. The first group includes, among others, enzyme reactors while the second group consists mostly of reactors used for pre-concentration.

4.2.1 Derivatising reactors

4.2.1.1 Redox reactors

Redox reactors are prepared by packing the micro or mini columns with redox material. The material may be dry or a slurry of the reagent. When immobilized, it is allowed to be trapped while the polymer is forming and hardening to form oxidizing beds. This type of reactor employs a string of oxidizing (e.g. MnO_2 or PbO_2) [6,7] or reducing agent [5,8,9], which reacts with the analyte of importance to either render it in a suitable oxidation state for further reaction or for direct detection. The driving force for this type of reactor is the reduction or oxidation potential of the immobilized reagent. For the determination of nitrate the cadmium metal acted as a reductor in the following equation:

$$Cd\ (s) + NO_3\ (aq) + H_2O\ (\ell) \rightleftharpoons Cd^{2+}\ (aq) + NO^-_2\ (aq) + 2\ OH^-\ (aq)\ ;\quad E_0 = 6.402\ V$$

Redox reactors are also used to prepare analytes for enzyme immobilization.

4.2.1.2 Complex-forming reactors

The complex formation reactors are prepared by packing the column with a finely divided reagent. In this case the complexing agent, or ligand, is immobilized and reacts selectively with the metal analyte of importance when the latter moves through the reactor [10]. A typical

reaction that may be used is:

$$Fe^{3+}(aq) + Tiron^{2-}(s) \Leftrightarrow [Fe(Tiron)]^{+}(aq)$$

In this case the tiron (1,2 - dihydroxybenzene- 3, 5 - disulphonate) is in the reactor and reacts when the iron passes through. This reaction takes place in acidic medium. The resulting complex can be detected spectrophotometrically at the wavelength of maximum absorption. This reactor works on the premises that the formation constant of the complex is high enough to overcome the interactive forces between the ligand and the support material, whether it be ionic or polar-polar interaction.

4.2.1.3 Precipitating reactors

This type of reactor is ideally suited for the indirect determination of anions. A very slightly soluble compound is immobilized in the reactor and reacts with the analyte to form an even less soluble compound, releasing more soluble ion into the carrier stream [11]. This ion should then be in an easily detectable state, for example chromate or dichromate whose absorbance is measured directly. A typical reaction that takes place is the following:

$$BaCrO_4(s) + SO_4^{2-}(aq) \rightarrow BaSO_4(s) + CrO_4^{2-}(aq)$$

The solubility product of the analyte with different counter-ions plays an important role in developing a method incorporating this type of reactor. In this case the solubility product for $BaCrO_4$ ($K_{sp} = 2.4 \times 10^{-10}$) is higher than that for $BaSO_4$ ($K_{sp} = 1.1 \times 10^{-10}$) and the latter would

thus precipitate, releasing the chromate into the carrier stream. The sulphate content of a sample can be indirectly determined in this fashion [11].

4.2.1.4 Enzyme reactors

Enzymes are extremely efficient biological catalysts that can increase the rate of some occasionally very complex chemical reactors by a few orders of magnitude. Many reactors would be analytically useless in the absence of enzymes. Enzyme reactors are prepared by enzymes immobilized on suitable supports; particularly controlled-pore glass (CPG). The CPG provides support of readily available particle size, pore diameter and specific surface area. Silica excel over organic polymers.

Technology for enzyme catalysed reactions for use in flow systems is also quite well known and these reactors comprise most of the solid-phase reactors currently in use [4,5,12,13]. The specificity of enzyme reactors ensure that there are few, if any, interferences for a given method and thus also reduce the enzyme consumption, which is an important factor when the high cost of enzymes are considered.

A reaction consisting of four steps for the determination of inosine in human blood plasma is given below as an example of the simplicity and specificity possible with immobilized enzyme reactors in flow injection systems. The reaction that takes place is the following:

$$\text{Inosine} \xrightarrow{PNP} \text{hypoxanthine} \xrightarrow{XOD} \text{xanthine} \xrightarrow{XOD} \text{uric acid} \xrightarrow{UOD} \text{alantoin}$$

where PNP = purine nudeoside phosphorylase

XOD = xanthine oxidase

and UOD = urate oxidase

In the last three steps of the above reaction hydrogen peroxide is evolved, which then reacts with K - (P-hydroxyphenyl) propionic acid (HPPA) in a horseradish peroxidase (HRP) mediated step to form a fluorosphore compound which can be detected fluorimetrically [4]. A diagram of the FIA system is given in Fig. 4.1 which can easily be adapted to an SIA system as postvalve location.

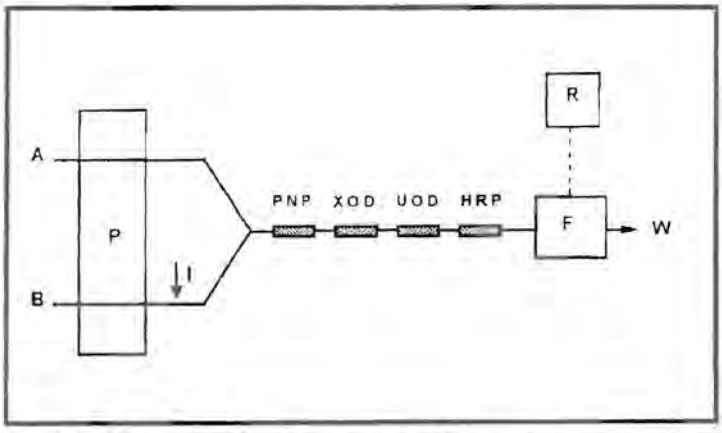

Fig. 4.1 Enzyme catalysed reaction in a flow system

In Fig. 4.1, **A** = HPPA; **P** = Peristaltic pump; **I** = Point of sample injection; **F** = Fluorescence detector; **R** = Recorder and **W** = Waste.

4.2.1.5 Immunoassay

The application of flow injection analysis (FIA) to immunology offers promise of faster and

more reproducible assays. It was found to be advantageous in that it is possible to utilize the kinetics of immunochemical binding. It uses immobilized reactors which binds the species of interest while allowing the rest of the matrix to pass through the reactor.

The bead injection (BI) is introduced as a novel flow system especially for immunoassay. The BI can be traced back to early literature of FIA. It was however, the SI technique that made it possible to handle suspended beads with precision and reliability. The introduction of BI resulted in an improvement to the SI system where in-line regeneration drawbacks were avoided. Other advantages of BI include improved assay sensitivity, because the use of surface bounded reagents minimizes sample dilution, lower limits of detection (because the analyte can accumulate on the beads) [14]. The detection method typically involves a tag such as an enzyme, radioisotope or fluoropore to monitor the reaction with a variety of detectors.

4.2.2 Non-derivatising reactors

4.2.2.1 Adsorptive reactors

The most commonly used material for packing adsorptive reactors is C18 bonded silica beads and to a lesser extent alumina and silica. Other packing material such as polyurethane foam (PUF) on a mini column are also used. Pre-concentration of metal ions is the most important use for this type of reactor, which consist of an adsorptive material like resins used for HPLC, packed in a conical container with both ends plugged with porous material.

Pre-concentration in a conical shape reactor takes place from the narrow to the wider end in a

conduit, with elution taking place in the opposite direction. The elution of the analyte through a narrow aperture introduces a well-defined sample zone into the carrier stream.

The adsorptive reactor may be used as a flow through sensor for individual as well as multi-element determination [15,16]. These reactors are based on the principle that the adsorptive material is placed in the flow cell of a flow system (FIA/SIA) and retains a product formed in the system for absorbance or reflectance measuring. Multi-element determination was done with the aid of a diode array spectrophotometer.

4.2.2.2 Reagent releaser reactors

Reagent releaser reactors are prepared by packing the reagents in cartridges or bound to resins. These reactors have as their aim the decrease in dispersion of a sample plug by eliminating the merging point in a flow system usually necessary for reagent addition. The reagent is thus added from the solid-phase directly into the sample, where it will release the relevant reagents into the carrier stream. The system is also simplified, as the merging points in the case of more than one reagent usually requires teflon connectors and extra tubing.

4.2.2.3 Beads

Bead injection (BI) is a technique based on the microfluidic manipulation of a precise volume of suspended sepharose beads that serve as a solid-phase carrier for reagents or reactive groups. It is composed of 80% solution and 20% matrix and are highly transparent to light. BI combines the advantages of solid-phase chemistry with the novelty of fluidic handling of microcarrier

beads, allowing automated surface renewal and postanalysis manipulations [116]

4.3 Modes of immobilization

There are three basic types of immobilization, namely natural, physical and chemical.

4.3.1 Natural

This type of immobilization is used when the reagent is naturally very slightly soluble in the relevant medium and the particles are of approximately the desired size and consistency [17]. Large particles can also be ground to the desired size if necessary [11]. Usually one would want the particles as small as possible to have the maximum surface area available for reaction, but this may provide problems as the basic-pressure resulting from usage of such small particles proves too much for normal peristaltic pumps to handle. This type of pump is mostly used in FIA to keep the total Piston-type pumps which can handle higher pressure, but this elevates the total cost. The Gilson mini pulse peristaltic pump is used in SIA. A compromise should be reached between the maximum surface area available with small particles and effective back-pressure produced in the system.

4.3.2 Adsorption

This type of immobilization, is mostly used when the reagent is a polar or even an ionic species [18]. The support for the polar reagent is a corresponding polar compound such as silica or

alumina and for the ionic species, a suitable ionic compound, such as an ion-exchange resin. The reagent is adsorbed onto the polar material either by precipitation, or heating and evaporation of the solvent. Other packing material such as polyurethane foam (PUF) on a mini column are also used. Pre-concentration and separation is the most commonly used function for this reactors.

In Chapters 5 and 8 the adsorption of lead (IV) dioxide onto silica gel is described for use in a redox reactor. There the immobilization was achieved by oxidising an aqueous lead(II) solution with sodium hypochlorite, whereafter a solid precipitate was formed. The precipitate (PbO_2) immediately adsorbed onto the very polar silica gel present in the reaction mixture.

4.3.3 Entrapment

This method is often used for enzyme immobilization when doing pharmaceutical analyses [6,7]. It involves making a slurry of the reagent to be immobilized, and physically "trapping" or encapsulating it in a hardening polymer. Polyester resins are particularly useful in this regard. Martinez Calatayud and Garcia Mateo [7] described the use of a polyester resin to immobilize Copper (II) carbonate. A copper(II) carbonate slurry was stirred together with AL-100-A polyester resin and a small volume of the relevant catalyst added. This mixture was then stirred until it started to harden. The resin with entrapped reagent ($CuCO_3$) could then be ground to the desired size and introduced into a reactor. This method for the immobilization of solid reagents provides a great degree of control over the amount of immobilizes reagent as well as the reagent to support ratio.

4.4 Shape of the reactor/ Reactor design

There are different reactor shapes that are used in FIA but now also in SIA. The shape that the reactor assumes, is indicative of whether a chemical reaction needs to take place or not.

4.4.1 Tubular

The most common reactors used are tubular or cylindrical in shape because of the flow through nature of the method. The reagent, either immobilized on a support material or naturally insoluble, can be packed into the tube, column or cylinder with both ends of the reactor closed off by glass wool or a similar porous inert material. Fig. 4.2 shows a cylindrical reactor that is used in Chapters 6 and 7, while Fig. 4.3 shows a packed tubular reactor used in Chapters 5 and 8.

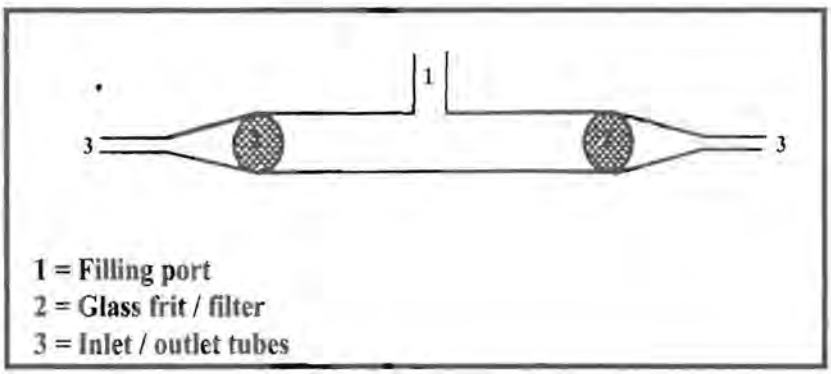

Fig. 4.2 Design of a cylindrical reactor

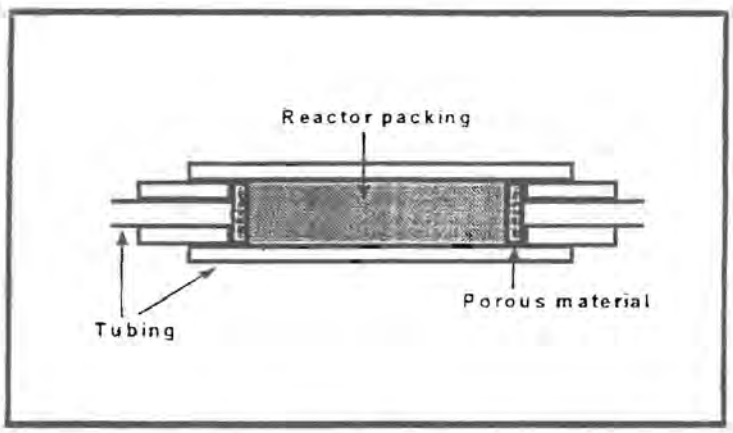

Fig. 4.3 Design of a packed tubular reactor

A open tubular reactor where the reagent is absorbed or impregnated on or in the tube wall is shown in Fig. 4.4. This reactor is less resistant to flow and the activity of its layers is rather low, so very long tubes are required to allow the reaction to proceed to the point at which detection becomes possible.

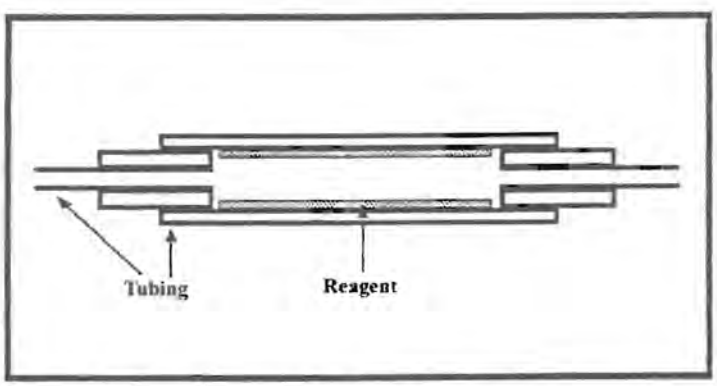

Fig. 4.4 Design of an open tubular reactor

4.4.2 Conical

A typical design of a push-fit conical reactor is shown in Fig. 4.5. The conical reactor is used when constructing pre-concentration reactors and enrichment factors of up to 50 have been achieved with it [19].

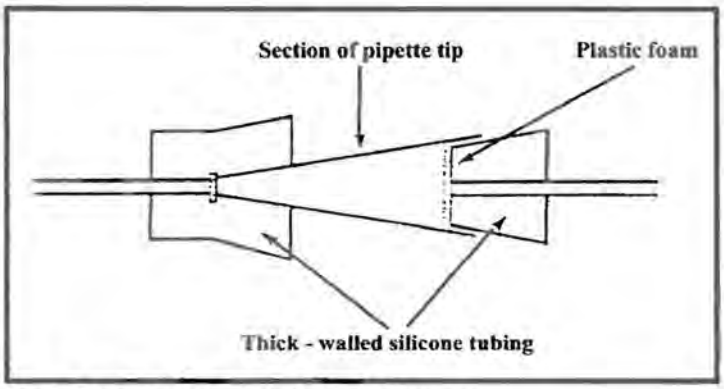

Fig. 4.5 Design of a push-fit conical reactor

The conical shape of a pre-concentration reactor ensures minimum dispersion of the retained analyte on elution, because retention takes place from the narrow to the wider end, while elution takes place in the opposite direction (Thus, elution of the analyte through a narrow aperture introduces a well-defined sample zone into the carrier stream).

A reactor with threaded fitting is shown in Fig. 4.6. This type of reactor can be constructed with push-fit or threaded fittings for coupling to the transmission tubing, with each type of fitting having its own advantages and disadvantages with regard to ease of construction and long term reliability. Reactors with threaded fittings are preferred over push-fit reactors

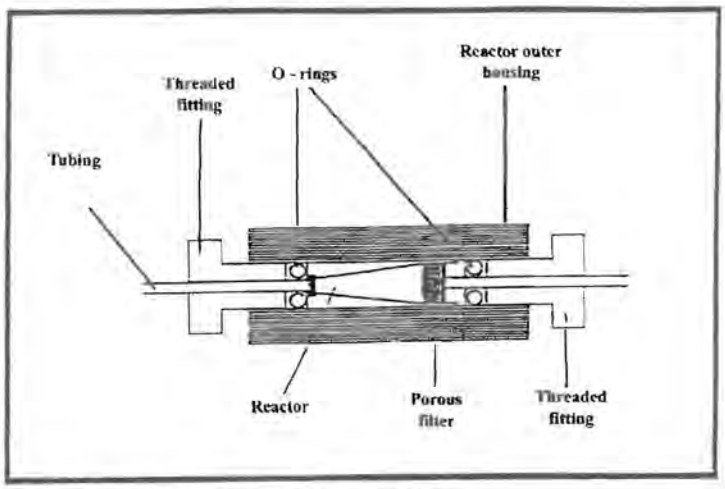

Fig. 4.6 Conical reactor with threaded fittings

4.4.3 Jet ring cell /Beads

Solid-phase titration is a novel technique that uses beads as individual micro-vessels containing a titrant and an indicator [20]. Beads injection (BI) is a novel approach to assays based on liquid-solid interactions.

The technique is based on the micro-fluidic manipulation of a precise volume of suspended beads that serve as a solid-phase carrier for reagents or reactive groups. Fig. 4.7 shows an SI system diagram modified for BI.

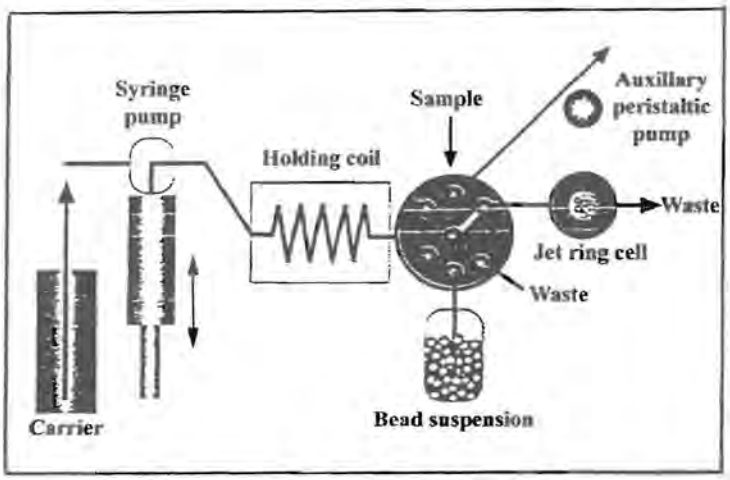

Fig. 4.7 An SIA diagram with beads and a jet ring cell

The use of beads as reagent carrier is restricted to biology, biotechnology and drug discovery in which there is an immediate need for kinetic interaction assays.

4.5 Position of reactor in the system

Reactors can be placed in many different positions along the FIA/SIA manifold depending on their analytical purpose. Illustration for both FIA and SIA system will be given in some cases for clarity.

4.5.1 Pre-valve position for the reactor

Fig. 4.8 and 4.9 show the position of the reactor in the FIA and SIA manifolds respectively.

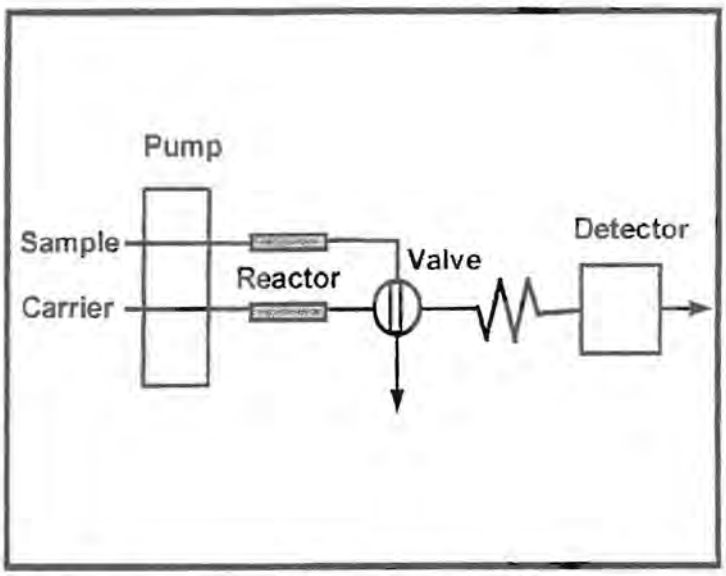

Fig. 4.8 Prevalve position for the reactor in a FIA system

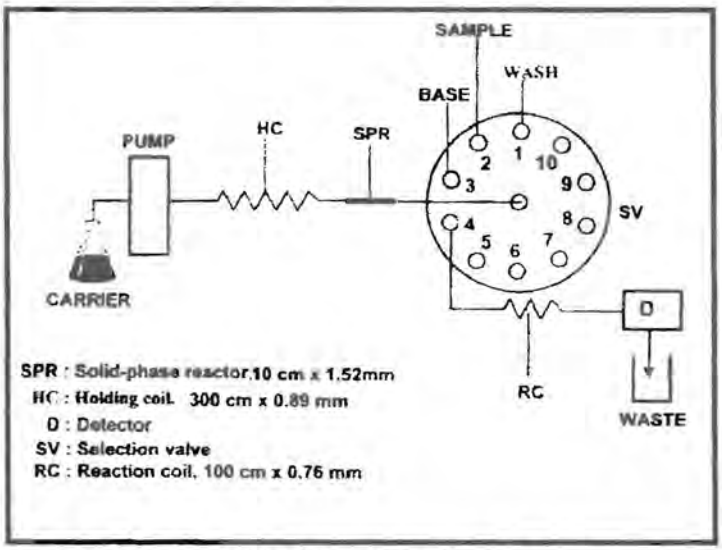

Fig. 4.9 Prevalve position for a reactor in a SIA system

This location is employed when there are impurities in either the carrier or sample stream and the aim is to minimize or remove the impurities. The reactor in this case is usually an adsorptive reactor packed with G8 bonded silica for the removal of less polar components or to a lesser extent, silica or alumina for the removal of more polar compounds. It may also be a redox material where the sample must first be reduced or oxidised before it can react, or combine with any reagent or before it can be propelled to the detector.

4.5.2 Between the injection valve and detector

Any type of reactor can be used in this location for any application, whether it be enzymatic, catalytic, redox, pre-concentration or complexation. The reactor in this case may act as sample converter or reagent releaser.

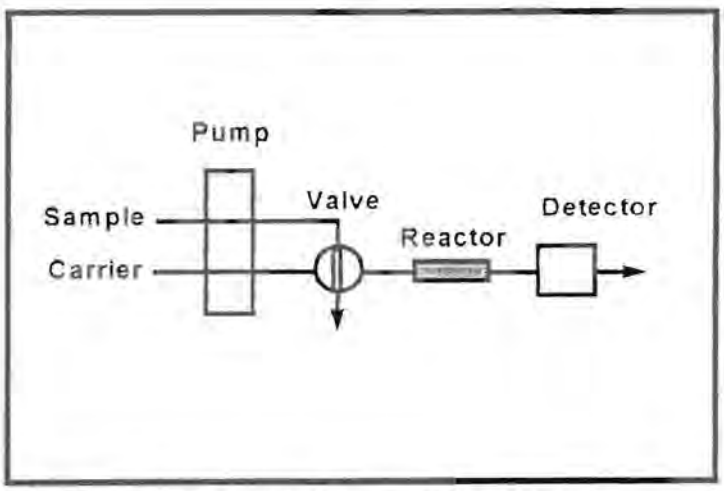

Fig. 4.10 Post-valve position for a reactor in a FIA system

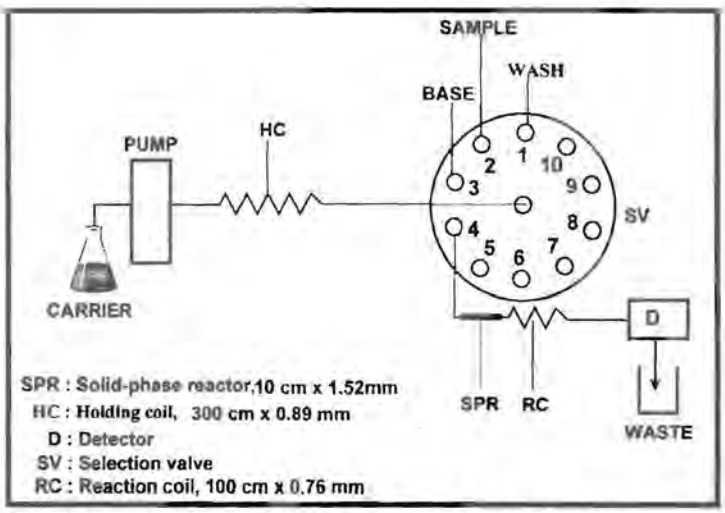

Fig. 4.11 Post-valve position for a reactor in a SIA system

4.5.3 In the injection system

This location is mostly used for pre-concentration with an adsorptive reactor placed in the sample loop of the injection system [21]. The released analyte can then be eluted with a suitable eluent and pumped to the detector. A schematic diagram of this arrangement applicable only to FIA is in Fig. 4.12. However, in the case of SIA, the same pre-concentration technique may be used, but instead, the adsorptive reactor is placed before the selection valve as in Fig. 4.9 where preconcentration can take place. The released analyte is then be eluted with a suitable eluent and pumped to the detector.

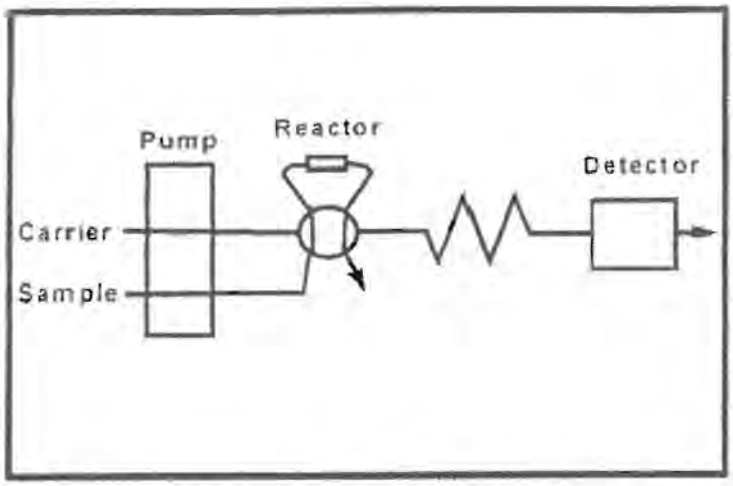

Fig. 4.12 Diagram of reactor placed in the injection system in a FIA manifold

4.5.4 In the detector

This location for the reactor is used to integrate reaction and detection for a number of advantages, some of which are decreased dispersion of the sample zone, increased sensitivity and increased sample throughput. The system can be extremely small. And there is no need for an additional reaction unit or transport tubing because the reactor is in the detector system. Diagrams of this arrangement are shown in Figures 4.13 and 4.14 for FIA and SIA systems respectively.

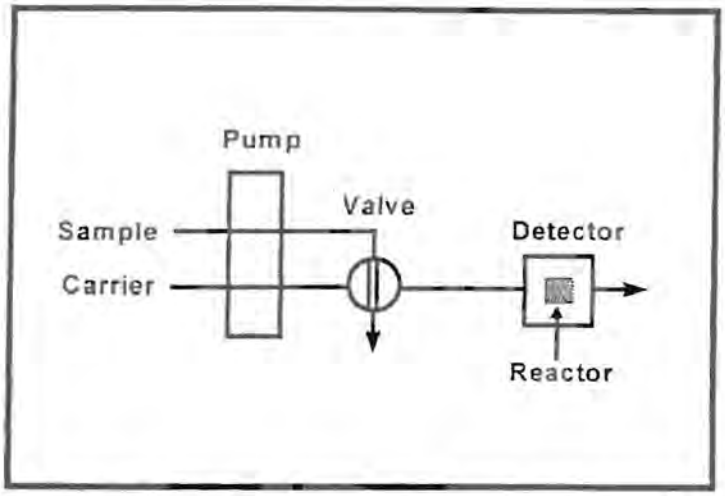

Fig. 4.13 Diagram of a FIA system with detector in the detection unit

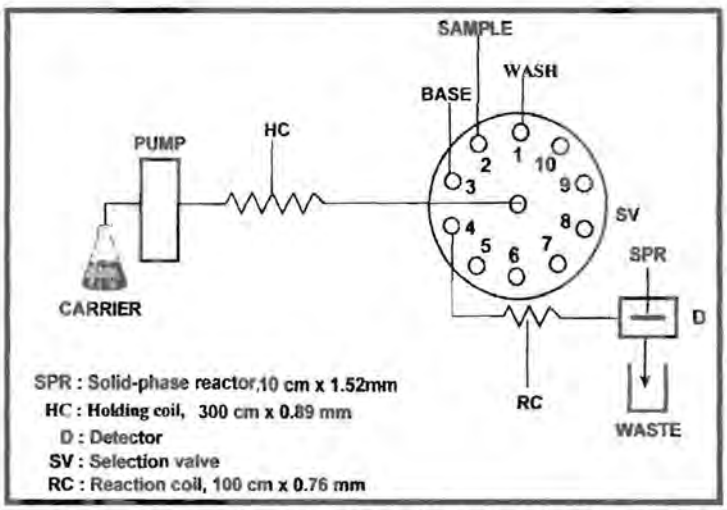

Fig. 4.14 Diagram of a SIA system with detector in the detection unit

4.6 Application of solid-phase reactors

To discuss the application of solid-phase reactors, the applications involved in FIA will be the starting point. A brief discussion of the reagent releaser will be given first followed by an analytical performance and reactor type given in Tabular form. This section will end with a brief discussion on SIA application.

4.6.1 FIA solid-phase reactors

Reagent releasers are very useful means of increasing sensitivity through substantially decreased dilution. A flow-through optosensor [116] in conjuction with a mono-channel FIA with fluorimetric detection, using sephadex SP-25 resin as active sorbent substrate was used for determination of vitamin B6 (pyridoxine).

Table 4.1 gives the analytical performance, the reactor and detector type for adsorptive reactors while Table 4. 2 shows the substances analysed and the performance of each detector type for ion-exchange reactors.

TABLE 4.1. Substances analysed using solid-phase adsorptive reactors in FIA.

Analyte	Range	%RSD	Detector	Ref
Pt	0.1 - 5 µg/ℓ	7 - 9	FAAS	23
Citrate, isocitrate	0.25 - 5 mmol/ℓ	2	Amperometry	24
Cr(III), Cr		1.2 - 5.9,1.2 - 5.7	FAAS	25
Pt	0 - 250 mg/ℓ	4.0	ICP-MS	26
Pt	20 - 80 µg/ℓ		ICP-AES	27
Co, Cu	0.3 - 6 µg/mℓ 0.1 - 15 µg/mℓ	2, 0.9	Spectrometrry	28
Cd, Pb	0.02 - 0.2 µg/ℓ	2.1 - 2.7	ETAAS	29
Cr			ETAAS	30
Zn	20 - 100 ng/ℓ	1.2	Spectrometry	31
Urea	0 - 120 mg/ℓ	< 1,9	Spectrometry	32
Hg	0 - 1 µg/mℓ	0.8 - 2.1	ICP-AES	33
V, Pb, Co, Cd			Spectrometry	34
Zn	0.04 - 40 ng/ℓ	3.3	Spectrometry	35
Ni	0.25 - 5 µg/ℓ	1.1	Spectrometry	36
Aspartame	20 - 80 µg/mℓ	0.2	Chemilumetry	37
Al	0.3 - 16 µmol/ℓ	3.7	Specrometry	38
Ag	0 - 800 ng/ℓ	1	Amperometry	39

TABLE 4.2 Substances analysed using Ion-exchange as solid phase reactor in FIA

Analyte	Range	%RSD	Detector	Ref
Trace metals			ETAAS	40
Chloracetic acid	0.005 - 0.1 mol/ℓ	1.5	Potentiometry	41
Pb		2.4	FAAS	42
Cd	0.056 - 56.2 mg/ℓ	7	Potentiometry	43
Cd			Potentiometry	44
Anion surfactants	0.005 - 0.5 mmol/ℓ	0.7	Phosphorescence	45
L- valine, L-leucine, L - isoleucine	30 nmol/ℓ - 5 µmol/ℓ	1.6	Potentiometry	46
Am, Pu			α- spectroscopy	47
Fe (total)	1 - 50 mg/ℓ	1.1	Spectrometry	48
Cu	0 - 100 µg/ℓ	< 2	Spectrometry	49
Se	100 - 200 ng/ℓ	1.5 - 2.3	ETAAS	50
Trace metals			AAS	51
Trace metals		3 - 5	ICP-MS/AAS	52
Trans-resveratrol	0 - 100 mg/ℓ	3.2 - 7.1	Spectrometry	53
Ascorbic acid	1.0 - 6.0 µg/mℓ	0.87 - 1.08	Spectrometry	54

Redox reactors develop a strong reducing or oxidizing agent which reacts with the analyte of importance to either render in a suitable oxidation state for further reaction or for direct detection. Redox reactors are also used to prepare analytes for enzyme immobilization. Table 4.3 gives the substances determined and the performance of the reactor and detector.

TABLE 4.3. Substances analysed using solid phase redox reactor in FIA.

Analyte	Range	%RSD	Detector	Ref
Adrenaline	0.5 - 20 µg/mℓ	2.0	Fluorimetry	55
Emetine hydrochloride	0.1 - 100 µg/mℓ	1.3	Fluorimetry	56
Phenothiazine derivatives	5 - 50 µg/mℓ	0.5 - 1.0	Spectrometry	57
Mn	0 - 5 mg/ℓ	1.8	Spectrometry	10
L -ascorbic acid	50 - 400 µmol/ℓ	0.75	Spectrometry	58
Sulfide	1.0 - 5.0 µg/ℓ	2.3	Spectrometry	59
Cystein	1 - 90 µg/mℓ	0.8	Spectrometry	60
Thioradazine, chlorpromazine	250 - 500 µg/mℓ	3.4 , 2.8	Spectrometry	61
Iproniazid, isoniazid	0 - 14 µg/mℓ	1.4	Spectrometry	62
H_2O_2	0.01 - 0.1 mol/ℓ		Spectrometry	63
Phenothiazine derivatives	5 - 150 g/mℓ	1.2	Potentiometry	64
Chlorpromazine	0.1 - 2 µg/mℓ	1.4	Potentiometry	65
Nitrate, Nitrite	0.02 - 400 µg/ℓ	1.56, 0.77	Spectrometry	9
Mn	1- 20 mg/ℓ	1.35	Spectrometriy	66

The use of immobilized enzymes in FIA emerges from a simple to a complex one. Many reactors would be analytically useless in the absence of enzymes. This is shown in Table 4.4 by the long list of various substances analysed and the performance of the chosen detector and reactor.

TABLE 4.4. Substances analysed using immoblized enzymes in FIA.

Analyte	Range	%RSD	Detector	Ref
Starch			Spectrometry	67
Ammonia. Glutamine			Potentiometry	68
Nitrophenyl phosphates	0 - 0.16 µmol/ℓ			69
Creatine, glucose , urea	0.2 - 20 mmol/ℓ		Electrochemical	70
Phosohate, pyrophosphate		1.5	Amperometric	71
Glycogen				72
Glutamic acid	10 - 500 µmol/ℓ	1.8	Spectrometry	73
Creatine, creatinine	5 - 400 µmol/ℓ	0.7	Spectrometry	74
Glucose uric acid, cholesterol			Amperometry	75
Nucleotides, Purine	0 - 10 µmol/ℓ	2.2 - 3.8	Amperometry	76
Creatinine			Amperometry	77
Methanol	4 - 80 µmol/ℓ	1.8	Fluorimetry	78
Glucose, glutamate, acetylcholine			Amperometry	79
Glucose, uric acid, cholesterol	5 - 700 mg/ℓ	2.8	Amperometry	80
Glucose,butyrate-3-hydroxy	10 µmol/ℓ - 1 mmol/ℓ 1 µmol/ℓ - 0.5 mmol/ℓ	0.88 1.1	Chemiluminescence	81
Glucose, penicillin			Spectrometry	82
L - Malic acid	20- 400 µmol/ℓ	1.2	Amperometry	83
Glycerol				84
Nitrogen containing compounds	0.005 - 8 mmol/ℓ	2	Fluorimetry	85
KI	0.06 - 100 µmol/ℓ		Chemiluminescence	86
Glutamate	0.05 - 20 mmol/ℓ	1.9 - 2.8	Spectrometry	87

Glycerol, ATP	2 -160 µmol/ℓ, 4 70 µmol/ℓ		Spectrometry	88
Lysine , glucose			Chemiluminescence	89
Glucose, choline	30 n mol/ℓ - 10µmol/ℓ	2	Chemiluminescence	90
Review			Chemiluminescence	91
Creatine, urea	0.05 - 1.5 mmol/ℓ	0.9 - 1.2	Spectrometry	92
Catechol, dopamine, phenol			Spectrometry	93
Biosystems			Ammonium-ion sensor	94
α-glycerophosphate			Spectrometry	95
inosine, hypoxanthine	0 - 20 µmol/ℓ	2.3	Amperometry	96
H_2O_2	40 - 80 mol/ℓ	1.1	Fluorimetry	97
ATP, ADP, AMP	2.5 - 2500 pmol 10 - 2500 pmol 25 - 5000 pmol	3.5 2.0 2.2	Fibre-optic sensor	98
Serine, sucrose	0 - 0.5 g/ℓ, 0 - 2.5 g/ℓ	1.7, 0.75	Amperometry	99
β - N - oxalyl, α,β - diamino propionic acid			Amperometry	100
Formaldehyde	0.5 - 100 µg/ℓ	0.92	Amperometric	101
D and L- amino acids			Amperometry	102
Glutamate	1 - 200 µmol/ℓ, 10 - 500 µmol/ℓ		Fluorimetry	103
Branched chain amino acids			Fluorimetry	104
NADP	0.01 - 5 µmol/ℓ	1.5 - 2.3	Fluorimetry	105

The application of FIA to immunology has resulted in a method which offers promise for faster and more reproducible assays. FIA was found to be advantageous in that it is possible to utilize the kinetics of immunochemical binding. Table 5 gives the various substances analysed and the

performance of the chosen reactor and detector.

TABLE 4.5. Substances analysed using immunochemical binding in FIA

Analyte	Range	%RSD	Detector	Ref
Immunoglobulin			Fluorimetry	106
Insulin	0.05 -2.25 ng/mℓ	4	Fluorimetry	107
Cr, imazethepyr	10 - 200 ng/mℓ		Fluorimetry	108
Biomolecules			Immunoassay	109
Bioligands			Spectrometry	110
Choline , phospholipidase	0.2 -1 ng/mℓ	1.8	Chemiluminescence	111
Eschericia, enterotoxin, staphylococcal			Fluorimetry	112
Pesticides			Immunoassay	113
microcarrier beads			beads	114
Drugs			Fluorimetry	2, 115
Atrazine	0.014 - 0.232 ng/mℓ		Fluorimetry	116
Naptalam		3.7	Fluorimetry	117

4.6.2 SIA solid-phase reactors

The use of solid-phase reactors incorporated into the SIA manifold is one of the areas which still needs a lot of exploration as little has been done compared to FIA. However, focus is now put on SIA. Shu *et al.* [118] developed a spectrophotometric method for the determination of lactic acid from industrial inorganics. A method for the simultaneous monitoring of glucose, lactic acid and penicillin [119] by SIA with glucose oxidase or lactate oxidase immobilized onto nylon

tubing was developed. The on-line monitoring of glucose and penicillin [120] with immobilized glucose oxidase and penicillinase on a piece of nylon tubing from industrial organics was accomplished spectrophotometrically.

Theophylline and caffeine [121] using a micro-column packed with Micro-prep High Q anion exchange beads were determined spectrophotometrically. The separation of radio-nuclides [122] using Sr-resin, TRU-resin and TEVA resin beads as slurry packed into a micro-column was developed.

4.7 Conclusion

FIA methodology using solid-phase has advanced to a very large extent that almost any analyte can be determined. The substances analysed ranges from agricultural, industrial, environmental, clinical, bioassay and biochemical (Tables 4.1 - 4.5). The number of publications in international journals and the journal for FIA is further evidence of the interest it has generated.

The simplicity and versatility of this technique allows the location of the solid reactor in the manifold in accordance to the nature of the analysis desired. The adaptation of the FIA technique to SIA has started to emanate, this is evident from the number of publications gradually coming out.

The same reactor types and shapes used in FIA are used in SIA. The only difference is with the location of the reactor in the manifold, with SIA needing fewer positions to execute the same

function.

Although the on-line coupling of solid-phase reactors to both the FIA and SIA manifold are related to one of the these three aspects, namely: miniaturization, integration of reaction (retention) and detection as well as multianalyte determinations, the SIA technique has enhanced sensitivity and is more cost effective. Thus SIA with solid-phase reactor incorporated into its manifold is a trend which has to be looked into.

4.8 References

1. M. D. Luque de Castro, **Trends Anal. Chem., 11** (1992) 149.
2. J. Martinez and J. V. Garcia Mateo, **Trends Anal. Chem., 12** (993) 428.
3. R. A. Messing, **Immobilised enzymes for industrial reactors, Academic Press,** New York,1975.
4. K. Zaitsu, K. Yamagashi and Y. Okhura, **Chem. Pharm. Bull., 36** (1988) 4488
5. Y. Hayashi, K. Zaitsu and Y. Okhura, **Anal. Chim. Acta, 186** (1986) 131.
6. J. Martinez-Catalayud, J. V. Garcia Mateo and Lahuerta Zamora, **Anal. Chim. Acta, 265** (1992) 81.
7. J. Martinez-Catalayud and J. V. Garcia Mateo, **Anal. Chim. Acta, 274** (1993) 275.
8. T. Pérez-Ruiz, C. Martinez-Lozano, V. Tomás and J. Carpena, **Analyst (London), 117** (1992) 1025.
9. J. F. van Staden and Makhapa Makhafola, **S. Afr. J. Chem., 52(1)** (1999) 49.
10. J. F. van Staden and L. G. Kluever, **Anal. Chim. Acta, 350** (1197) 15.
11. A. Sakuragawa, S. Nakayama and T. Okutani, **Anal. Sci., 10** (1994) 77.
12. A. Fernandez, J. Ruz, M. D. Luque de Castro and M . Valcárcel, **Clin. Chim. Acta, 148** (1985) 131.
13. C. W. Bradberry and R. N. Adams, **Anal. Chem., 55** (1983) 2439.
14. J. Růžička and L. Scampavia, **Anal. Chem. News and Features,** (1999) 251A.
15. D. Chen, M. D. Luque de Castro and M. Valcárcel, **Microchem. J., 44** (1991) 215.
16. B. Fernández-Band, F. Lazaro, M. D. Luque de Castro and M. Valcárcel, **Anal. Chim. Acta, 229** (1990) 177.

17. R. Montero, M. Gallego and M. Valcárcel, **Anal. Chim. Acta, 234** (1990) 433.

18. J. Martinez-Calatayud and S. Sagrado Vivez, **J. Pharm. Anal., 7** (1989) 1165.

19. Z. Fang, **Flow-Injection Separation and Preconcentration**, VCH, Weinheim, 1993.

20. D. H. Holman, G. D. Christian and J. Růžička, **Anal. Chem., 69** (1997) 1763.

21. M. Karlson, J. C. Person and J. Möller, **Anal. Chim. Acta, 244** (1991) 109.

22. A. Ruiz-Medina, M. L. Fernandez-de-Cordova and A. Molina-Diaz, **Fresenius' J. Anal. Chem., 363** (1999) 265.

23. A. Cantarero, M. M. Gomez, C. C. Camara and M. A. Palacios, **Anal. Chim. Acta, 296** (1994) 205.

24. K. Matsomoto and T. Tsukatani, **Anal. Chim. Acta, 321** (1996) 157.

25. R. M. Cespon-Romeo, M. C. Yebra-Biurrun and M. P. Bernejo-Barrera, **Anal. Chim. Acta, 327** (1996) 37.

26. M. M. Hidalgo, M. M. Gomez and M. A. Palacios, **Fresenius' J. Anal. Chem., 354** (1996)420.

27. J. F. van Staden, C. J. Rademeyer and S. M. Linsky, **S.Afr. J. Chem., 50** (1997) 115.

28. E. Vereda, A. Rios and M. Valcarcel, **Analyst 122** (1997) 85.

29. E. Ivanova, W. Van Mol and F. Adams, **Spectrochimica Acta, Part B53** (1998) 1041.

30. S. Nielsen and E. H. Hansen, **Anal. Chim. Acta, 366** (1998)163.

31. D. S. de Jesus, R. J. Cassella, S. L. C. Ferreira, A. C. S. Costa, M. S. de Carvalho, R. E. Santelli, **Anal. Chim. Acta, 366** (1998) 263.

32. S. Jorgi, D. Narinesingh and T T. Ngo, **Anal. Lett., 31** (1998) 543.

33. P. Canada-Rudner, J. M. Cano-Pavon, F. Sanchez-Rojas and A. Garcia-de-Torres, **J. Anal. At. Spectron, 13** (1998) 1167.

34. D. Beauchemin and A. A. Spech, **Canadian J. Anal. Sci. And Spectrosc., 43** (1998) 43.

35. S. G. L. Teixeira, F. R. P. Rocha, M. Korn, B. F. Reis, S. G. L .C. Ferreira, A. C. S. Costa, **Anal. Chim. Acta, 383** (1999) 309.

36. S. L. C. Ferreira, D. S. de Jesus, R. J. Cassella, A. C. S. Costa, M. S. de Carvallo and R. E. Santelli, **Anal. Chim. Acta, 378** (1999) 287.

37. O. Fatibello-Filho, L. H. Marcolino-Junior and A. V. Pereira, **Anal. Chim. Acta, 384** (1999) 167.

38. K. J. Powel, **Analyst, 123** (1998) 797.

39. Q. S. Pu, Q. Y. Sun, Z . D . HU and Z. X. Su, **Analyst, 123** (1998) 239.

40. P. E. Carreiro J. F. Tyson, **Analyst, 122** (1997) 95.

41. C. Puig-Lleixa, J. Bartroli, M. Del-valle, D. Montllo and A. Tomico, **Anal. Chim. Acta, 359** (1998) 311.

42. G. H. Tao and Z. L. Fang, **Fresenius' J. Anal. Chem., 366** (1998) 156.

43. C. M . C .M. Couto, J. L. F .C. Lima, B. S. M. Montenegro, B. F. Reis and E. A. G. Zagatto, **Anal. Chim. Acta, 366** (1998) 155.

44. M. Trojanowicz, P. W. Alexander and D. B. Hibbert, **Anal. Chim. Acta, 370** (1998) 267.

45. R. Badia, M. E. Diaz-Garcia, **Anal. Chim. Acta, 371** (1998) 73.

46. N. Kiba, M. Tachibana, K. Tani and T. Miwa, **Anal. Chim. Acta, 375** (1998) 65.

47. J. W. Grate and O. B. Egorov, **Anal.Chem., 70** (1998) 3929.

48. J. F. van Staden and L. G. Kluever, Fresenius. **J. Anal. Chem., 362** (1998) 319.

49. F.C. Carmago, E.A.G. Zagato and C.C. Oliveira, **Anal. Sci., 14** (1998) 565.

50. P. E. Carreiro, J. F. Tyson, **Spectrochimica Acta, B53** (1998) 1931.

50. P. E. Carreiro, J. F. Tyson, **Spectrochim. Acta, B53** (1998) 1931.

51. G. M Greenway, S. M. Nelms, I. K. Skhosana and S. J. L. Dolman, **Spectrochim. Acta, Part B 51 B** (1996) 1909.

52. S. N. Willie, H. Tekgul and R.E. Sturgeon, **Talanta, 47** (1998) 439.

53. L. Arce, M. I. Tena, A. Rios and M. Valcarcel, **Anal. Chim. Acta, 359** (1998) 27.

54. A. Molina-Diaz, A. Ruiz-Medina and M. L. Fernandez de Cordova, **Fresenius J. Anal. Chem., 363** (1999) 92.

55. A. Kojlo and J. M. Calatayud, **Anal. Lett., 28** (1995) 239.

56. S. L . Ortiz and J. Martinez Calatayud, **Anal. Lett., 28** (1995) 971.

57. A. Kojlo and J. M. Calatayud, **Talanta, 42** (1995) 909..

58. A. V. Pereira, O. Fatibello-Flho, **Anal. Chim. Acta, 366** (1998) 55.

59. J. F. van Staden and L. G. Kluever, **Anal. Chim. Acta, 369** (1998) 157.

60. M. Catala-Icardo, L. Lahuerta-Zamora and J. Martinez Calatayud, **Analyst, 123** (1998) 1685.

61. M. Catala-Icardo, L. Lahuerta-Zamora and J. Martinez-Calatayud, **Lab. Robotics. Autom. 10** (1998) 33.

62. J. A. Garcia-Bautista, J. V. Garcia-Mateo and J. Martinez-Calatayud, **Anal. Lett., 31** (1998) 1209.

63. J. A. Garcia-Bautista, J. V. Garcia-Mateo, J. Martinez-Calatayud, **J. Flow. Injection. Anal., 15** (1998) 61.

64. M. Polasek, J. Dolejsova and R. Karlicek, **Pharmazie, 53** (1998) 168.

65. A. Kojlo, **Anal. Lett., 30** (1999) 2353..

66. K. Kargosha and M. Noroozifar, **Anal. Chim. Acta, 413** (2000) 57.

67. J. Emneus, G. Nilson and L. Gorton, **Starch/Staerke, 45** (1993) 264.

68. B. O. Palson, B. Q. Shen, M. E. Meyerhoff and M. Trojanowicz, **Analyst, 118** (1993) 1361.

69. Y. Shan, I. D. Mckelvie and B. T. Hart, **Anal. Chim., 65** (1993) 3053.

70. C. S. Rui, H. I. Ogawa, K. Sonomoto and Y. K ato, **Biosci. Biotechnol.Biochem, 57** (1993) 191.

71. T. Yao, and T. Wasa, **Electroanalysis (NY), 5** (1993) 887.

72. J. Emneus and L. Gorton, **Anal. Chim. Acta, 276** (1993) 319.

73. C. D. Stalikas, M. I. Karayannis, S. M. Tzouwara-Karayanni, **Analyst, 118** (1993) 723.

74. G. Moges and G. Johansson, **Anal. Lett., 27** (1994) 495.

75. T. Yao, M. Satomura and T. Nakahara, **Anal. Chim. Acta, 296** (1994) 271.

76. T. Yao, K. Tsureyaman and T. Nakahara, **Electroanalysis (NY), 6** (1994) 165.

77. C. S. Rui, Y. Kato and K. Sonomoto, **Biosens-Bioelectron, 9** (1994) 429.

78. C. G. de Maria, T. Manzano, R. Duarte, A. Alfonso, **Anal. Chim. Acta, 309** (1995) 241

79. T. Yao, S. Suzuki, H. Nishino and T. Nakahara, **Electroanalysis (NY), 7** (1995) 1114

80. .T. Yao, M. Satomura and T. Nakahara, **Electroanalysis (NY), 7** (1995) 143.

81. N. Kiba, H. Koemado and M. Furusuwa, **Anal. Sci., 11** (1995) 605.

82. R. W. Min, J. Nielsen and J. Villadsen, **Anal. Chim. Acta, 320** (1996) 199.

83. M. I. Prodrommidis, S. M. Tzouwara-Karayannis, P. Vadigamaand and A. Maines, **Analyst,121** (1996) 435.

84. M. I. Prodrommidis, C. D. Stalikas, S. M. Tzouwara-Karayannis, **Talanta, 43** (1996) 27.

85. H. Mana and U. Spohn, **Anal. Chim. Acta, 325** (1996) 93.

86. K. Hayash, T. Okugawa, Y. Kozuka, S. Sasaki, K. Ikebukuro and I. Karube, **Anal. Lett.,**

29 (1996) 2499.

87. R. Shi and K. Stein, **Analyst , 121** (1996) 1305.

88. E. R. Kiranas, M. I. Karayannis and S. M. Tzouwara-Karayanni, **Anal. Lett., 30** (1997) 537.

89. A. M. Almuaibed and A. Townshend, **Anal. Chim. Acta, 338** (1997) 149.

90. M. Emteborg (b.Stigband), K. Irgum, C. Gooijer, U. A.T. Brinkman, **Anal. Chim. Acta, 357** (1997) 111.

91. N. Kiba, **J. Flow. Injection-Anal., 14** (1997) 123.

92. M. Jurkiewicz, S. Alegret, J. Admirall, M. Garkia and Fabregas, **Analyst,123** (1998) 1321.

93. A. W. O. Lima, E. K. Vidsiunas, V. B. Nascimento and L. Angnes, **Analyst , 123** (1998) 2377.

94. M. Jurkiewicz, S. Alegret and E. Fabregas, **Anal. Chim. Acta, 370** (1998) 47.

95. E. R. Kiranas, M. I. Karayannis and S.M. Tzouwara-Karayanni, **Talanta, 45** (1998) 1015.

96. M. A. Carsol and M. Mascini, **Talanta, 47** (1998) 335.

97. Y. Z. Li and A. Townshend, **Anal. Chim. Acta, 359** (1998) 149.

98. P. E. Michel, S. M. Gautier-Sauvigne and L. J. Blum, **Anal.Chim. Acta, 360** (1998) 89.

99. P. Sosnitza, F. Irtel, R. Ulber, M. Busse, R. Faure, L. Fischer and T. Scheper, **Biosensor and Bioelectronics, 13** (1998) 1251.

100. G. Akalu, G. Johansson and B. M. Nair, **Food Chemistry, 62** (1998) 233.

101. N. Kiba, L. Sun, S. Yokose, M. T. Kazue, T.T. Suzuki, **Anal. Chim. Acta, 378** (1999) 169.

102. M. Varadi, N. Adanyi, E. E. Szabo and N. Trummer, **Biosensor and Bioelectronics, 14**

(1999) 335.

103. C. D. Stalikas, M. I. Karayannis and S. M. Tzouwara-Karayanni, **Egypt. J. Chem., 3** (1994)113.

104. N. Kiba, M. Tachibana, K. Tani and T. Miwa, **Anal. Chim. Acta, 375** (1998) 65.

105. T. Yao, H. Ogawa and T. Nakahara, **Talanta, 42** (1995) 1297.

106. C. H. Pollema and J. Ruzicka, **Anal. Chem., 66** (1994) 1825.

107. M.Y. Khokhar, J. N. Miller and N. J. Seare, **Anal. Chim. Acta, 290** (1994) 154.

108. J. Růžička, **Anal. Chim. Acta, 308** (1995) 14.

109. B.Willumsen, G. D. Christiaan and J.Růžička, **Anal. Chem., 69** (1997) 3482.

110. J. Růžička and A. Ivaska, **Anal. Chem., 69** (1997) 5024.

111. M. G. Yaqoob, J. A. Nabi and M. Masoon-Yasinzai, **J. Biolumin. Chemilumin., 12** (1997)135.

112. H. Yu, **Anal. Chim. Acta, 376** (1998) 77.

113. Z. L. Zhi, **Lab. Robotics. Autom., 11** (1999) 83.

114. J. Růžička and L. Scampavia, **Anal. Chem., 71** (1999) 257A.

115. P. S. Hodder and J. Růžička **Anal. Chem., 71** (1999) 1160.

116. M.A. Gonzalez-Martinez, R. Puchades, A. Maquieira, I. Ferrer, M. P. Marco and D. Barcelo, **Anal. Chim. Acta, 386** (1999) 201.

117. T. Galeano-Diaz, M.I. Aledo-Valenzuela and F. Saliaas, **Anal. Chim. Acta, 384** (1999) 185.

118. H. C. Shu, H. Hakanson and B. Mattiason, **Anal. Chim. Acta, 300** (1995) 277.

119. R. W. Min, J. Nielsen and J. Villadsen, **Anal. Chim. Acta, 312** (1995) 149.

120. R. W. Min, J. Nielsen and J. Villadsen, **Anal. Chim. Acta, 320** (1996) 199.

121. B. Dockendorf, D. A. Holman, G. D. Christian and J. Růžička, **Anal. Comm., 35** (1998) 357

122. O. B. Egorov, M. J. Ohara, and J. W. Grate, **Anal. Chem., 71** (1999) 345.

CHAPTER 5

Determination of manganese using a solid-phase reactor in an SIA system

5.1 Introduction

Manganese is a grey metal with a reddish tone. It is relatively abundant, constituting about 0.085% of the earth's crust. Among the heavy metals only iron is more abundant, heavier than manganese, harder and have a higher melting point (mp; Mn = 1244°C, Fe = 1535°C). Although widely distributed, it occurs in a number of substantial deposits mainly as oxides, the most important of which is pyrolusite, manganese (II) oxide, MnO_2 , is a grey-green to dark green powder made by roasting the carbonate in hydrogen or nitrogen by action of steam on manganese (II) chloride, $MnCl_2$ at 600°C. Less important ores are: braunite, Mn_2O_3 ; manganite, $Mn_2O_3.H_2O$ and hausmanite, $MnO.Mn_2O_3$. Manganese is also present in a fairly abundant impurity in most iron ores and hydrous oxide carbonate deposits [1,2]. Its presence in ground water and natural waters is considered to be due to the chemical erosion of the earth's crust [3].

Manganese exhibits complex behaviours in natural water systems, cycling readily among oxidation states in response to changing environmental conditions [4,5]. The behaviour of manganese in seasonably anoxic hypolimnetic waters generally follows the model developed by Delfino and Lee [6], who traced the migration of the boundary between oxidized and reduced forms from below the sediment-water interface up into the water column as anoxia developed

during stratification. Manganese thus resembles iron in its response to changing redox conditions, and the bio-geochemistries of the two elements are closely linked [7].

The concentration of manganese found in natural water is generally quite low, in the range 0.1-1.0 mg/ℓ [8], although in certain reservoirs at times it is as high as 10 mg/ℓ [9]. However, in South Africa the mining industry also contributes to the presence of manganese in natural waters and the concentrations may rise to a level of 200 mg /ℓ even higher in certain effluent streams [8].

Although manganese in ground water is generally present in the soluble divalent ionic form because of the absence of oxygen, part or all of the manganese in water treatment plants may be in a higher valence state. There is however, evidence that manganese occurs in surface waters both in suspension in the quadrivalent and trivalent state in a relatively stable, soluble complex.

Special means of removal such as chemical precipitation and pH adjustment, aeration and use of special ion-exchange materials has been used. Hence, the determination of manganese in public and industrial waters is important because it can cause discolouration of products, stains to laundry and reduction of pipeline carrying capacities due to encrustation. Furthermore the effect of its deficiency in both plants and animals cause diseases. Manganese at elevated concentration is toxic to a variety of organisms.

5.2 Properties of Manganese

Manganese is roughly similar to iron in its physical and chemical properties, the main difference being that it is harder and more brittle, but less refractory. It is quite electropositive and readily dissolves in dilute, non-oxidizing acids. It is not particularly reactive towards non-metals at room temperatures, but at elevated temperatures it reacts vigorously. It burns in chlorine gas to give $MnCl_2$, reacts with fluorine to give MnF_2 and MnF_3, burns in nitrogen above 1200°C to give Mn_3N_2 and combines with oxygen giving Mn_3O_4 at high temperatures. It also combines directly with boron, carbon, sulfur, silicon and phosphorus, but not with hydrogen. In neutral or acid solutions it exists as the very pale pink hexa-aquo ion, $[Mn(H_2O)_6]^{2+}$, which is quite resistant to oxidation. In basic media, however, the hydroxide, $Mn(OH)_2$ is formed and this is readily oxidized even by air [1,10]

5.3 Oxidation states of Manganese

As with Ti, V and Cr, the highest oxidation state of manganese corresponds to the total number of 3d and 4s electrons. This +7 state occurs only in the oxo compounds, MnO_4^-, Mn_2O_7 and MnO_3F, and these compounds show some similarity to corresponding compounds of the halogens. Manganese (VII) is a powerful oxidizing ion, usually being reduced to Mn(II). The intermediate oxidation states are known, but only a few compounds of Mn(V) have been characterized; nevertheless, Mn(V) species are frequently postulated as intermediates in the reduction of per-manganates. Although Mn(II) is the most stable state, it is quite readily oxidized in alkaline solution. Thus the only compounds that appear in stable ionic species in

solution are in the +2 as Mn(II) and the +7 as MnO_4^- [1,4,11].

5.4 Manganese (II) compounds: Mn^{2+}

Since the divalent state is the most important and most stable state in solution and the analyses is in water, only compounds in this oxidation state will be discussed. Manganese(II) is found in both solid salts and their aqueous solutions. In solution this ion is only slightly hydrolysed and its hydroxide is among the more soluble and more strongly basic of the precipitable hydroxides. In atmospheric oxygen the gelatinous white solid, rapidly darkens because of oxidation. It is a well defined compound, having the same crystal structure as magnesium hydroxide [1,2].

Manganese (II) forms as intensive series of salts with all common anions. Most are soluble in water, although the phosphate and carbonates are slightly so. The soluble salts of manganese include the chloride, $MnCl_2 \cdot 4H_2O$; sulphate, $MnSO_4 \cdot 4H_2O$ and nitrate, $Mn(NO_3)_2 \cdot 6H_2O$. All of these are red solids, but at a concentration greater than 0.5 mol/ℓ in water they assume a pink colour [1,10].

Manganese(II) sulfide, MnS has a pink colour and precipitates when sulfide ions in basic solution are added, and has a relatively large K_{sp} value (1×10^{-14}) and hence dissolves easily in 6 mol/ℓ HCl. Manganese(II) hydroxide, $Mn(OH)_2$ forms a pink precipitate when a solution containing Mn^{2+} is made basic. Its K_{sp} value is large enough (4×10^{-14}). The compound $Mn(OH)_2$ does not form stable complexes with either of these two species [1,2,10].

The majority of manganese(II) complexes are of a high spin. In octahedral fields, this configuration gives spin-forbidden as well as parity forbidden transitions, thus accounting for the extremely pink colour of such compounds. In tetrahedral environments, these transitions are therefore twice stronger and the compounds have a noticeable pale yellow-green colour.

Manganese(II) forms many complexes, but with the equilibrium constants for their formation in aqueous solution are not high compared to those for the divalent cations of succeeding elements [Fe(II)-Cu(II)], because the Mn(II) ion is the largest of these and it also has no ligand field stabilization energy in its complexes. Many hydrated salts contain $[Mn(H_2O)_6]^{2+}$ ion, and direct action of ammonia anhydrous salts leads to the formation of ammoniates, $[Mn(NH_3)_6]^{2+}$ ion. Chelating ligands such as ethylenediamine form $[Mn(OH)_2EDTA]^{2-}$. Hydrated salts such as trans-$[MnCl_2(H_2O)_2]^{2-}$ and trans-$[MnCl_6(H_2O)_4]^{2-}$ are also known.

5.5 Industrial uses of Manganese

Metallic manganese, as such is not used to any appreciable extent in industry. But the iron-manganese alloy called ferromanganese, which contains 75 to 80% manganese, is largely used in the manufacture of special steels. These steels are used to make rails, safe and many types of machinery.

The addition of small quantities of ferromanganese improves the quality of steel by removing traces of oxygen and sulfur on forming MnO_2 and MnS which are separated by slag. The addition of larger quantities of ferromanganese forms steel of great toughness. MnO_2 is used as

a dryer for paints since it catalyses the oxidation (drying) of the paint oils by oxygen of the air; as a decolouriser of glass, since it oxidises any green iron (II) compound present to a much paler yellow iron (III) compound; and as a depolariser in dry cells, since it reacts with the H_2 liberated at the carbon cathode. Potassium permanganate, $KMnO_4$, find some use as a strong oxidant, especially in analytical procedures [10].

5.6 Biological importance of Manganese

The biological role of manganese has stimulated much study of especially complexes of Mn(II) and Mn(VII) oxidation states. Manganese is an essential element in several biological systems in trace amounts, virtually to all forms of life. Manganese is involved in the oxidation of water to oxygen in the photo-system II where redox changes are linked to the four-electron oxidation of water. It is the only metal that has been found to be associated with the water-splitting apparatus in all the oxygen-evolving organisms studied to date [13]. In plants the bacterial enzyme super-oxide dismutase [1,2] catalyses the decomposition of O_2^-. The precise nature and role of manganese in this, is not clear and nothing is known about the chemical details of its participation [14]. Nevertheless searches for model systems have led to study polydentate [15] and macro-cyclic ligands [16] such as polyamine carboxylate, 8- quinolinolates, polyhydroxo compounds and porphyrins.

Although manganese is an essential element in plant and animals, at elevated concentrations are toxic to a variety of aquatic organism [13]. In addition, reduced manganese makes water unpalatable and causes fouling and corrosion in water systems and cooling towers. Deficiencies

cause diseases of both plants and animals in larger numbers. The adult human body contains approximately 15 mg of manganese.

In the quality of water for human consumption the maximum admissible concentration is 0.05 mg/ℓ and the guide value is 0.02 mg/ℓ; the WHO and European Standards quotes 0.05 mg/ℓ as the level above which trouble may arise; the Russian Standards allow 0.1 mg/ℓ as the upper limit; earlier surface water criteria in the United States suggested a similar value of 0.05 mg/ℓ [17]. If manganese precipitates out in water as manganese (II) hydroxide in a distribution system so that the consumers receive a blackened discolouration in the water, this gives rise to greater concern than does rusty water 17].

The skeleton in animals is one of the most affected by manganese deficiency. In chicken the skeletal disorder perosis or "slipped tendon disease" results, in rats a condition known as chondrodystrophy, a type 7 skeletal disproportionate growth is observed [18]. When deficiency is imposed during prenatal period, the offsprings show congenital irreversible ataxia, characterized by lack of equilibrium, abnormal body reflexes and retractions of the head [19]. The same abnormal behaviour shown by offspring of manganese deficiency animals is also seen in a genetic mutant, the pallid mouse. In this strain the inability of the animal to swim, as well as the abnormal development of the otoliths, can be completely prevented by giving pregnant females a diet supplemented with manganese [20]. Manganese deficiency also affects brain function, this has been shown in that manganese deficient rats are much more susceptible to convulsion than are normal rats [20]. Ultra-structural defects were also observed in mice whose mitochondria showed evidence of membrane defects, the outer membrane was damaged and in some cases appeared to be missing [21].

5.7 Choice of analytical method

Various techniques are employed to determine manganese. These techniques include AAS, colorimetry, XRF spectrometry, ICP-AES, stripping voltammetry and HPLC [22]. Although these techniques deliver accurate results with some having low detection limits, the apparatus are expensive and not suitable for on-site, on-line routine analysis. Furthermore these techniques usually require labourious sample preparation using large sample volumes and involve complicated procedures which are time consuming. Spectrophotometric methods coupled with flow injection analysis proved to be a better alternative, but due to its high sample and reagent consumption, were ruled out in favour of the sequential injection system. In papers by Bowie *et al.* [22] and Gaikwad *et al.* [23] flow-injection analysis (FIA) is used with chemiluminescence (CL) mode of detection. However, in a paper by van Staden and Kluever [8] and a very recent paper by Kargosha and Noroozifar [9], FIA is used with a spectrophotometer as a mode of detection. Among the advantages of using flow-injection over other manual techniques [22] is a decrease in the amount of sample handling accompanied by the minimum of sample preparation steps.

Homogeneous reactions with sample and reagent both in the liquid phase are used in most of the FIA manifolds [24-26]. This set-up may provide some disadvantages, particularly if the reagent is expensive, slightly soluble or only available in the solid form. In fact one of the disadvantages of FIA is the relatively high reagent consumption per analysis.

The use of solid-phase reactors incorporated into FIA manifolds may offer certain advantages

over homogeneous systems [8, 27-30]. Reagent consumption is greatly decreased and the system is simplified with fewer junction for mixing of reagent, sample and carrier streams.

Sequential injection analysis (SIA), launched in 1990 [31, 32] is a technique that has a tremendous potential especially for on-line process measurements and in the monitoring of the environment, due to the simplicity and convenience with witch sample manipulations can be automated. The versatility of the technique is centred around a selection valve where each port of the valve allows a different operation to be performed [31-33]. The basic components of the system are a peristaltic pump with only one carrier stream, a single selection valve, a single channel and a detector. The concept is based on the sequential injection of a wash solution, sample zone and reaction zone(s) into a channel [34-37]. In this way a stack of well-defined zones adjacent to each other is obtained in a holding coil. After the valve has been selected to the detector position, the flow in the carrier stream is reversed and the zones mutually disperse and penetrate each other as they pass through a reaction coil to the detector. The flow reversal as a result of the injection step therefore creates a composite zone in which the sample and reagent zone penetrate each other due to combined axial and radial dispersion.

Some of the prerequisites needed for an analyser in the determination of manganese (II) in natural and effluents streams were that the system should be simple and robust, reliable with low frequency of maintenance and that the consumption of reagents should be very low. Sequential injection analysis seemed to be an ideal technique for such an analyser and this Chapter reports on a solid-phase reactor incorporated into a sequential injection analysis (SIA) system for the determination of manganese (II).

5.8 Manganese determination

Manganese (II) from a sample is oxidised by solid PbO_2 , embedded in silica gel beads, to produce the permanganate ion which is determined spectrophotometrically [38] at 526 nm.

5.8.1 Experimental

5.8.1.1 Reagents and solutions

All reagents were prepared from analytical-reagent grade chemicals unless specified otherwise. All aqueous solutions were prepared with doubly distilled water.

5.8.1.1.1 Stock manganese solution

A stock manganese (II) solution containing 1000 mg/ℓ Mn^{2+} was prepared by dissolving 3.639 g of manganese (II) chloride tetrahydrate (Merck, pro analysis) and diluting to 1ℓ with water. Working manganese (II) solutions in the range 0.1 to 7 mg/ℓ were prepared by appropriate dilution of the stock solution with 0.1 mol/ℓ HNO_3.

5.8.1.1.2 HNO_3 solution

A 0.5 mol/ℓ HNO_3 solution was prepared by dilution of 195 mℓ HNO_3 (55%), UNIVAR; SAARCHEM) with de-ionised water to 5 ℓ. The solution for the carrier stream was prepared by

appropriate dilution of this solution.

5.8.1.2 Instrumentation

The sequential injection system depicted in Fig 5.1 was constructed from the following components: a Gilson minipuls peristaltic pump (Model M312, Gilson, Villiers-le Bel, France); a 10-port electrically actuated selection valve (Model ECSD1OP; Valco Instruments, Houston, Texas); and a Unicam 8625 UV-Visible spectrophotometer equipped with a 10-mm Helma-type (Helma GmbH and Co., Mulheim/Baden, Germany) flow-through cell (volume 80 $\mu\ell$) for absorbance measurements.

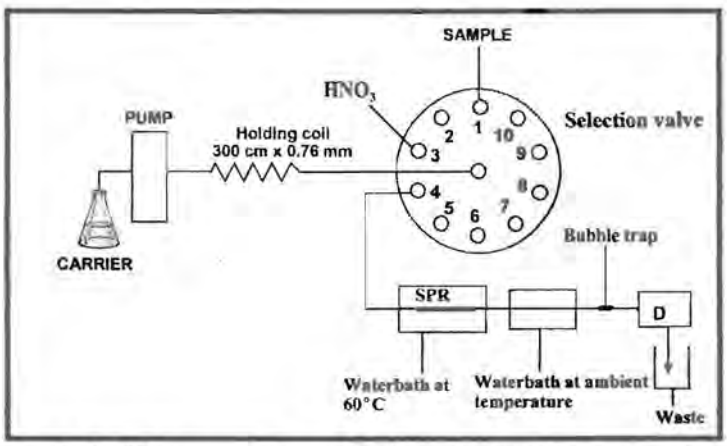

Fig. 5.1 A SIA system diagram for determination of manganese in water

Data acquisition and device control was achieved using a PC30-B interface board (Eagle Electric, Cape Town) and an assembled distribution board (Mintek, Randburg). The FlowTEK [38] software package (obtainable from Mintek) for computer-aided flow analysis was used

throughout for device control and data acquisition. All data given (mean peak height values) are the average of 10 replications.

5.8.1.3 The solid-phase reactor

The solid-phase reactor (SPR) was constructed using PTFE tubing with an internal diameter of 1.52 mm (Fig. 5.2). The reactor packing consisted of lead (IV)dioxide suspended on silica gel beads (35-70 mesh, 40 Å; Aldrich-Cemical Co. Gillngham-Dorset). The lead (IV) doxide was prepared as described by Rüter and Neidhart [29], the only difference being the use of commercial sodium hypochlorite (3.5% m/v when packed) for supplying the sodium hypochlorite. The bleach was added drop-wise to a solution of 150 g lead(II) acetate in 500 mℓ water in which 75 g of the previously mentioned silica gel was suspended with fast stirring. The bleach was added until precipitation of the lead (IV) dioxide was complete. The NaOCl oxidizes divalent lead to lead oxide according to the equation :

$$Pb(CH_3COO)_2 + NaOCl \rightarrow PbO_2 + 2CH_3COOH + NaCl$$

The mixture was then stirred for a further 60 minutes, vacuum-filtered, washed successively with dilute nitric acid and de-ionised water and the formed lead(IV) dioxide dried in a dessicator. The packing of each reactor was done by attaching the Teflon tube to a vibrating shaker after plugging the bottom end with glass wool. The prepared packing was then introduced via a funnel.

After packing each reactor had to be conditioned (run in) for at least 60 minutes before use.

Conditioning involved pumping de-ionised water through the reactor at a flow rate of 2.2 mℓ/min for 45 minutes and then the carrier for 15 minutes at the same rate. This was to ensure that there were no air pockets and to ensure close packing of the beads.

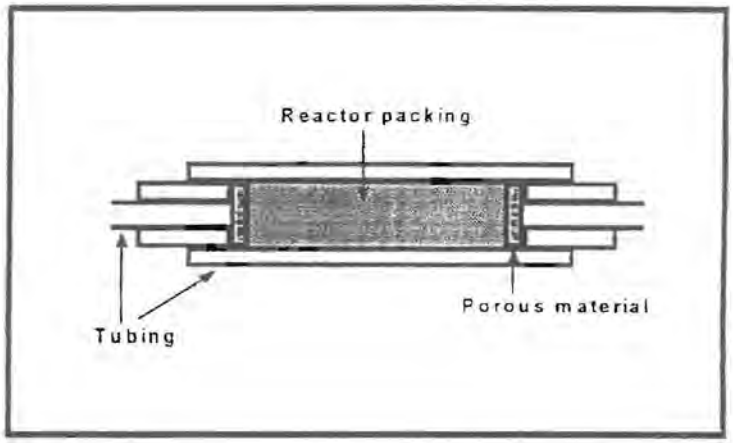

Fig. 5.2 Design of a tubular packed reactor

The lifetime of each reactor was established by comparing peak heights for the same standards from day to day. When the peak heights started to decrease systematically and drastically, the reactor had to be replaced. Another indication that the reactor was losing its oxidation capacity was the colour of the packing itself. At the beginning of a new conditioned reactor the colour of the packing was dark brown which gave a greyish appearance inside the PTFE tubing. After the reactor was in use for several samples (500-600) experiments and depending on the concentration of the manganese in the samples the colour of the packing at the front end of the reactor started to disappear. This meant that all of the PbO_2 had been stripped off the beads.

5.8.1.4 Procedure

A schematic diagram for the sequential injection analysis system in shown in Fig 5.1. The whole procedure, from sample injection to data processing and storage was computer controlled via the FlowTEK-program [38] except the water bath which had to be controlled manually. The whole procedure involved designing a method which allows a single cycle of the experiment to be run Fig 5.3 and Table 5.1 shows the device sequence analysis for one cycle.

The equation for this reaction is:

$$2Mn^{2+} + 5PbO_2 + 4H^+ \Rightarrow 2MnO_4^- + 5Pb^{2+} + 2H_2O$$

The reaction is thus pH dependent and the oxidation of Mn^{2+} is accompanied by a rise in the pH of the solution which results in a decrease in the efficiency of the reaction. The reaction conditions are kept at optimum by using an acidic carrier stream. After being placed in the carrier stream, the sample zone was pumped through the solid-phase reactor, which was immersed in the temperature controlled water bath.

For this study the determination of manganese was chosen. Mn^{2+}-ions in the sample zone was oxidised to MnO_4^- in the solid-phase reactor and the permanganate zone was channelled through a cooling system and then to a spectrophotometer for measurements at 526 nm. The decision to take measurements at this wavelength was based on a scan of the specified solution over the 200 to 1100 nm range.. The data obtained was converted to a response time graph illustrated on the computer screen as a peak profile. The maximum peak height was automatically

sequential injection system depends on the efficiency of the redox reaction at the inter-face between the solid and liquid phases of SPR. In addition to reactor packing, the reactor length and temperature had major effects and had to be optimized.

5.8.2.1.1 Reactor length

The response and precision of the system were studied by varying the reactor length between 8 and 16 cm (8, 10, 12, 14 and 16cm) with internal diameter fixed at 1.52 mm. A 7 mg/ℓ manganese (II) standard solution was used to optimized the system and the results are shown on Table 5.2. The internal diameter (i.d) of the SPR was kept constant at 1.52 mm because, i.d's smaller than that caused a dramatic deterioration in precision and also cause back pressure, while i.d's larger than 1.52 mm cause the response to drop, hence larger dispersion [8].

TABLE 5.2 Optimisation of reactor length

Reactor length (cm)	Peak height	%RSD
8	0.328	1.3
10	0.318	1.0
12	0.329	3.8
14	0.296	6.4
16	0.314	4.0

From results obtained it was concluded that with a longer reactor all the manganese was oxidized compared to the shorter reactor length. However, the 10 cm reactor length was found to be the ideal one for this type of analysis and was chosen as the optimum. It gave the best precision,

complete oxidation as well as a sharp peak compared to the longer reactors which gave a broad peak, but lower precision. Fig. 5.4 shows the responses and precision of this optimization.

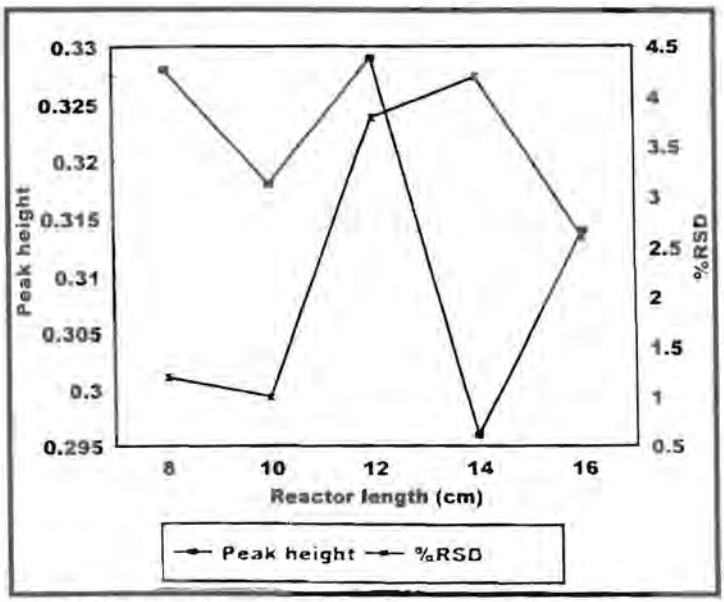

Fig. 5.4 Effect of reactor length on response and precision

5.8.2.1.2 Reactor temperature

The reactor temperature was varied between 60°C and 80°C with optimum results being obtained at 60°C. This confirmed the work done by van Staden and Kluever [8]. The response decreases with increase in temperature due to a faster reaction, and the reproducibility also showed a substantial decrease. Table 5.3 shows the results obtained and Fig. 5.5 the response and precision of this optimization.

TABLE 5.3 Optimization of reactor temperature

Temperature (°C)	Peak height	% RSD
60	0.328	1.2
65	0.318	1.4
70	0.313	1.6
75	0.322	3.4
80	0.247	1.97

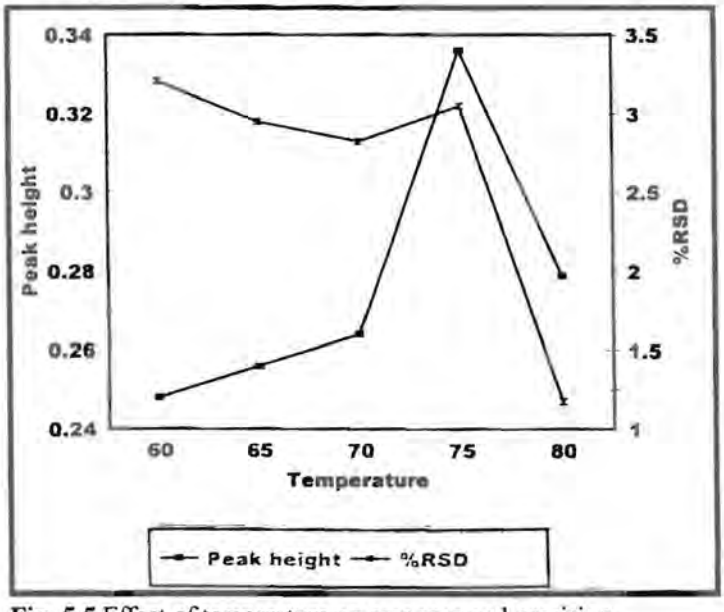

Fig. 5.5 Effect of temperature on response and precision

In the work done by Rüter and Neidhart [29], the highest possible temperature of 90 °C was used. Van Staden and Kluever [8] found this temperature to be unacceptable because of the high %RSD achieved at temperatures above 70°C as well as the problems experience with gas bubbles.

5.8.2.2 Chemical parameters

5.8.2.2.1 Acid concentration

As mentioned in the introduction, acidic conditions are required for the oxidation of Mn^{2+} ions to MnO_4^- ions. A manganese(II) concentration of 7 mg/ℓ was chosen as optimum. However, the choice of acid concentration in the carrier stream should give optimum performances without destruction of the SPR. Originally a problem was experienced with bubble formation when the carrier stream passed the heated reactor. This was at first attributed to a gas formed during the redox reaction, but it was later established that it was due to the carrier when heated. The problem was eventually solved by first bubbling nitrogen through the carrier and designing a glass tubing which trapped and eliminated the bubble before it could reach the detector. The bubble trap was 1 cm long with outlets of 0.76 mm internal diameter and a protrusion of 1 mm internal diameter where the bubble was trapped and destroyed (Fig 5.6).

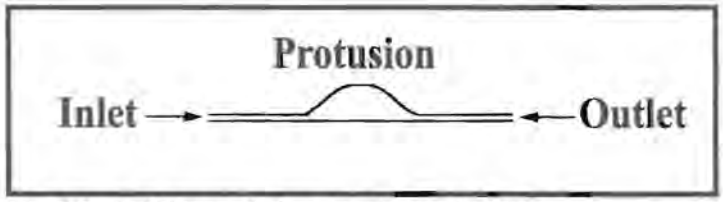

Fig. 5.6 Bubble trap designed to destroy bubbles

The bubble trap slowed down the flow rate because of that protrusion and hence the peak height was decreased by 5%. Table 5.4 shows the response with and without the bubble trap.

TABLE 5.4 Optimization of carrier concentration

(HNO_3) mol/ℓ	With bubble trap		Without bubble trap	
	Peak height	% RSD	Peak height	% RSD
0.05	0.308	3.8	0.3234	4.0
0.10	0.318	3.0	0.3349	3.9
0.15	0.312	1.4	0.3286	2.8
0.20	0.328	1.2	0.3444	2.0
0.25	0.312	1.4	0.3286	2.0

The effect of acid concentration between 0.05 mol/ℓ and 0.25 mol/ℓ was studied. The peak heights increased with increase in acid concentration, as was expected because the reaction is pH dependent. The precision improved between 0.10 and 0.25 mol/ℓ HNO_3 concentration. Below 0.1 mol/ℓ the precision was bad. At a concentration of 0.20 mol/ℓ the precision was 1.2%. Thus 0.20 mol/ℓ was therefore chosen as optimum concentration. This is a slight deviation from the work done by van Staden and Kluever [8] and Rüter and Neidhart [29] who both used 0.10 mol/ℓ as carrier concentration. Fig. 5.7 shows the response and precision of this optimisation.

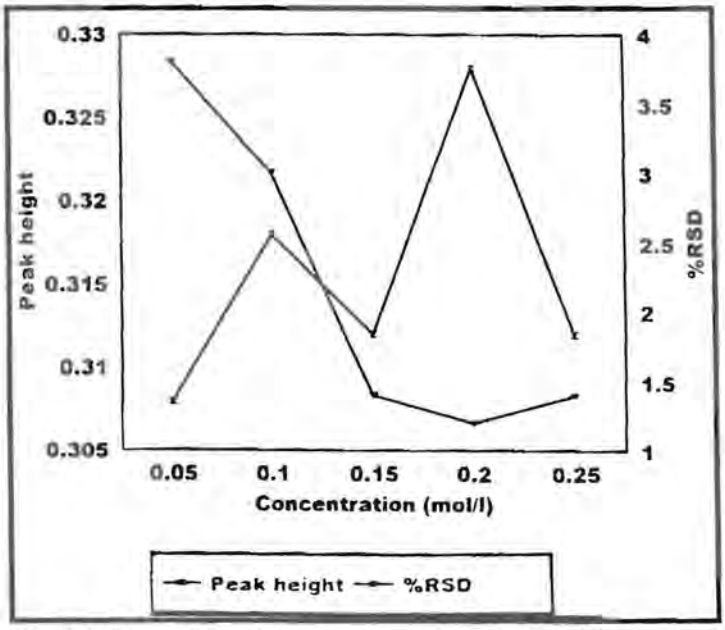

Fig. 5.7 Effect of concentration on response and precision

5.8.2.3 Physical parameters

5.8.2.3.1 Flow rate

The contact time between the sample zone containing manganese (II) and the solid phase reactor (SPR) is of utmost importance for the reaction to give the best analytical results. This period was influenced by the SPR parameters and by the flow rate. Flow rates between 0.9 mℓ/min and 2.5 mℓ/min were evaluated and Table 5.5 shows the results for this optimization.

TABLE 5.5 Optimization of flow rate

Rate (mℓ/ min)	Peak height	% RSD
0.9	0.292	3.8
1.3	0.282	1.5
1.7	0.308	2.7
2.2	0.325	1.2
2.5	0.328	1.7

The peak heights for higher flow rates were almost gaussian, with a small tailing effect due to fast rinsing of the SPR and a narrower longitudinal diffusion, but at the same time the peak heights increased substantially. The reason for this, is that at lower flow rates the manganese(II) took longer to flow through the SPR, producing a longer reaction time resulting in a higher yield of permanganate ions. The optimum flow rate was found to be 2.2 mℓ/min. The relative peak height was 0.33 at this flow rate with a 1.2% RSD. Fig. 5.8 shows the optimization of this flow rate.

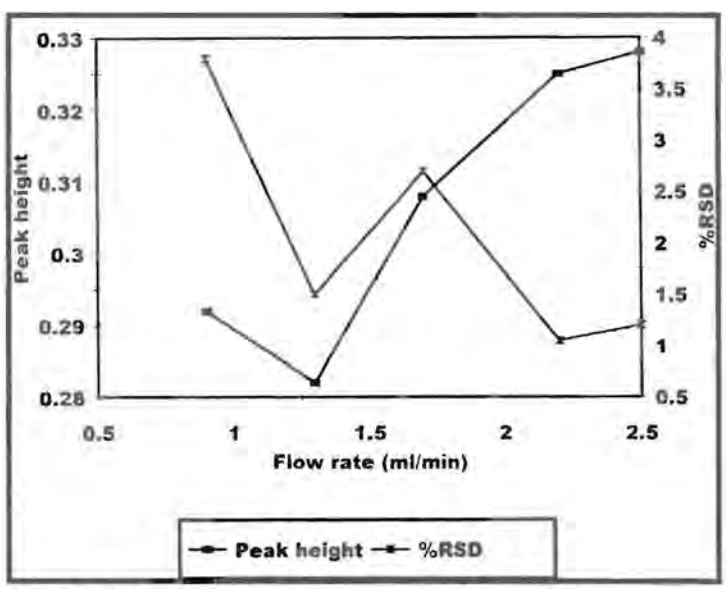

Fig. 5.8 Effect of flow rate on response and precision

5.8.2.3.2 Tube length

The tube length was optimised by distinguishing between the holding coil and the tube between the SPR and the detector. The holding coil was kept constant at a length of 3 m with an internal diameter of 0.76 mm. The tube length was varied between 20 and 60 cm with the internal diameter fixed at 0.76 mm. The optimum length of tubing between the SPR and the detector was 40 cm with a 1.1% RSD, which was the lower limit imposed by the system configuration. Table 5.6 shows the results for the optimization of this tube and Fig. 5.9 shows the response and precision of this optimization.

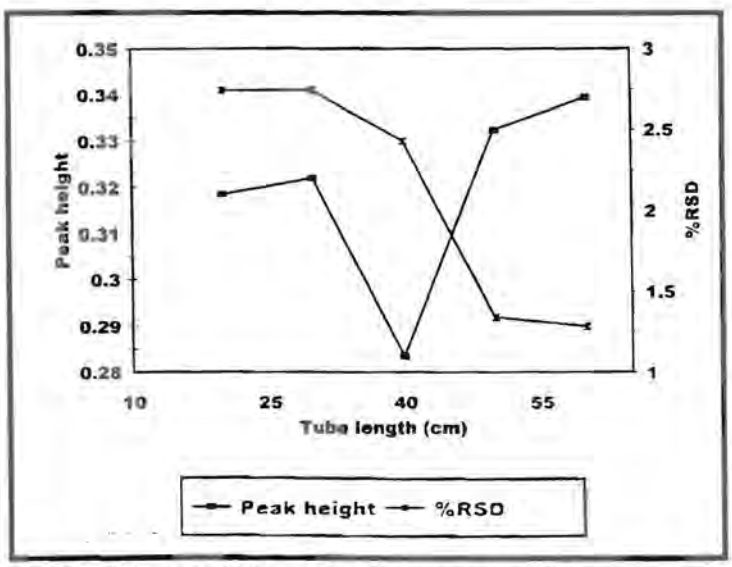

Fig. 5.9 Effect of tube length on response and precision

TABLE 5.6 Optimization of tube length

Tube length (cm)	Peak height	% RSD
20	0.341	2.1
30	0.341	2.2
40	0.330	1.1
50	0.292	2.5
60	0.290	2.7

5.8.2.3.3 Sample volume

The effect of sample volume was evaluated between 60 µℓ and 100 µℓ. Table 5.7 shows the results obtained for this optimization. The peak height increased with increase in volume of the sample, however the precision decreased as well. A value of 80 µℓ was chosen as optimum because it gave by the lowest %RSD of 1.04. Fig. 5.10 shows the response and precision of this optimization.

TABLE 5.7 Optimization of sample volume

Sample volume (µℓ)	Peak height	% RSD
60	0.268	1.2
70	0.273	1.4
80	0.328	1.2
90	0.288	2.3
100	0.338	4.3

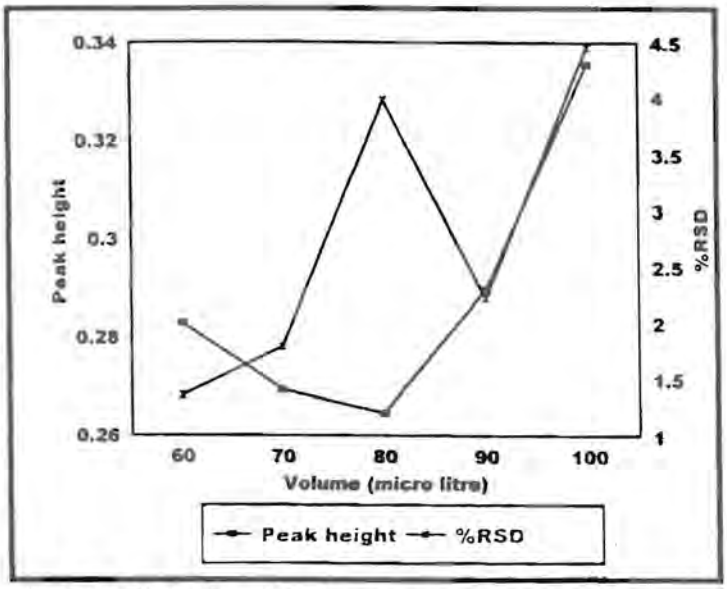

Fig. 5.10 Effect of sample volume on response and precision

5.8.3 Method evaluation

The system was evaluated with regard to linear range, accuracy, precision, detection limit, sample interaction (carry-over), interference, sampling rate and general problems experienced. The optimum conditions used are given in Table 5.8.

TABLE 5.8 Optimum (conditions) parameters

Parameter	**Optimum value**
Reactor length	10 cm
Reactor diameter	1.52 mm
Acid concentration	0.20 mol/ℓ
Flow rate	2.2 mℓ/min
Sample volume	80 µℓ
Tube length	40 cm
Tube diameter	0.76 mm

5.8.3.1 Linearity

The linearity of the SIA system was evaluated for analyte concentration ranging from 1 to 50 mg/ℓ under optimum conditions. The response was found to be linear in the range 1 to 7 mg/ℓ. Fig. 5.11 shows the calibration graph, the linear equation as well as the correlation co-efficient. The relationship obtained between response and concentration is given by the equation:

$$H = 0.01889x + 0.193 \ (r = 0.999, n = 7)$$

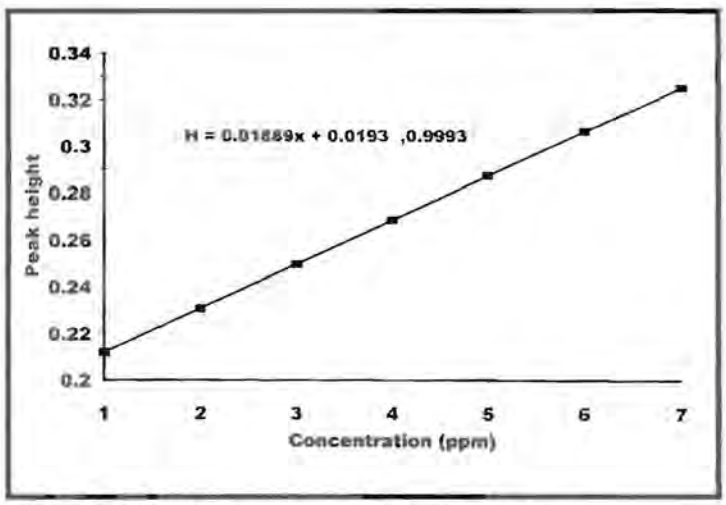

Fig. 5.11 Calibration graph using optimum conditions

where H is the relative peak height and x the analyte concentration (mg/ℓ). Real samples (water for domestic use and effluent streams) were analysed by the proposed SIA system. The results obtained are a mean of 10 repetitive analyses of each sample. Tables 5.9 and 5.10 shows the results obtained with the proposed system and the standard (ICP) method.

TABLE 5.9 Manganese in domestic water samples using SIA and ICP methods*.

Sample	Concentration of Mn in mg/ℓ		Relative standard deviation (%)	
	SIA	ICP	SIA	ICP
A	1.500	1.504	2.9	6.3
B	1.500	1.010	2.6	6.2
C	2.100	2.110	2.7	6.3
D	1.20	1.204	3.0	6.0
E	2.500	2.510	2.8	6.2

*n=10

TABLE 5.10 Manganese in effluent streams using SIA and ICP methods*.

Sample	Concentration of Mn in mg/ℓ		Relative standard deviation (%)	
	SIA	ICP	SIA	ICP
1	12.370	12.440	2.0	1.4
2	5.000	5.010	2.7	6.3
3	5.500	5.510	2.9	6.2
4	5.200	5.220	2.5	6.1
5	5.300	5.330	2.7	6.2

*n=10

5.8.3.2 Accuracy

The accuracy was evaluated by comparing results obtained with those from the standard (ICP) method. The results compared well (Tables 5.9 and 5.10). Since the majority of the tap water samples could only give a response in the SIA procedure after spiking, the accuracy of the method was also determined from these results using the method of standard addition.

5.8.3.3 Recovery

Real tap water samples which were found to contain no manganese at all were spiked with a 5 mg/ℓ standard manganese (II) solution to evaluate the recovery of the system. The formula used is:

$$\%\ Recovery = \frac{obtained}{\exp ected} x100\%$$

The expected concentration of manganese(II) for effluent streams spiked with 5.00 mg/ℓ Mn(II) standard solution was calculated with the calibration curve. The sample was analysed and the concentration (4.75 mg/ℓ) was compared with the expected concentration as shown above. The recovery ranged between 96.86 to 103.35 %.

5.8.3.4 Precision

The precision of the method was determined by 10 repetitive analyses of real sample solutions (Tables 5.9 and 5.10) as well as 10 repetitive analyses of standard solutions ranging from 1 to 7 mg/ℓ (calibtration graph, Fig 5.11). All these were carried out under optimum conditions. The % RSD for the standard solution was less than 1.8% and for real samples less than 2.9%.

5.8.3.5 Sample inter-action

The sample inter-action or carry-over was calculated according to the following formula:

$$\text{Interaction} = \frac{A_3 - A_1}{A_2} \text{ x } 100$$

$$\text{Interaction} = \frac{A_3 - A_1}{A_2} \times 100$$

where A_1 = peak height for sample without interaction

A_2 = peak height for sample with ten times the concentration of A_1

A_3 = peak height for interacted sample with the same concentration as A_1

In this study, A_1 was obtained with a 7 mg/ℓ manganese(II) standard solution and A_2 with a 70 mg/ℓ manganese(II) standard solution. A_3 was obtained by running in A_1 after having run in A_2. The values for A_1 and A_3 were 0.325 and 0.385 respectively. The value for A_2 was 6.12 giving an interaction value of 0.98% at a sampling rate of 50 samples per hour.

5.8.3.6 Detection limit

The detection limit was calculated using the formula:

$$DL = \frac{[(3\sigma + K) - C]}{m}$$

where $\sigma = 0.0016$ is the standard deviation of the baseline,

$K = (0.20)$ average signal value of the baseline

$C = 0.193$, which is the intercept of the calibration graph

$m = 0.01889$, which is the slope of the calibration graph.

The calculated detection limit was found to be 0.62 mg/ℓ.

5.8.3.7 Interferences

According to the work done by Rűter and Neidhart [30] only interferences for the determination of permanganate at 520 mm are reducing substances and coloured metal ions (iron(III), nickel(II), vanadium(V), copper(II), cobalt(II)) in high concentration as well as anions (halides, sulphate, phosphate, carbonate, acetate, thiocyanate, oxalate, sulphite).

In this determination at 526 nm the only ion found to be present in detectable amounts was iron (Fe) in the range 0.286 - 0.835 mg/ℓ. This did not cause any interference as the interference or tolerance level was found at 5 mg/ℓ. Finally the amount of manganese in the household water collected was found to contain very little amounts of manganese.

5.8.3.8 Sampling rate

The time taken for samples with low concentrations is 50 seconds per sample. The increased time is due to longer return-to-baseline times, implying longer washing-out times for flow cell. Thus a range of sampling rates are obtained varying between 50 and 72 samples per hour, depending on the manganese(II) concentration.

5.8.3.9 General problems

As was mentioned in subsection 5.8.2.2.1, the biggest problem encountered with this system was the bubbles that formed when the carrier passed through the water-bath. As mentioned the problem could be overcome by bubbling nitrogen through the carrier and placing a bubble trap between the detector and the water-bath (at ambient temperature).

Another problem was leaving the packed reactor in the laboratory exposed to the atmosphere. It was found that the response deteriorated compared to a freshly packed reactor. This problem was solved by storing the packed reactors in a dessicator until use.

5.9 Statistical comparison of techniques used

The statistical comparison was done between the SIA and ICP (standard method) to establish whether the proposed SIA method can be accepted as giving reliable results in manganese determination. The null hypothesis was used [40, 41]. For the null hypothesis, Ho we assert that the two methods agree, that is, the population mean difference is zero, H_o: $\mu_d = 0$. For the alternative hypothesis H_t:$\mu_d \neq 0$, where μ_d is the population paired by difference. The t-test with multiple samples (paired by difference) was applied to examine whether the two methods differed significantly at 95% level. The test is two tailed, as we are interested in both $\mu_d<0$ and $\mu_d>0$.

The mean, $\bar{x}_d$ standard deviation, S_d and $t_{calculated}$, $t_{calc.}$ are determined from the following equations:

$$\bar{x}_d = \frac{\sum x_d}{N}$$

$$S_d = \sqrt{\frac{\sum (x_d - \bar{x}_d)^2}{N-1}}$$

and

$$t_{calc.} = |\bar{x}_d| x \frac{\sqrt{n}}{s_d}$$

Table 5.11 gives the mean differences between SIA and ICP results for domestic water.

TABLE 5.11 Differences between SIA and ICP results for domestic water

Sample	x_{di}	$x_{di}^2 \times 10^{-4}$
A	0.004	0.16
B	0.010	1.0
C	0.010	1.0
D	0.004	0.16
E	0.010	1.

From Table 5.11 the following is deduced:

$$\sum x_{d1} = 0.038$$

and

$$\sum x_{d1}^2 = 3.32 \times 10^{-4}$$

Substituting for the mean and standard deviation with N = 5, we obtain:

$$\bar{x}_{d1} = 0.0076$$

and

$$S_{d1} = 0.0068$$

Table 5.12 gives the mean differences between SIA and ICP results for for effluent streams

TABLE 5.12 Differences between SIA and ICP results for effluent streams.

Sample	x_{d2}	x_{d2}^2
1	0.07	0.0049
2	0.01	0.0001
3	0.01	0.0001
4	0.02	0.0004
5	0.03	0.0009

From Table 5.12 the following is deduced:

$$\Sigma x_{d2} = 0.014 \qquad \text{and} \qquad \Sigma x_{d2}^2 = 0.0064$$

Substituting for the mean and standard deviation with N = 5, we obtain:

$$\bar{x}_{d2} = 0.0028$$

and

$$S_{d2} = 0.0397$$

From Table 5.11, $\bar{x}_{d1} = 0.0076, S_{d1} = 0.0068$ and $n = 5$.

Substituting for t_{calc} we find:

$$t_{calc} = 2.48$$

From Table 5.12, $\bar{x}_{d2} = 0.0028, S_{d2} = 0.0397$ and $n = 5$.

Substituting for t_{calc} we find:

$$t_{calc} = 0.1574$$

For both the determinations of manganese in tap water and effluent streams, there are five determinations, therefore $v = 4$. At 95% confidence level $t_{0.05,4}$ is 2.78. The critical t-values are therefore ±2.78. Since the calculated value is less than the critical value, the null hypothesis, H_0 cannot be rejected and it follows that at 95% of all samples drawn from the same population have a mean content within the acceptable range or only 5% of such samples fall outside the acceptable range. Hence it may be concluded that there is no significant statistical difference between the SIA and ICP techniques.

5.10 Conclusions

Mn determination by SIA with a solid-phase reactor incorporated into the SIA manifold is an improvement on the FIA system. In contrast to FIA, SIA once designed, does not need to be

physically reconfigured, even if essential parameters such as flow rates, sample and reagent volumes, reactant ratios and reaction times are to be altered. The system is easier to use and has the advantage of material saving. The system was found to be suitable for manganese determination in tap and domestic waters and effluent streams with a relative standard deviation of better than 3%.

5.11 References

1. F. A. Cotton and G. Wilkinson, **Advanced Inorganic Chemistry-A Comprehensive text,** Wiley & sons, New York, 1980.
2. J. V. Quagliano and L. M. Vallarino, **Chemistry 3rd ed.,** Prentice Hall, New Jersey, 1969.
3. E. Griffen and J. Am, **Water works Assoc., 52** (1960) 1326.
4. D.A. Crerar, R..K. Cormick, H. L. Barney. **General problems:** ***Geology and Geochemistry of Manganese,*** Ed by J. Varentsov and G. Grasselly; Springler verslag, Stuttgort, Germany, 1980.
5. W. Stumm, **Chemical processes lakes,** Wiley& sons, New York, 1985.
6. J. J. Delfino and G. F. Lee, **Environ. Sci. Technol. 2.,** (1968) 1094.
7. W. Balzer, **Geochim. Cosmochim. Acta, 46** (1982) 1153.
8. J. F. van Staden and L. G. Kluever, **Anal. Chim. Acta, 350** (1997)15.
9. K. Kargosha and M. Noroozifar, **Anal. Chim. Acta, 413** (2000) 57.
10. W. L. Masterdom, E. J. Slowinski and C. L Stanitski, **Chemical Principles with qualitative analysis,** Saunders, U.S.A, 1986.
11. A. Tulinsky and B. M. L Chen, **J. Am. Chem. Soc., 199** (1977) 3647.
12. C. E. Bomberger and D. M. Richardson, **J. Inorg. Nucl. Chem., 39** (1977)151.
13. C. Kies, **Nutritional Bio-availability of Manganese:** ***ACS Symposichem. Series 354, Am. Chem. SCC.,*** Washington, 1987.
14. J. Hauck, **Inorg. Nuch. Chem. Lett., 12** (1976) 893.
15. M. W. Coleman and L. T. Taylor, **Inorg. Chem., 16** (1977) 1114.
16. L. J. Boucher, **Co-ord. Chem. Rev., 7** (1972) 289.

17. A. H. Goodman, **Potable water Quality:** ***Developments in water treatment-2,*** Ed. by W. M. Lewis, Applied Science, London, 1980.

18. H. H. Sandstead, **J. Lab. Clin. Med., 98** (1981) 457.

19. G. K. Davis, **Ann. New York Alad. Sci., 355** (1980)130.

20. A. Wise, **Nutr. Abstr. Rev., Ser. A, 50** (1980) 319.

21. W. G. Pond, E. F. Walker jr., D. Kirkland, **J. Anim. Sci., 41** (1975) 1053.

22. A. R. Bowie, P. R. Fielden, R. D. Lowe and R. D. Snook, **Analyst, 120** (1995) 2119.

23. A. Gaikwad, M. Silva and D. Perez-Benditio, **Anal. Chim. Acta, 302** (1995) 275.

24. J. Ružička, E. H. Hansen, **Flow Injection Analysis, 2nd ed.,** Wiley & sons, New York, 1988.

25. Valcarsel, M. D. Luque de Castro, **Flow Injection Analysis. Principles and Applications,** Horwood, Chichester, 1987.

26. J. L. Burguera, **Flow Injection Atomic Spectrometry,** Marcel Dekker, New York, 1987.

27. M. D. Luque de Castro, **Trends Anal. Chem., 11** (1992)149.

28. J. Martinez Calatayud and J. V. Garcia Mateo, **Trends Anal. Chem., 12** (1993) 428.

29. J. F. van Staden and L. G. Kluever, **Anal. Chim. Acta, 369** (1998) 157.

30. J. Rűter and B. Neidhart, **Microchim. Acta., 18** (1984) 271.

31. J. Ružička and G. D. Marshall, **Anal. Chim. Acta, 237** (1990) 329.

32. J. Ružička, G. D. Marshall amd G. D. Christian, **Anal. Chem., 62** (1990) 1861.

33. G. D. Marshall, **Sequential-Injection Analysis,** PhD-thesis, University of Pretoria, 1994.

34. J. Ružička and T. Gűbeli, **Anal. Chem., 63** (1991) 1680.

35. T. Gűbeli, G. D. Christian and J. Ružička, **Anal. Chem., 63** (1991) 2407.

36. D. J. Tucker, B. Toivola, C. H. Pollema, J. Ružička and G. D. Christian, **Analyst, 119**

(1994) 975.

37. G. D. Marshall and J. F. van Staden, **Process Control and Quality, 3** (1992) 251.

38. E. B. Naidoo and J. F. van Staden, **Fresenius J. Anal. Chem., 370 (6)** (2001) 776.

39. G. D. Marshall and J. F. van Staden, **Analytical Instrumentation, 20** (1992) 79.

40. D. McCormick and A. Roach, **Analytical Chemistry by open learning. Measurement, Statistic and Computation.** Wiley and sons, Chichester, 1995.

41. D. A. Skoog, D. M. West and F. J. Holler, **Fundamentals of Analytical Chemistry, 7th ed.** Saunders, USA,. 1996.

CHAPTER 6

Determination of iron as Fe(II) in multi-vitamins, haematinics and natural waters using a sequential injection analysis (SIA) system.

6.1 Introduction

Iron is the second most abundant metal, after aluminium, and fourth most abundant element in the earth's crust. The core of the earth is believed to consist mainly of iron and nickel, and the occurrence of many iron meteorites suggests that it is abundant throughout the solar system. The major iron ores are hematite (Fe_2O_3), Magnetite (Fe_3O_4), Limonite [FeO(OH)], and Siderite ($FeCO_3$) [1].

However, from a biological viewpoint iron falls into the category of trace elements, which are most conveniently classified as essential, non-essential and toxic. The trace elements classified as essential for plants are those elements which cannot be substituted by others in their specific biochemical roles and that have a direct influence on the organism so that it can neither grow nor complete some metabolic cycle. In human and animals systems, trace elements are defined as being essential if depletion consistently results in a deficiency syndrome and repletion specifically reverses the abnormalities. Deficiency of iron causes anaemia and excess causes

liver cirrhosis and haemochromatosis.

The iron containing proteins in a normal adult are haemoglobin, myoglobin, transferrin, ferritin, hemosiderin, catalase, cytochrome *C*, peroxidase, cytochrome and oxidase, flavoprotein dehydrogenase, oxidases and oxygenases.

A wide range of human activities contributes to iron pollution of the aquatic environments. The major activities including mining, industrial processing, agricultural and domestic effluents of sewage, the impact of iron input, duration of input, physical and chemical form and associated ligands or chemicals [2].

Iron occurs primarily in two oxidation states, Fe(II) and Fe(III). In deep waters, especially in lakes where there is no oxygen, iron is in the Fe(II) state and in surface water it is in the Fe(III) state.

The maximum admissible concentration in water recognised by the European Economic Community (EEC) Directive on Quality of water for Human Consumption is 0.2 mg/ℓ while the guide value which is desirable is given as 0.05 mg/ℓ. The Russian standards, the World Health Organisation (WHO) and the EEC Surface Water Directive allows values up to 0.3, 0.1 and 2 mg/ℓ respectively. However, in most potable water supplies a concentration of 0.05 mg/ℓ would appear to be a satisfactory upper limit [3]. It is however, important to understand the specific range of iron concentration the body allows; which will in turn dictate the daily requirement. The daily requirement for men is 10 mg and 15 mg for women [6]. But, Heinrich *et al.* [7] has shown that the amount of average requirement is 1.5 mg/day in males and non-

menstruating females and 14.8 mg/day in menstruating females.

The high presence of iron can give rise to an astrigent taste, discolouration, deposits of rusts and could promote iron bacteria growth.

Finally, iron is vital and required for various biological features in the human body. Deficiency are known to occur in vulnerable populations such as pregnant women, infants and children as well as mal-nutritioned individuals. In order to avoid such deficiencies, an adequate supply of iron that can be utilized for biological functions is needed. Individual components of the diet and iron status of each individual will affect the bio-availability [6]. However, besides diet iron requirements may be supplied by administering multivitamins and haematinics.

6.2 The biochemistry and biological uses of iron

Trace amounts of iron is truly ubiquitous in living systems. It is versatile and unique. It is important for the prevention of anaemia. It is at the active centre of molecules responsible for oxygen transport and electron transport and it is found in, or with, such diverse metalo-enzymes as nitrogenases and dehydrases.

The iron containing proteins in a normal adult perform a specific function as is given by the following proteins:

Haemoglobin - oxygen transport in plasma

Myoglobin - oxygen storage in muscle

Transferrin - iron transport via plasma

Hemosideria - iron storage in cells

Catalase - metabolism of H_2O_2

Cytochrome - terminal oxidation

Cytochrome and oxidase - terminal oxidation

Peroxidase - metabolism of H_2O_2

Flavo protein dehydrogenase,

oxidases and oxygenase - oxidation reactions, incorporation of molecular oxygen [1].

Iron is used or administered to iron deficiency subjects to prevent anaemia. However, if not monitored on individual with excess it may cause liver cirrhosis and haemochromatosis.

6.3 Choice of analytical method

The determination of iron in its various oxidation states in a variety of matrices has been studied and described by numerous researchers [7-12]. Methods used include kinetic spectrometry [8-11], Polarography [13] Graphite Furnace Atomic Absorption Spectrometry (GFAAS) [13] and Flame Atomic Absorption Spectrometry (AAS) [14]. Most of these classical technique have been modified for use in-flow system by making use of the flexibility and ease offered by flow injection analysis (FIA) [9, 15-17].

Speciation of Fe(III) and Fe(II) [18-20] was also described. Faizullah and Townshed [21] determined Fe(II) after complexing with 1,10 Phenanthroline, then reducing the Fe(III) present

with a reducing column. Lynch *et al.* [22] described the use of different complexing agents in the same manifold for determining Fe(II) and Fe(III).

Simultaneously, Masatoshi and Shigeki [23] developed a method for the sequential spectrophotometric determination of Fe(III) and Fe(II) by a copper(II) catalysed reaction with Tiron in a double-injection flow injection system. Oliveira *et al.* [24], proposed an asynchronous merging zones method with simultaneous introduction of the sample and modifier (ascorbic acid) for sequential determination of Fe(II) and Fe(III) in pharmaceutical products. Luque-Perez *et al.* [25] indirectly determined ascorbic acid by reducing Fe(III) to Fe(II) with ascorbic acid and monitoring the Ferroin complex spectrophotometrically. Van Staden and Kluever [26, 27] modified an existing FIA homogeneous system to a heterogeneous systems by incorporating solid-phase reactors into the FIA manifolds.

The homogeneous SIA technique was also used for the determination of iron [28-30]. This technique launched in 1990 [31, 32], is a technique that has great potential for on-line measurement in many routine laboratories due to its simplicity and the convenience with which sample manipulation can be automated. The pre-requisite needed for the determination of iron, in pharmaceutical products and natural waters, was an enhanced technique, which is robust and versatile, reliable with a low frequency of maintenance. The system should be simplified with fewer junctions for reagents and less sample preparations and carrier streams. SIA seemed the ideal technique for this analysis.

6.4 Total iron determination

An iron(III) sample was reduced on-line to iron(II) by a cadmium reductor incorporated into SIA manifold, complexed with 1,10 Phenantroline to a red stable complex and detected at 515 nm with a UV/VIS spectrophotometer[33]. The choice of this wavelength was made after a scan of the standard solution over a range of 200 - 1100 nm.

6.4.1 Experimental

6.4.1.1 Reagents and solutions

All solutions are prepared from analytical grade reagents unless specified otherwise. De-ionised water from a Molulab system (Continental Water Systems, San Antonio, TX, USA) was used to prepare all aqueous solutions and dilutions.

6.4.1.1.1 Stock iron (II) solution

A stock iron(II) solution containing 1000mg/l iron(II) was prepared by dissolving $FeSO_4 \cdot (NH_4)_2SO_4 \cdot 6H_2O$ (Kanto Chemical Co., extra pure) and diluting to 1 litre with water. Working standards in the range 1 to 100 mg/ℓ were prepared by appropriate dilution of the stock solution with 0.01 mol/ℓ perchloric acid.

6.4.1.1.2 Perchloric acid solution

A 0.01 mol/ℓ perchloric acid was prepared by diluting 4.4 mℓ of perchloric acid (Merck, GPR, 70%) to 5 ℓ with deionised water.

6.4.1.1.3 1.10 Phenanthroline solution

.A 0.25% 1,10 Phenanthroline solution (Aldrich, 99+%) was prepared by dissolving 0.625 g of 1,10 Phenanthroline in 50 ml 0.01 mol/ℓ perchloric acid and diluting to 250 mℓ with water.

6.4.1.1.4 Acetic acid solution

A 0.1 mol/ℓ acetic acid solution was prepared by diluting 1.45 mℓ of acetic acid (Chemical suppliers, 99.9%) to 250 mℓ with deionised water.

6.4.1.1.5 Hydroxyl ammonium chloride solution

A 10% hydroxyl ammonium chloride (Searle, GPR, 97%) was prepared by dissolving 10 g in water and making up to 100 mℓ with deionised water.

6.4.1.1.6 Sodium acetate solution

A 0.1 mol/ℓ sodium acetate solution was prepared by dissolving 1.36 g of sodium acetate (Merck, extra pure) in water and making up to 100 mℓ.

6.4.1.1.7 Buffer solution

A buffer solution in the pH range range 3 to 5 was prepared by mixing 65 mℓ of 0.1 mol/ℓ acetic acid solution with 35 mℓ 0.1 mol/ℓ sodium acetate solution and adding 1 ml of 10% hydroxyl ammonium chloride to the resulting solution.

6.4.1.1.8 Hydrochloric acid solution

A 1 mol/ℓ HCl solution was prepared by diluting 100 mℓ of concentration HCl (Merck, 32%) and making up to a litre. chloroform (Merck, pro analysis) was used to extract the unwanted organic material from the samples.

6.4.1.2 Instrumentation

A sequential injection system is depicted in Fig. 6.1. It was constructed from the following components:

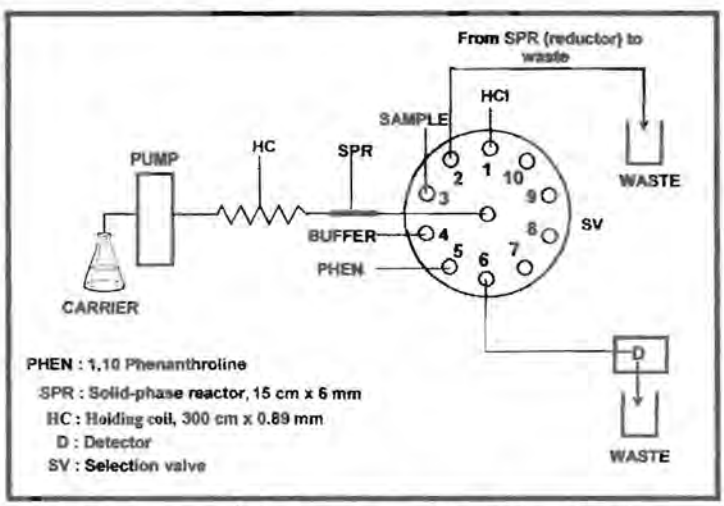

Fig. 6.1 A diagram of a SIA system used in this investigation

a Gilson minipuls peristaltic pump (Model M312, Gilson, Villiers-Le Bel, France); a 10-port electrically actuated selection valve (Model ECSDIOP, Valco Instruments, Houston, Texas) and a Unicam 8625 UV-Visible spectrophotometer equipped with a 10-mm Hellma-type (Hellma GmbH and Co., Mulheim/Baden, Germany) flow- through cell (volume 80 $\mu\ell$) for absorbance measurements.

Data acquisition and device control was achieved by using a PC30-B interface board (Eagle Electric, Cape Town) and an assembled distribution board (Mintek,Randburg). The flowTEK [34] software package (obtainable from Mintek) for computer-aided flow analysis was used throughout for device control and data acquisition.

6.4.1.3 Operation of the system

The whole SIA procedure involved designing a method which allows a single cycle of the experiment to be run. Fig. 6.2 and Table 6.1 shows the device sequence for one cycle.

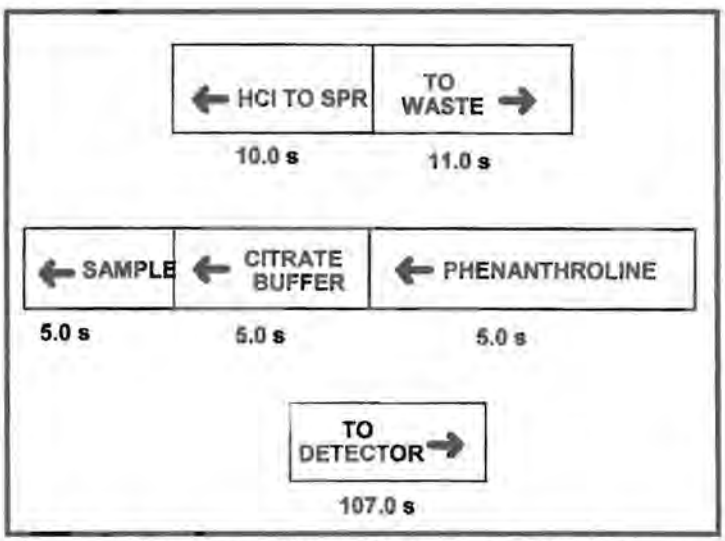

Fig. 6.2 Device sequence diagram for one cycle of the SIA system

The whole procedure, from sample injection to data processing and storage was computer controlled via flowTEK program.

TABLE 6.1 Device sequence for one cycle of the SIA system

Time (s)	Pump	Valve	Description
0	Off	Position 1	Pump off. Select HCl stream.
1	Reverse		Draw HCl solution through SPR for regeneration.
10	Off		Pump stop.
11	Off	Position 2	Select waste stream.
12	Forward		Pump solution from SPR to waste
23	Off		Pump stop
24	Off	Position 3	Select sample stream
25	Reverse		Draw sample
29	Off		Pump stop
30	Off	Position 4	Select buffer stream
31	Reverse		Draw buffer solution
35	Off		Pump stop
36	Off	Position 5	Select 1.10 Phenanthroline stream
37	Reverse		Draw 1.10 Phenanthroline
41	Off		Pump stop
42	Off	Position 6	Select detector stream
43	Forward		Pump zones through reductor to detector
150	Off	Position 1	Valve return home

The zones were stacked in the holding coil and then transported by the carrier stream (0.01 mol/ℓ perchloric acid) through the reactor where all the iron(III) that may be present is reduced to iron(II). The iron(II) then complexes with 1,10 Phenanthroline and is detected at 515 nm with

a spectrophotometer. The working wavelength at 515 nm was established by scanning the standard solution from 200 to 1100 nm.

The complex formation can be described by the equation:

$$Fe^{2+} + 3\ pheH^{+} \rightarrow Fe(phe)_3^{2+} + 3\ H^{+}$$

The data obtained is then converted to a response time graph on the computer screen as a peak profile. The maximum relative peak height was then automatically processed and stored on a computer via the FlowTEK program.

6.4.1.4 The solid-phase reactor preparation

The reactors were made of glass with varying lengths (12, 15, 17, 19 and 21 cm) but with the same internal diameter of 6 mm. Fig. 6.3 shows such a reactor. The columns were then filled with cadmium granules (Merck, 0.3-1.5 mm).

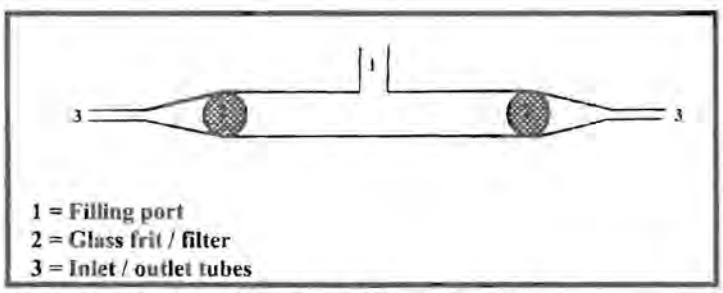

Fig. 6.3 A diagram of the cylindrical reactor used

The particles were held by a glass frit at each end so that they did not block the SIA system. A vibrator was used for close packing of the columns. The cadmium granules used for packing the glass column were prepared by washing with acetone for 10 minutes, adding 2 mol/ℓ hydrochloric acid, de-ionised water and methanol and dried in a desiccator. An acidified cadmium reactor was chosen over a copperised one because copper has a tendency of interfering in the determination of iron. The cadmium reactor was regenerated by passing approximately 470 $\mu\ell$ of 1 mol/ℓ hydrochloric acid at the beginning of every cycle. This was to ensure consistency in the reduction efficiency and capacity of the reactor.

6.4.1.5 Sample preparation

The multivitamin and haematinic samples were digested in 50 mℓ (6% V/V) hydrochloric acid on a hot plate. When a fifth of the solution was remaining a further 30 mℓ of the (6% V/V) hydrochloric acid was added and the digestion continued until approximately 10 mℓ was remaining. Three 50 mℓ portions of chloroform (Merck, pro analysis) were added to the samples with vigorous shaking to separate the organic material from the inorganic. The separation at each instance was allowed two hours. A final 50 mℓ portion was added and left overnight for final separation.

The aqueous layer was collected into a 100 mℓ standard flask and made to volume with a 0.01 mol/ℓ perchloric acid solution. Further dilutions were made from the prepared samples to bring their concentrations within detectable range in the SIA system.

6.4.2 Method optimization

The method was optimised with regard to the following parameters: iron(II) concentration, flow rate, sample and reagent volume, reactor length, carrier type and hydrochloric acid concentration for reactor regeneration (reactor efficiency). Both the relative peak height and % RSD were used as criteria for establishing the most appropriate parameter value in each case.

6.4.2.1 Solid-phase reactor

The cadmium reactor forms the heart of the manifold of the proposed system. The performance of the SIA system depends on the efficiency of the reactor at the interface between the solid and the liquid phases of the cadmium reactor. In addition the reactor packing had to be thorough and the reactor length and efficiency had to be optimised.

6.4.2.1.1 Reactor length

The response and precision of the system were studied by varying the reactor length between 12 and 21cm with the internal diameter fixed at 6 mm. The five reactors (12, 15, 17, 19 and 21 cm) were compared for reduction efficiency. It was found from the results obtained (Table 6.2) that the first three cadmium reactors did not show a significant difference in response; there was, however for the longer lengths. The 15 cm reactor length was chosen as the optimum length because of its good precision as seen in Table 6.2. Fig.6.4 shows the effect of reactor length on response and precision.

TABLE 6.2 Effect of reactor length on response and precision

Length (cm)	12	15	17	19	21
Relative peak heights	5.262	5.281	5.31	5.872	6.521
% RSD	2	1.1	5.8	5.34	4.38

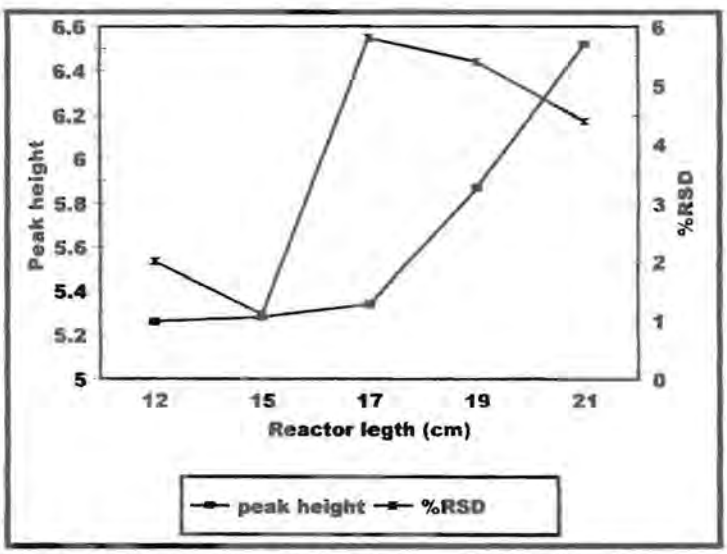

Fig. 6.4 Influence of reactor length on response and precision

6.4.2.2 Chemical parameters

6.4.2.2.1 Fe(II) concentration

The Fe(II) concentration was evaluated between 1 to 100 mg/ℓ. The effect of concentration is presented in Table 6.3 and Fig. 6.5. It is clear from Figure 6.4 that the response steadily increases with an increase in concentration. The 50 mg/ℓ concentration gave the best precision and was chosen as the optimum concentration.

TABLE 6.3 Effect of Fe(II) concentration on response and precision

Concentration mg/ℓ	Peak height	% RSD
1	0.304	1.43
10	1.145	0.68
20	2.166	1.7
30	3.206	1.57
40	4.337	1.28
50	5.329	0.42
60	6.230	1.92
70	7.458	1.5
80	8.260	1.9
90	8.834	0.8
100	8.841	1.0

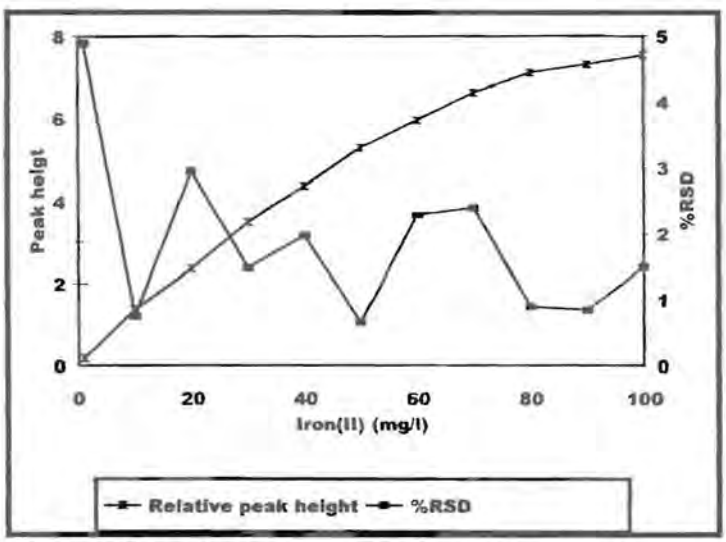

Fig. 6.5 Effect of iron (II) concentration on response and precision

6.4.2.2.2 Carrier concentration

The use of 1 mol/ℓ hydrochloric acid as both reactor regeneration and carrier could not work because bubbles were given off now and then. However, the use of 0.1 mol/ℓ perchloric acid resulted in a better consistency in response and there were no bubbles. The perchloric acid concentration was then studied between 0.005 and 0.1 mol/ℓ and the results given in Fig. 6.6 and Table 6.4. The response increases up to a concentration of 0.05 mol/ℓ. The best precision was however given by a concentration of 0.01 ml/ℓ which was chosen as the optimum.

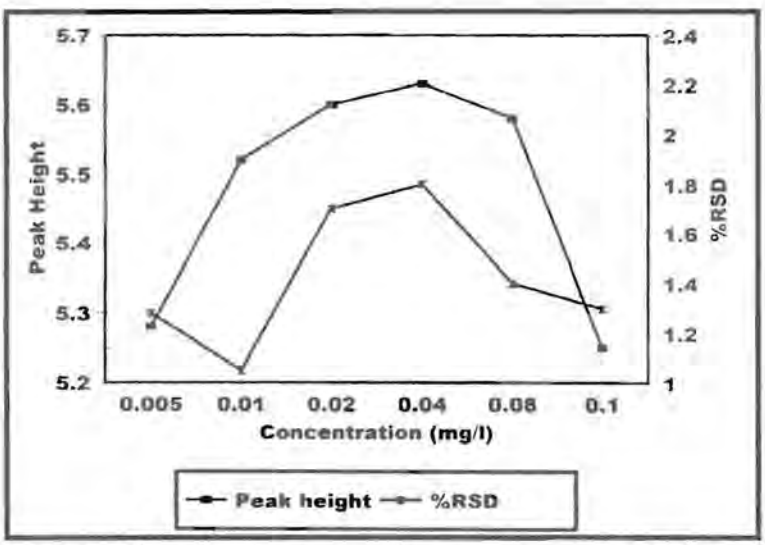

Fig. 6.6 Effect of carrier concentration on response and precision

TABLE 6.4 Effect of carrier concentration on response and precision

Concentration mg/ℓ	Peak height	% RSD
0.005	5.28	1.28
0.01	5.52	1.05
0.02	5.6	1.7
0.04	5.63	1.8
0.08	5.58	1.4
0.1	5.25	1.3

6.4.2.3 Physical parameters

The contact time between the iron and the cadmium reactor is of utmost importance. It was however, found that most of the iron in the pharmaceutical preparation is in the Fe(II) state, with very little in the Fe(III) state. Although the amount of iron present in the water samples analysed was lower, all the iron was in the Fe(III) state and had to be reduced. The 15 cm reactor was found to be optimum and effective with 470 $\mu\ell$ 1 mol/ℓ HCl passed through the reactor for every SIA cycle.

6.4.2.3.1 Flow rate

The flow rate was evaluated between 1.13 and 3.96 mℓ/min. The results and effect of this are illustrated in Table 6.5. Fig. 6.7 shows the response and precision of this optimization. The response increases with an increase in flow rate, due to less dispersion and better zone overlapping. The 2.83 mℓ/min flow rate however gave the best precision and was chosen as

optimum.

TABLE 6.5 Effect of flow rate on response and precision

Rate (mℓ/min)	1.13	1.71	2.26	2.83	3.29	3.96
Relative peak heights	0.557	1.929	2.544	3.612	3.951	4.033
% RSD	5.6	4.6	3.3	2.1	2.4	7.5

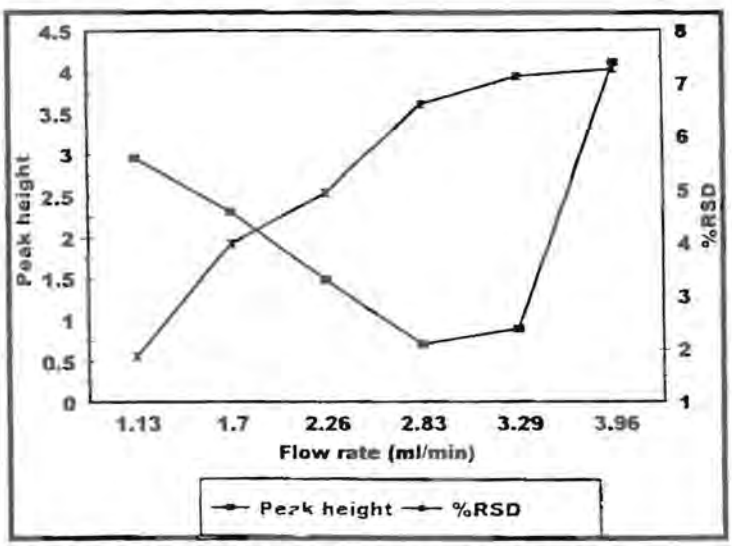

Fig. 6.7 Influence of flow rate on response and precision

6.4.2.3.2 Sample volume

Sample volume was evaluated from 142 to 424 $\mu\ell$ and the results are given in Table 6.6. Fig. 6.8 gives the response and precision of this optimisation. Although the sensitivity increases with an increase in sample volume, the best precision was obtained with a sample volume of 236 $\mu\ell$ which was chosen as optimum sample volume.

TABLE 6.6 Effect of sample volume on response and precision

Volume (mℓ)	142	236	330	424
Relative peak heights	2.847	3.951	4.404	4.376
% RSD	3.3	2.4	3.2	3.1

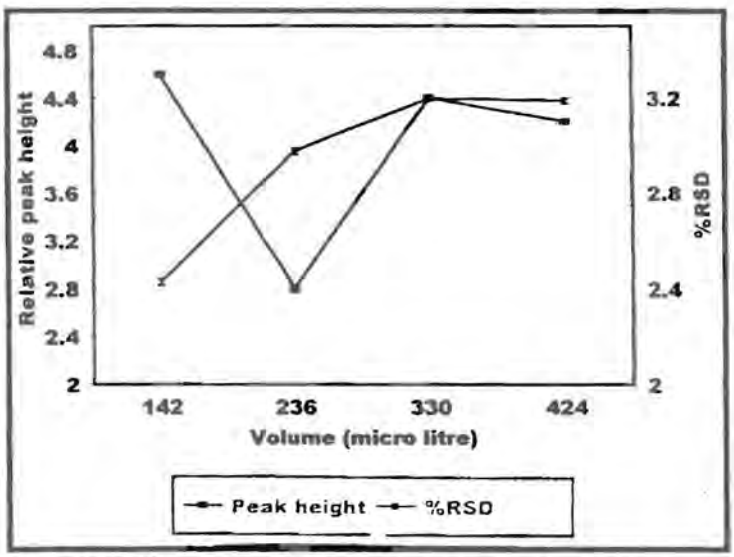

Fig. 6.8 Effect of sample volume on response and precision

6.4.2.3.3 Reagent volume

The reagent volume was evaluated from 94 to 283 $\mu\ell$ (Table 6.7). A volume, 236 $\mu\ell$ was chosen as optimum reagent volume due to the best precision. Fig. 6.9 gives the response and precision for this optimization.

TABLE 6.7 Effect of reagent volume on response and precision

Volume (mℓ)	94	142	189	236	283
Relative peak heights	1.766	4.464	6.847	8.62	8.72
% RSD	2.9	3.2	1	0.8	4.2

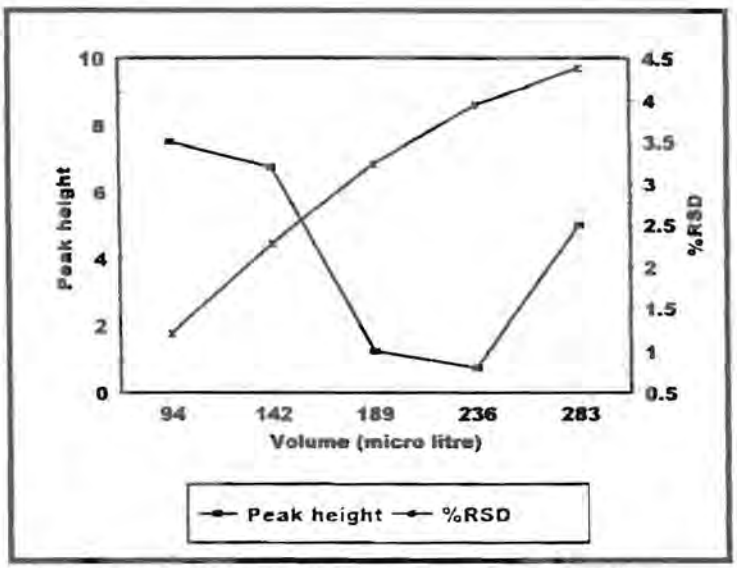

Fig. 6.9 Effect of reagent volume on response and precision

6.4.3 Method evaluation

6.4.3.1 Linearity

The linearity of the system was evaluated for the analyte concentration between 1 and 100 mg/ℓ. The response was found to be linear in the range 1 to 60 mg/ℓ (Fig. 6.9). The relationship between the response and the concentration is given by the equation:

$$H = 0.149x + 0.1722, (r = 99.99\%, n = 10),$$

where H is the relative peak height and x the analyte concentration in parts per million mg/ℓ(ppm).

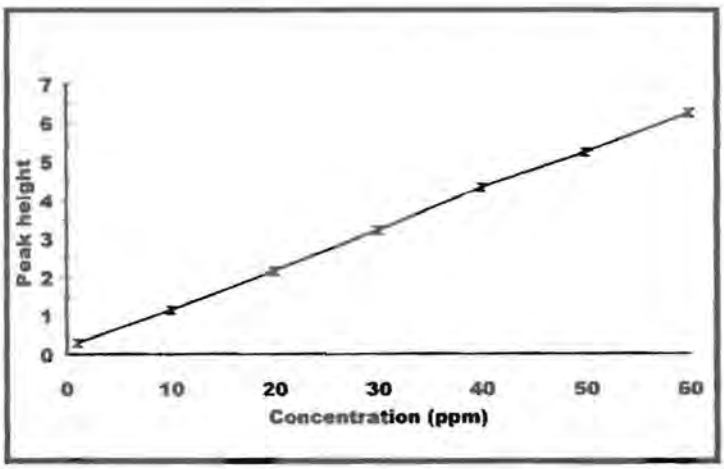

Fig. 6.10 A calibration graph using optimum values

All these were carried out and under optimum conditions (Table 6.8).

TABLE 6.8 Optimum values for the SIA system.

Parameter	**Optimum value**
Reactor length	15 cm
Reactor diameter	6 mm
Carrier concentration	0.01 mol/ℓ
Flow rate	2.83 mℓ/min
Sample volume	236 $\mu\ell$
Reagent volume	236 $\mu\ell$

Real samples (multivitamins and haematinics) and water samples were analysed with the proposed system. The results obtained are a mean of 10 repetitive analyses of each sample. The accuracy was compared to certified values and the standard method (Table 6.9 and 6.10).

TABLE 6.9 Iron in multivitamin and haematinics using SIA and spectrophotometric methods as well as certified values in mg/tablet (capsule) and % RSD's in brackets.

Sample	Certified values	Proposed SIA method	Standard spectrophotometric method
Filibon	15	16.04 (2.3%)	15.3 (4.2%)
Ferrimed	50	47.75 (1.6%)	51.52 (4.3%)
Pregamal	56	52.65 (1.8%)	51.02 (4.5%)
Ferrous C	28	27.19 (1.2%)	27.16 (2.7%)

TABLE 6.10 Iron in effluent streams using SIA and ICP methods

Sample	Concentration in mg/ℓ		Relative standard deviation (%)	
	SIA	ICP-AES	SIA	ICP-AES
A	0.759	0.861	2.3	2.2
B	0.331	0.296	1.3	2.8
C	0.266	0.241	0.3	3.9

6.4.3.2 Accuracy

The accuracy of the proposed SIA analyser was evaluated by comparing results obtained with those from the certified results, standard ICP-AES and spectrophotometer. Tables 6.9 and 6.10 shows that the results compared well, especially between the certified results and SIA results.

6.4.3.3 Recovery

The recovery of the system was evaluated by comparing results obtained with the proposed SIA system and rthe cerified results (Table 6.9). The percentage recovery after analysing the samples with the SIA system was determined according to this equation:

$$\%\,\mathrm{Recovery} = \frac{obtained}{\mathrm{expected}} x100$$

The percentage recovery between certified results and SIA results ranged from 103.1% to 106.9%.

6.4.3.4 Precision

The precision of the method was determined by 10 repetitive analyses of the standard solutions as well as 10 repetitive analyses of the real samples. All these were carried out under optimum conditions. The relative standard deviation for the standard was 1.5% and for the real samples was less than 2.3% (Tables 6.9 and 6.10).

6.4.3.5 Detection limit

The detection limit was calculated using the formula:

$$DL = \frac{[(3\sigma + k) - c]}{m}$$

where σ (0.00529) is the standard deviation of the baseline, k is the average response of the baseline (0.175) and c (0.1722) the intercept and m (0.1049) the slope of the calibration graph. The detection limit was found to be 0.178 mg/ℓ.

6.4.3.6 Sample interaction

The sample interaction carryover effect between consecutive samples was determined by analysing sample with low analyte concentration followed with a high analyte concentration which was again followed by the sample with a low analyte concentration. The sample interaction was then calculated using the following formula:

$$\text{Sample interaction} = \frac{(A_3 - A_1)}{A_2} x100\%$$

where A_1 is the peak height (1.35) of a sample containing to 10 mg/ℓ Fe(II), A_2 is a peak height (5.52) containing 50 mg/ℓ Fe(II) and A_3 is a peak height (1.42) containing 10 mg/ℓ Fe(II). The sample interaction was ± 1.3% which may be considered negligible.

6.4.3.7 Interferences

The only possible interferences that may disturb this analysis are Ag, Bi, Ni, Cu and Co. Fortunately of al these, only Cu was found to be present, but in very low levels which may not affect the results. Table 6.11 gives the elements present in samples analysed and their amounts. In the work done by van Staden and Kluever [27] these levels of cations did not interfere with the analysis of Fe (II) as shown by the recoveries obtained.

TABLE 6.11 Elements present in samples analysed as mg/tablet or capsule

Element	Amount/tablet (capsule)	Element	Amount/tablet (capsule)
Ca	< 5 mg	Na	< 1 mg
K	< 0.83 mg	Mg	< 0.15 mg
Mn	< 0.05 mg	Zn	< 0.085 mg
Mo	< 0.025 mg	Cu	< 0.15 mg

6.5 Statistical comparison of techniques used

The comparison was done between the SIA results and the certified values (Table 6.9) and between the SIA results and the standard spectrophotometric method results (Table 6.10), for pharmaceutical products.

TABLE 6.12 Differences between SIA and certified results for pharmaceutical products

Sample	x_d	x_d^2
Filibon	-1.04	1.082
Ferrimed	2.25	5.063
Preganal	3.35	0.656
Ferrous C	0.81	11.225

TABLE 6.13 Differences between SIA and spectrophotometric results for pharmaceutical products

Sample	x_d	x_d^2
Filibon	0.74	0.55
Ferrimed	-3.77	14.21
Preganal	1.63	2.66
Ferrous C	0.03	0.0009

A further comparison was done between SIA and the standard ICP method for the water samples and Table 6.14 gives the mean differences between the SIA and ICP-AES.

TABLE 6.14 Difference between SIA and ICP-AES results for water samples

Sample	x_d	x_d^2
A	0.103	0.0104
B	-0.049	0.0024
C	-0.039	0.0015

The above comparisons were done to establish whether the SIA system can be accepted as giving reliable results in the iron determination or not. The null hypothesis was used [35, 36]. For the null hypothesis the two methods should agree ideally when the population, H_o mean difference is zero; $H_o: \mu_d = 0$. The alternative hypothesis, $H_1: \mu_d \neq 0$, implies that the two methods failed the test. The t-test with multiple samples (paired by difference) was applied to examine whether the two methods differed significantly at 95% confidence level.

The mean, $\bar{x}_d$ and the standard deviation, s_d are calculated from the following equations:

$$\bar{x}_d = \frac{\sum x_d}{N}$$

and

$$s_d = \sqrt{\frac{\sum (x_d - \bar{x}_d)^2}{N-1}}$$

From Table 6.12 between certified and SIA results the following is deduced:

$$\sum x_d = 5.37 \qquad \text{and} \qquad \sum x_d^2 = 18.02$$

Substituting the above where $N = 4$, we find the mean and standard deviations as:

$$\bar{x}_{d1} = 1.34 \qquad \text{and} \qquad S_{d1} = 1.34$$

From Table 6.13, for SIA and standard method, the following is deduced:

$$\sum x_d^2 = 17.42 \qquad \text{and} \qquad \sum x_d = 1.396$$

Substituting the above for the mean and standard deviation with N = 4, we find:

$$\bar{x}_{d2} = 0.349 \qquad \text{and} \qquad S_{d2} = 2.350$$

From Table 6.14 between SIA and the ICP-AES the following id deduced:

$$\sum x_d = 0.014 \qquad \text{and} \qquad \sum x_d^2 = 0.0143$$

Substituting the above for mean and standard deviation with N = 3, we find:

$$\bar{x}_{d3} = 0.0047 \qquad \text{and} \qquad S_{d3} = 0.0842$$

Now, in the determination of iron in pharmaceutical products there are four determinations (n=4), therefore υ=3 and at 95% confidence level $t_{0.05,3} = 3.18$. The critical values are therefore ± 3.18. The $t_{calculated}$ values are in accordance with the following equation:

$$t_{calculated} = \frac{|\bar{x}_d|}{s_d} \times \sqrt{n}$$

Now between SIA and certified results $t_{calculated.}$ ($t_{calc.}$) is given as:

$$t_{calc.} = 2.00$$

and between SIA and spectrophotometry as:

$$t_{calc.} = 0.297$$

Finally, $t_{calc.}$ is at 1.15 between SIA and certified results. The results indicates that there is no significant difference between the methods at 95% confidence level. Between SIA and spectrometry the t_{calc} is 0.297 which indicates that the two techniques gives the same results, as such there is no statistical significant difference between the techniques

In the determination of iron in water samples there are three determinations (n=3), therefore υ=2 at 95% confidence level $t_{0.05,2} = 4.30$. The $t_{calculated}$ value is obtained as:

$$t_{calc.} = 0.097$$

Therefore the $t_{calc.}$ value, 0.097 implies that there is no significant difference between the two methods at 95% confidence level.

It can therefore, be concluded that, in the determination of iron in pharmaceutical products, the SIA and standard method (spectrophotometry) at 95% confidence level give the same results. It can in the same breath be conducted that SIA and the ICP method in the determination of iron in water samples gives the same results at 95% confidence level. The null hypothesis can therefore be accepted at 95% confidence level.

6.6 Conclusions

The total iron determination by SIA with a cadmium reductor incorporated into the SIA manifold is an improvement on the homogeneous methods applied in FIA and SIA systems. In contrast to the FIA system, the cadmium reductor in SIA was regenerated on-line without having to disconnect the system and replace with a new reductor. Thus, once designed it does not have to be physically reconfigured. The SIA system is easier to use and was found suitable for determination of total iron as Fe(II) in pharmaceutical products and water samples within a wide range as shown by the detection limit.

6.7 References

1. F. A. Cotton and G. Wilkinson, **Advanced inorganic chemistry-A comprehensive text,** Wiley & sons, New York, 1980.
2. N. I. Ward, **Trace elements:** ***Environmental analytical chemistry***, **Ed.** by F. W. Fifield and P. J. Haines, Chapman & Hall, USA.
3. A. H. Goodman, **Potable water quality:** ***Developments in water treatment***, Ed. By W. M. Lewis, Applied Science, London,. 1980.
4. M. Bloomfield and L. J. Stephen, **Chemistry and the Living Organism, 6th ed.,** Wiley & sons, New York., 1996.
5. H. C. Heinrich, E. E. Gabbe and A. A. Pfau, **Nutrient availability:** ***Chemical and biological aspects,*** Ed. by. D. A. T. Southgate, I. T. Johnson and G. R. Fenwick., 1989.
6. B. Lönnerdal, **Nutrient availability:** ***Chemical and biological aspects,*** Ed. by D. A. T. Southgate, I. T. Johnson and G. R. Fenwick., 1989.
7. S. M. Sultan and F. E. O. Suliman, **Analyst, 121** (1996) 617.
8. S. N. Bhadani, M. Tiwari, A. Agrawal and C. S. Kawipurapu, **Mikrochim Acta, 117**(1994) 15.
9. R. Kuroda, T. Nara and K. Oguma, **Analyst, 113** (1998)1557.
10. K. Oguma, S. Kozuka, K. Kitada and R. Kuroda, **Fresenius' J. Anal. Chem., 341** (1991) 545.
11. J. Liu and H. Ma, **Talanta, 40** (1993) 969.
12. T. P. Tougas, J. M. Jnatti and W. G. Collier, **Anal. Chem., 57** (1985) 1377.
13. H. S. Zhang, X. C. Yang and L. P. Wu, **Fenxi Huaxue, 24** (1996) 220.

14. S. Blain and P. Treguer, **Anal. Chim. Acta, 308** (1995) 425.

15. O. Abollino, M. Aceto, G. Sarzanini and E. Mentasti, **Anal. Chim. Acta, 305** (1995) 200.

16. Y. L. Zhang, **Lihua-Jianyan, 30** (1994) 14.

17. J. M. Barrero, C. Camara, M. G. Perez-Conde, C. San-Jose and L. Fernandez, **Analyst, 120** (1995) 431.

18. R. M. Liu, D. J. Liu, G. H. Liu, A. L. Sun and Z. H. Zhang, **Fenxi Huaxue, 22**(1994) 1241.

19. S. J. Cosano, M. D. Luque de Castro and M. Valcarcel, **J. Autom. Chem., 15** (1993) 47.

20. S. J. Cosano, M. D. Luque de Castro and M. Valcarcel, **J. Autom. Chem., 15** (1993)141.

21. A. T. Faizullah and A. Townshed, **Anal. Chim. Acta, 167** (1985) 225.

22. T. P. Lynch, N. J. Kemoghan and J. N. Wilson, **Analyst, 109** (1984) 843.

23. E. Masatoshi and A. Shigeki, **Fresenius' J. Anal. Chem., 358** (1997) 546.

24. A. F. Oliveira, J. A. Nóbrega and O. Fatibello-Filho, **Talanta, 49** (1999) 505.

25. E. Luque-Pèrez, A. Rios and M. Valcarcel, **Fresenius' J. Anal. Chem., 366** (2000) 857.

26. J. F. van Staden and L. G. Kluever, **Anal. Chim. Acta, 350** (1997)15.

27. J. F. van Staden and L. G. Kluever, **Fresenius J. Anal. Chem., 362** (1998)319.

28. J. Růžička and G. D. Marshall, **Anal. Chim. Acta, 237** (1990) 329.

29. J. Růžička, G. D. Marshall and G. D. Christian, **Anal. Chem., 62** (1990) 1861.

30. J. F. van Staden, H. du Plessis and R. E. Taljaard, **Anal. Chim. Acta, 357** (1997)141.

31. A. N. Araújo, J. Gracia, J. L. F. C. Lima, M. Poch, M. Lúcia and M. F. S. Saraiva, **Fresenius' J. Anal. Chem., 357** (1997)1153.

32. E. Rubi, M. S. Jiménez, F. Bauzá de Mirabó, R. Forteza and V. Cerdá, **Talanta, 44** (1997) 553.

33. J. F. van Staden and E. B. Naidoo, **S. Afr. J. Chem., 53** (2000).

34. G. D. Marshall and J. F. van Staden, **Anal. Inst., 20** (1992)79.

35. D. McCormick and A. Roach, **Measurement, Statistics and Computation. Analytical Chemistry by Open Learning.** Wiley & sons, New York, 1995.

36. D. A. Skoog, D. M. West and F. J. Holler, **Fundamentals of Analytical Chemistry. 7th ed.,** Saunders, USA, 1996.

CHAPTER 7

Determination of nitrate and nitrite in water using a solid-phase reactor in a SIA system

7.1 Introduction

Nitrate and nitrite play an important role in the nitrogen cycle which involves the complex interaction of different ecosystems of the biosphere. Both nitrate and nitrite are present in food and water, and it is from these sources that humans are exposed to these ions.

Excessive amounts in water supplies indicate pollution from sewage or agricultural effluents. In many ways the analytical chemistry of nitrate is linked to that of nitrite. The presence of nitrite in drinking water would indicate recent pollution. Although it is rare to find appreciable levels in waters in the United Kingdom (UK), there are reports that nitrite may occur to an appreciable extent in some continental waters, in distribution. It may well be that, this is because waters contain no residual disinfectants when put into supply and that there is no bacteriological action taking place in the distribution systems oxidising ammonia or reducing nitrate.

Nitrate is chemically stable throughout the relevant range of pH. It can be reduced to nitrite when in contact with metals, such as occurs during cooking of food in aluminium utensils [1].

Nitrite is very unstable, particularly at acidic pH values [2] at which it can disproportionate to yield nitrate and nitrogen oxide and/or react with many components of foods including amines, phenols and thiols.

The occurrence of waters high in nitrate content seemed to be more common in the UK than in Europe, although, of recent times the nitrate content of some European sources does seem to have increased to similar levels to those found in the UK. This is one of the reasons for high degree of purification of sewage effluents before they are discharged into river water with a corresponding low level of ammonia content.

It has been assumed that the increasing use of fertilisers in agriculture has been coincident with the increase in nitrate content of ground-waters. However, the situation is more complex and the high nitrate in ground-waters may be due to the intensity of agriculture, to better land drainage which results in less de-nitrification in waterlogged sods to increasing use of ground-water.

The World Health Organisation (WHO) Standards include nitrate among those constituents which if present in excessive amounts may give rise to trouble. In the European Standards it is recommended that less than 50 mg/ℓ as nitrate should be present in drinking water, but between 50 and 100 mg/ℓ of nitrate is acceptable and that more than 100 mg/ℓ as nitrate is recommended. The International Standards suggested that a maximum of 45 mg/ℓ be expressed as nitrate because of the risk to infants. The European Economic Community (EEC) Directives suggest a maximum admissible concentration of 50 mg/ℓ and the United States National Interim Primary Water Quality Standards give a maximum content of nitrate (as N) of 10 mg/ℓ (equivalent to 45

mg/ℓ as nitrate). The same value is quoted in the Russian Drinking Water Standards. However, the value given as maximum admissible concentration in the Directive on Water for Human Consumption is 0.1 mg/ℓ.

In the UK, water authorities follow WHO standards laid down in 1970. These recommended that NO^-_3 - N in drinking water should be less than 11.3 mg/ℓ. Values of 11.3 - 22.6 mg/ℓ are acceptable, those in excess of 22.6 mg/ℓ are unacceptable [3, 4].

Nitrate is necessary for plant growth. According to Christy *et al.* [5], probably more than 90% of the nitrogen absorbed by plants is in the form of nitrate. Nitrite gives cured meat its characteristic colour and flavour and it is important in the control of bacteria, particularly *Clostridium botulimum* [6]. It is also used for pigment and other colourants [7].

Nitrate in water could in the presence of some bacteria react with the secondary or tertiary amines present in foodstuffs to produce the carcinogenic materials, nitrosoamines. It has been suspected for some years that the effect of exposure to nitrate and nitrite may cause human cancer [8]. There is evidence that high intra-gastric nitrite concentrations correlate with an increased risk of stomach cancer [9]. The reduction of nitrate to nitrite in the gastric lumen is an important source of nitrite for the formation of N-nitroso compounds. High nitrate levels in domestic water causes cyanosis in young babies and infant methaemoglobinaemia [10, 11] has been traced to high nitrite content.

7.2 Choice of analytical technique

The determination of total oxidized nitrogen is a subject of interest in the routine laboratory analysis of potentially polluted waters. However, the determination of nitrate is difficult because of the relatively complex procedures required, the high probability that interfering constituents will be high and the limited concentration ranges of the various techniques. Consequently the determination of total oxidized nitrogen as nitrate is not recommended for waters, but rather as nitrite.

Several methods are commonly used at present for these, but impose restrictions that make the analysis time-consuming and tedious. These methods include gravimetry, titrimetry, spectroscopy and electro-analytical techniques. It falls into one of the five main categories:

- the reduction of nitrate to ammonia [12, 13]
- photo-induced reduction of nitrate to nitrite [14]
- direct spectrophotometry [15, 16]
- potentiometric methods using ion-selective electrodes [17]
- reduction of nitrate to nitrite [18, 19, 20]

Many colorimetric methods have been proposed for the determination of micro-amounts of nitrite [21-28] which is a modified version of the Shinn [29]. These methods involved a reaction of nitrite with a primary aromatic amine to form a diazonium salt which is coupled with another aromatic compound to form the azo dye of which the absorbance is measured. The strategy commonly adopted is based on the reduction of nitrate to nitrite which is then

spectrophotometrically determined after diazotation and coupling reaction.

A number of flow injection analysis (FIA) methods[30-35] have been developed using this modification. Sequential injection analysis (SIA) methods have also been developed for determination of nitrate and nitrite in waste waters and aqueous extracts of atmospheric aerosols [36]; for the determination of nitrite in fertilizers process streams, natural and waste water effluents [37] and the simultaneous determination of nitrate and nitrite in water samples [38].

In the above methods employed, either a homogeneous or heterogeneous reactor is used. However, good the FIA and SIA systems already in use maybe, a system more advanced where as automated pump in the place of a semi automated burette and an acidified cadmium reactor in the place of a copperised one was developed. Furthermore this reactor is regenerated on line, these are some of the features which makes this new technique so unique. Hence, a SIA system incorporating an acidified cadmium reactor into its manifold was used for the determination of nitrate and nitrite.

The SIA technique launched in 1990 [39] is a technique that has tremendous potential especially for on-line process measurements and in monitoring of the environment. It is simple and convenient to operate. The technique considerably decreases sample and reagent consumption and thus the waste generated. In addition, devices based on SIA yield robust and stable systems that are suitable for routine monitoring.

The SIA system described herein allows for the determination of oxidized nitrogen in water samples from different sources as nitrite.

7.3 Determination of total oxidized nitrogen

A water sample containing nitrate was reduced on-line with a solid-phase reactor, diazotised and coupled to produce a reddish azo dye which is detected a 540 nm with a UV/VIS spectrophotometer. The wavelength at 540 nm was chosen from a scan of the standard nitrite solution over a range of 200-1100 nm.

7.3.1. Experimental

7.3.1.1 Reagents and solutions

All reagents were prepared from analytical grade chemicals unless specified otherwise. All aqueous solutions were prepares from doubly distilled, de-ionised water. A De-ioniser from Modulab system (Continental Water System, Sant Antonio, TX, USA) was used throughout. The solutions were all degassed before introduction into the system and stored in an oxygen free environment.

7.3.1.1.1 Stock nitrate solution

A 0.6070 g of oven dried sodium nitrate (Merck, pro analysis) was dissolve and diluted to 1ℓ with double de-ionised water. A 2 mℓ solution of chloroform (Merck, pro analysis) was added to this solution to maintain stability and stored in a cool place. The solution was then standardised with potassium permanganate (Protea Laboratories service (Pty) Ltd.). Working

standards in the range of 0.25 to 50 mg/ℓ were prepared by appropriate dilution of the solution with deionised water.

7.3.1.1.2 Stock nitrite solution

A 0.5057 g of oven dried sodium nitrite (Riedel-De Haën AG, Seelze-Hannover) was dissolved and diluted to 1ℓ with double deionised water. A 2 mℓ solution of chloroform (Merck, pro analysis) was added to this solution to maintain stability and stored in a cool place. The solution was standardised with potassium permanganate (Protea Laboratories service). Working standards in the range of 0.25 to 50 mg/ℓ were prepared by appropriate dilution of the stock solution with deionised water.

7.3.1.1.3 Buffer solution

The buffer solution was prepared by dissolving 30 g of ammonium chloride (Merck, Darmstadt) and 0.2 g EDTA-disodium salt (GPR, Essex, England) in de-ionised water and diluting to 500 mℓ. The pH was adjusted to 6.5 using ammonia (25% NH_3, SAARCHEM). The carrier solution was prepared by dissolving 13 g ammonium chloride (Merck, Darmstadt) and 2.0 g EDTA. The pH of the solution was 4.75 and was not adjusted to any particular value. The appropriate dilutions were made from this solution during optimisation of the carrier concentration.

7.3.1.1.4 Chromogenic reagent

The chromogenic reagent was prepared by dissolving 5 g sulphanilamide (BDH, Poole, England)

and 0.5 g of N–(1-naphthyl) ethylenediammonium dichloride in a mixture of 50 mℓ hydrochloric acid (32% HCl, Chemical suppliers) and 300 mℓ de-ionised water and diluting to 1ℓ. The solution was stored in an amber bottle.

7.3.1.2 Instrumentation

The sequential injection system depicted in Fig. 7.1A was constructed from the following components: a Gilson minipuls peristaltic pump (Model M312, Gilson, Villiers-Le Bel, France); a 10-port electrically actuated selection valve (Model ECSDIOP, Valco Instruments, Houston, Texas) and a Unicam 8625 UV-Visible spectrophotometer equipped with a 10-mm Hellma-type (Hellma GmbH and Co., Mülheim/Baden, Germany) flow-through cell (volume 80 $\mu\ell$) for absorbance measurements. .

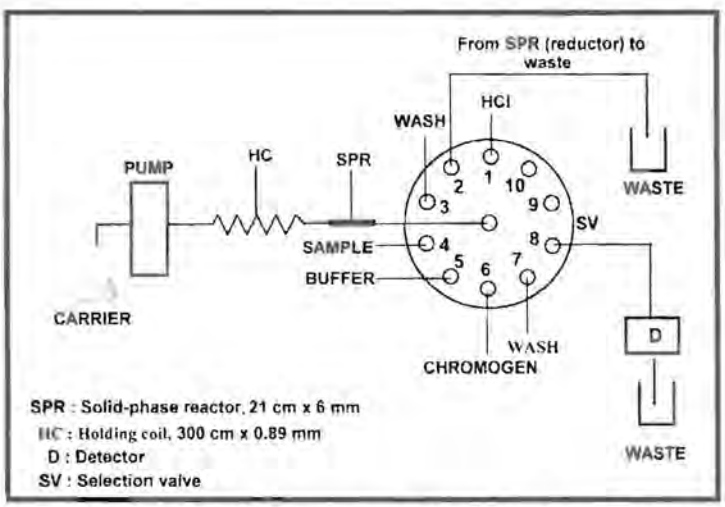

Fig. 7.1A A SIA system diagram used in nitrate determination

Data acquisition and device control was achieved using a PC30-B interface board (Eagle Electric, Cape Town) and an assembled distribution board (Mintek, Randburg). The flowTEK

[40] software package (obtainable from Mintek) for computer-aided flow analysis was used throughout for device control and data acquisition. All data given (mean peak height values) are the average of 10 replicates.

7.3.1.3 Operation of the system

A schematic diagram for the SIA system is depicted in Fig. 7.1A. The whole procedure, from sample injection to data processing and storage was computer controlled via the flowTEK program. The whole SIA procedure involved designing a method which allows a single cycle of the experiment to be run. This procedure is well illustrated in Fig. 7.1B and Table 7.1.

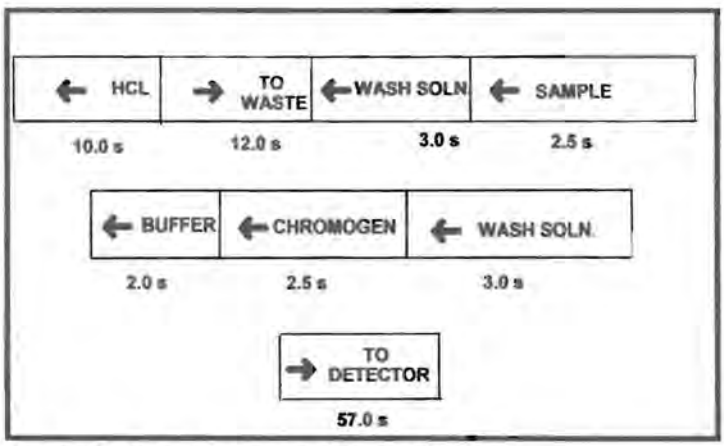

Fig. 7.1B A device sequence for one SIA cycle

When all the zones were placed in the holding coil (HC), they were then flushed with the carrier stream through the reductor to reduce the nitrate to nitrite. The oxidised nitrogen as nitrite was diazotised in the system with sulphanilamide and coupled with N-(1-napthyl) ethylenediammonium dichloride to form a highly coloured azo dye which was detected at 540 nm with a spectrophotometer. The data obtained is converted to a response time graph on the

computer screen as a peak profile. The maximum peak height was then automatically processed and stored on a computer via the FlowTEK program.

TABLE 7.1 Device sequence for one cycle of the SIA system

Time (s)	Pump	Valve	Description
0	Off	Position 1	Pump off. Select HCl stream.
1	Reverse		Draw HCl solution for regeneration.
10	Off		Pump stop.
11	Off	Position 2	Select waste stream.
12	Forward		Pump solution to waste.
23	Off		Pump stop.
24	Off	Position 3	Select wash stream.
25	Reverse		Draw wash solution.
27	Off		Pump stop.
28	Off	Position 4	Select sample stream.
29	Reverse		Draw sample solution.
30.5	Off		Pump stop.
31.5	Off	Position 5	Select buffer stream.
32.5	Reverse		Draw buffer solution.
33.5	Off		Pump stop.
34.5	Off	Position 6	Select chromogen stream.
35.5	Reverse		Draw chromogen solution.
37	Off		Pump stop.
38	Off	Position 7	Select wah stream.
39	Reverse		Draw wash solution.
41	Off		Pump stop.
42	Off	Position 8	Select detector stream.
43	Forward		Pump zones through reductor to detector.
100	Off	Position 1	Pump stop. Valve return home.

7.3.1.4 The solid-phase reactor

The reactor columns were made of glass with varying length (12 cm, 15 cm, 17 cm, 19 cm and 21 cm) but with the same internal diameter of 6 mm. The reactor is shown in Fig. 7.2.

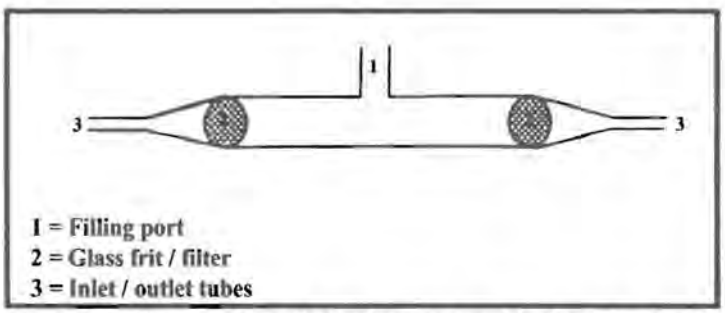

Fig. 7.2 A diagram of a cylindical reactor used in the reduction nitrate to nitrite

The columns were then filled with cadmium granules (Merck, 0.3 - 1.5 mm). The particles were held by a glass frit at each end so that they did not block the SIA system. A vibrator was used to effect close packing of the columns. The cadmium granules prior to being packed in the glass column were prepared by washing with acetone for 10 minutes, adding 20 mℓ of 2 mol/ℓ HCl solution, de-ionised water and methanol then drying in a dessicator. An acidified cadmium reactor was chosen over copperised one because copper has a tendency of interfering in the determination of nitrite in water. Furthermore van Staden and Makhafola [35], have shown that the life span of the acidified cadmium reactor was longer than the copperised one. The cadmium reactor was regenerated by passing approximately 270 $\mu\ell$ of 2 mol/ℓ HCl solution at the beginning of every cycle. This was to ensure consistency in the reduction efficiency and capacity of the reactor.

7.3.1.5 Sample preparation

The samples were obtained from the Institute for Water Quality Studies (Department of Water Affairs and Forestry). The samples were all collected from different localities (streams, rivers, dams, hydro plants, tunnels and effluent streams) at a depth of half a metre. The sample were then preserved in mercury (II) chloride. The samples received were ready for direct analysis. Samples selected were in the pH range 6.8 to 8.2. The buffer solution allowed the adjustment of the pH of the samples.

7.3.2 Method optimization

The method was optimized with regard to the following parameters: nitrite concentration, carrier concentration, flow rate, sample, reagent and buffer volume, reactor length and reduction efficiency. Both the relative peak height and %RSD were used as criteria for establishing the most appropriate optimum value in each case.

7.3.2.1 Solid-phase reactor parameters

The solid phase cadmium reactor forms the heart of the manifold of the proposed system. The performance of the SIA system depends on the reduction efficiency of the reactor at interface between the solid and liquid phases of the reactor. In addition the reactor packing had to be thorough and its length and efficiency had to be optimised.

7.3.2.1.1 Reactor length

The response and precision of the system were studied by varying the reactor length between 12 and 21 cm with the internal diameter fixed at 6 mm. The five reactors (12 cm, 15 cm, 17 cm, 19 cm and 21 cm) were compared for reductor efficiency. From results obtained it was found that the last three reactors did not show a significant difference in response, there was however, for the shorter reactor lengths. The 21 cm reactor length was chosen as optimum because of its good precision. This is illustrated by Fig. 7.3 and given in Table 7.2.

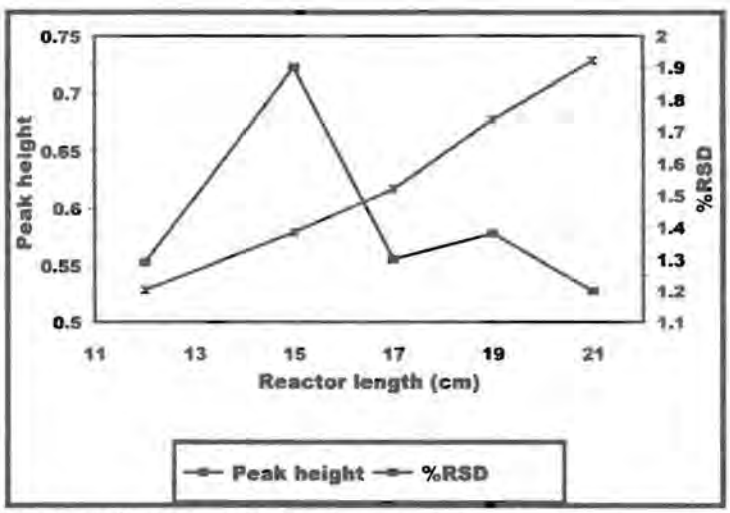

Fig. 7.3 Effect of reactor length on response and precision

TABLE 7.2 Effect of reactor length on response and precision

Length (cm)	12	15	17	19	21
RPh	0.529	0.579	0.617	0.677	0.728
%RSD	1.3	1.9	1.3	1.4	0.7

7.3.2.2 Chemical parameters

7.3.2.2.1 Nitrate concentration

The nitrate concentration was evaluated between 0.5 and 50 mg/ℓ and the 2.5 mg/ℓ concentration was chosen as the optimum concentration for optimising the remaining parameters. The results of this optimisation is presented in Table 7.3 and Fig. 7.4.

TABLE 7.3 Effect of nitrate concentration on response and precision

Conc (mg/ℓ)	0.5	1.0	2.5	5	10	25	50
RPh	0.402	0.412	0.618	0.736	1.708	2.325	5.367
%RSD	1.5	1.0	0.8	1.2	1.8	2.5	5.0

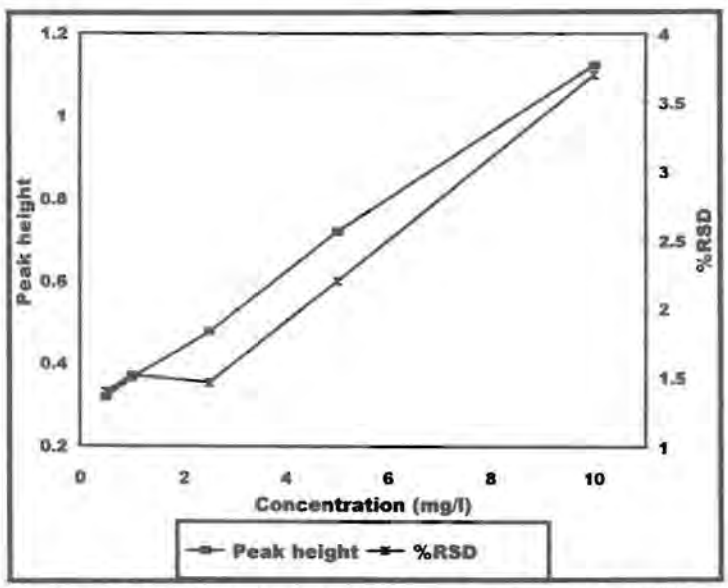

Fig. 7.4 Effect of nitrate concentration on response and precision

7.3.2.2.2 Carrier Concentration

The carrier was evaluated between pure de-ionised water and solution of 13 g ammonium chloride and 2 g EDTA per litre. However, it was a concentration corresponding to 1.3 g ammonium chloride and 0.2 g EDTA per litre of solution that was chosen as the optimum, because it gave the best response and precision as shown in Table 7.4 and by Fig. 7.5.

TABLE 7.4 Effect of carrier concentration on response and precision

Conc (mg/ℓ)	0	0.7	1.3	2.6	6.5	1.3
RPh	0.683	0.731	0.730	0.715	0.692	0.677
%RSD	2.1	1.3	1.0	1.4	1.9	1.4

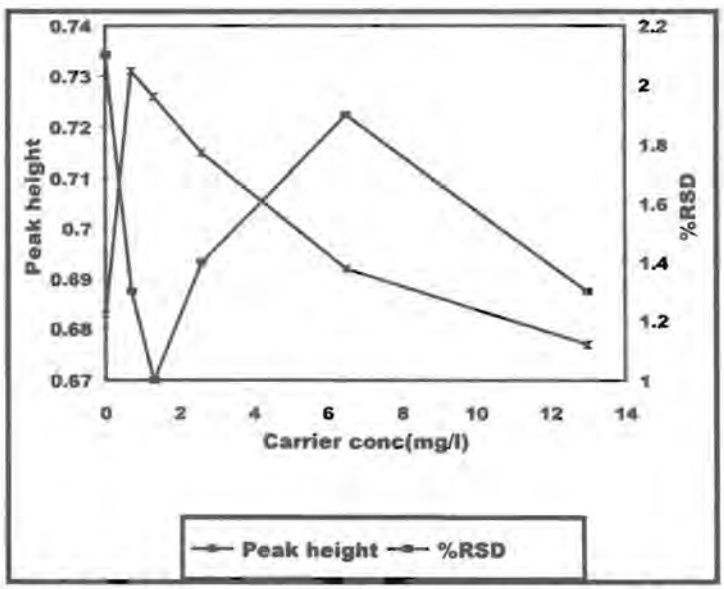

Fig. 7.5 Effect of carrier concentration on response and precision

7.3.2.3 Physical parameters

The contact time between the sample and the reactor is of utmost importance. The 21 cm reactor length was found to be optimum and effective with 270 $\mu\ell$, 2 mol/ℓ HCl solution passing through the reactor for every SIA cycle.

7.3.2.3.1 Flow rate

The flow rate was evaluated between 1.86 and 3.71 mℓ/min. The 3.25 mℓ/min flow rate was chosen as optimum as given by Fig. 7.6 and in Table 7.5.

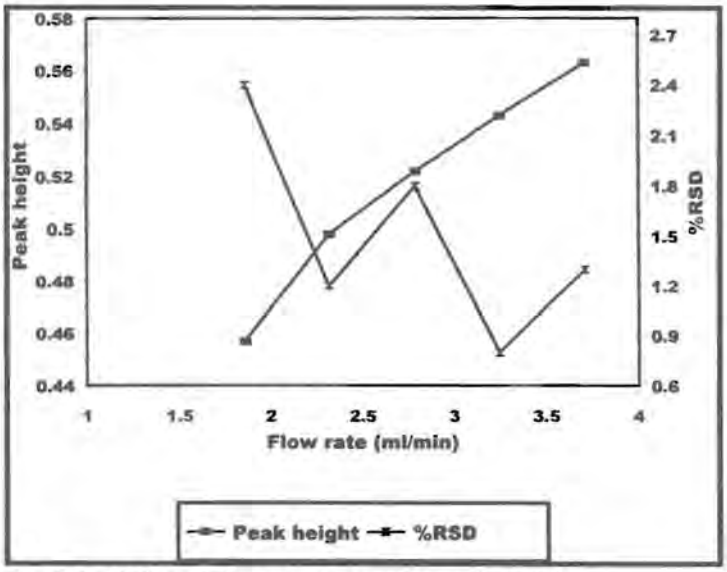

Fig. 7.6 Effect of flow rate on response and precision

TABLE 7.5 Effect of flow rate on response and precision

Rate (mℓ/min)	1.86	2.32	2.79	3.25	3.71
RPh	0.457	0.498	0.522	0.543	0.566
%RSD	2.4	1.2	1.8	1.0	1.8

7.3.2.3.2 Sample volume

The sample volume was evaluated between 25.0 and 140.0 $\mu\ell$. The sample volume was found to be optimum at 82.5 $\mu\ell$. The results are well presented in Table 7.6 and Fig. 7.7.

TABLE 7.6 Effect of sample volume on response and precision

Volume ($\mu\ell$)	27.5	55	82.5	110	137.5
RPh	0.377	0.486	0.629	0.765	0.877
%RSD	1.2	1.7	0.5	1.2	0.8

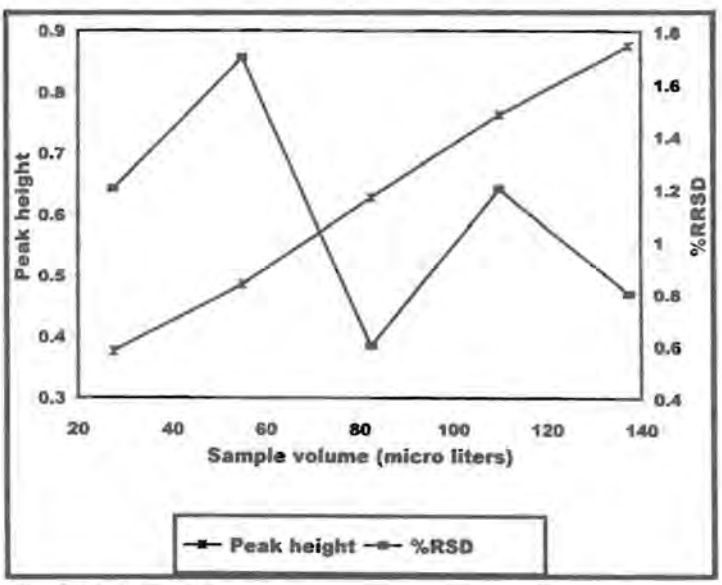

Fig. 7.7 Effect of sample volume on response and precision

7.3.2.3.3 Reagent volume

The reagent volume was evaluated between 25.0 and 140.0 $\mu\ell$. The reagent volume was found to be optimum at 82.5 $\mu\ell$. The results are shown in Table 7.7 and illustrated in Fig. 7.8.

TABLE 7.7 Effect of chromogen volume on response and precision

Volume ($\mu\ell$)	27.5	55	82.5	110	137.5
RPh	0.504	0.507	0.513	0.528	0.558
%RSD	3.6	1.5	0.8	1.6	1.0

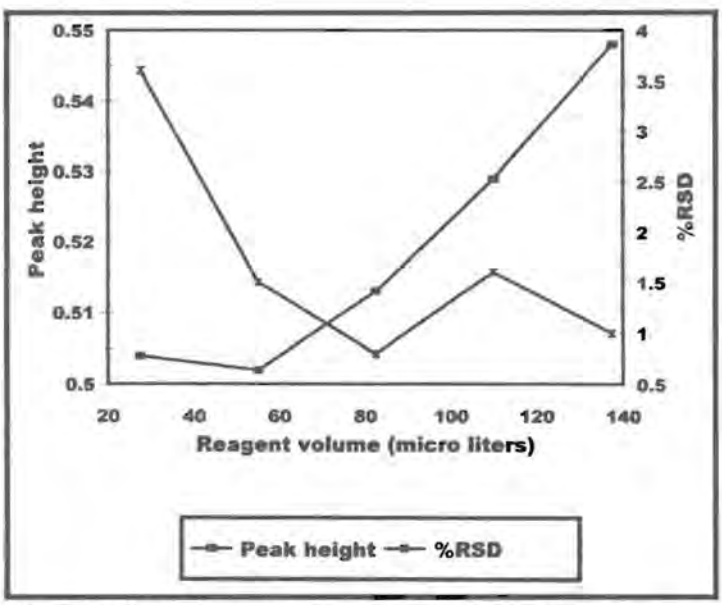

Fig. 7.8 Effect of reagent volume on response and precision

7.3.2.3.4 Buffer volume

The buffer volume was evaluated between 25.0 and 140.0 $\mu\ell$. The buffer volume was found to be optimum at 55 $\mu\ell$. The results are well presented in Table 7.8 and illustrated in Fig. 7.9.

TABLE 7.8 Effect of buffer volume on response and precision

Volume ($\mu\ell$)	27.5	55	82.5	110	137.5
RPh	0.662	0.608	0.574	0.589	0.596
%RSD	1.4	0.8	1.7	1.7	0.8

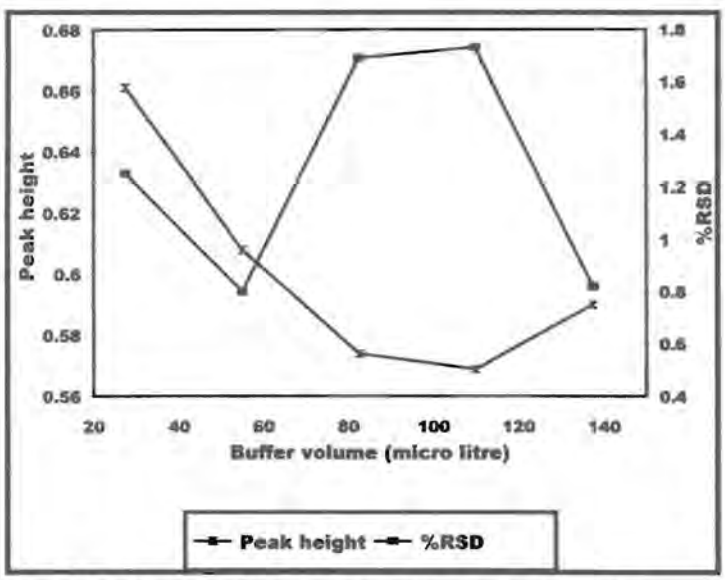

Fig. 7.9 Effect of buffer volume on response and precision

7.3.3 Method evaluation

7.3.3.1 Linearity

The linearity of the system was evaluated for analyte concentration between 0.25 and 50 mg/ℓ. The response was however, found to be linear in the range 0.25 to 5 mg/ℓ. The relationship between the response and the concentration is given by te equation : $H = 0.0877x + 0.2060$ (r = 99.94%), where H is the peak height and x the analyte concentration in mg/ℓ. The calibration graph is illustrated in Fig. 7.10.

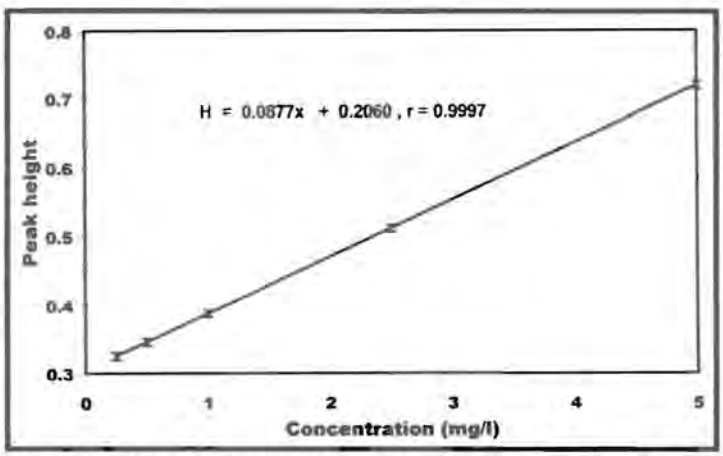

Fig. 7.10 Calibration graph obtained under optimum conditions

7.3.3.2 Accuracy

Water samples from different sources were analysed with the proposed system. The results obtained are a mean of 10 repetitive analysis of each sample (Table 7.9). The accuracy was compared to the standard method results (Table 7.9).

TABLE 7.9 SIA results for water samples analysed

Sample ID	pH	Peak height	mg/ℓ (NO_3^- - N + NO_2^--N)
Unknown	8.2	0.257 (1.2%)	0.65
Mtafufu-Ntafufu	7.8	0.277 (1.2%)	0.88
Tshinane	7.7	0.294 (1.4%)	1.07
Vink	8.3	0.284 (1.5%)	0.96
Wolwekloof tunnel	6.9	0.306 (0.9%)	1.02
Van Rhyreveldspas dam	7.5	0.347 (1.4%)	1.68
Mgwale-clackburg	7.8	0.248 (1.5%)	0.48
Tsitsa-Tsitsa bridge	7.3	0.242 (1.2%)	0.47
Duiwe river	7.0	0.276 (1.1%)	0.80
Mutshedi dam	7.4	0.366 (1.0%)	1.13

TABLE 7.10 Comparison of SIA and Standard method (AAS) results and their paired differences.

Sample Id	SIA method	Standard method	x_d x 10^{-2}	x_d^2 x 10^{-3}
unknown	0.65	0.63	2.0	0.4
Mtafufu-Ntafufu	0.88	0.78	10.0	10.0
Tshinane	1.07	0.97	10.0	10.0
Vink	0.96	1.05	-9.0	8.1
Wolweklof tunnel	1.20	1.16	4.0	1.6
Van Rhyreveldspas dam	1.68	1.77	-9.0	8.1
Mgwale-Clackburg	0.48	0.45	3.0	0.9
Mutshedzi dam	1.13	0.99	14.0	19.6
Tsitsa-Tsitsa bridge	0.47	0.46	1.0	0.1
Duiwe river	0.80	0.72	7.9	6.2

7.3.3.3 Precision

The precision of the method was determined by 10 repetitive analysis of the standard solution as well as that of the water samples. All these were carried out under optimum conditions. The standard deviation for the standards was <1.0% and the samples <1.5%.

7.3.3.4 Detection limit

The detection limit was calculated using the formula:

$$\text{Detection limit} = \frac{[(3\sigma + k) - c]}{m}$$

where σ (0.00455) is the standard deviation of the baseline, k (0.1932) is the average response of the baseline and c (0.0877) is the slope of the calibration graph. The detection limit was found to be 0.01 mg/ℓ.

7.3.3.5 Recovery

The recovery of the proposed system was determined by comparing the expected results with those obtained with the proposed system as follows:

$$\text{Recovery (\%)} = \frac{\text{obtained}}{\text{expected}} \times 100$$

Real samples were spiked with 5 mg/ℓ nitrate solution and analysed with the SIA method. The results ranged between 96.4% and 106.8%.

7.3.3.6 Sample interaction

The sample interaction carryover between consecutive samples was determined by analysing samples with low analyte concentration followed with a high analyte concentration which was again followed by the sample with a low analyte concentration. The sample interaction was then calculated using the following formula:

$$\text{Sample interaction} = \frac{A_3 - A_1}{A_2} \times 100\%$$

where A_1 is the peak height (0.2937) of a sample containing 1 mg/ℓ, A_2 is a peak height (0.7361) of a sample containing 5 mg/ℓ and A_3, is a peak height (0.3033) of a sample containing 1 mg/ℓ. The sample interaction was 1.3 % which may be considered negligible.

7.3.3.7 Interferences

The only possible interferences that may disturb the accuracy of this analysis are: iron, copper, phosphates, chromium (VI), magnesium, manganese and chloro-amines. Fortunately all these ions were found to be at acceptable levels and did not affect the results. Table 7.11 gives some of the ions, their ranges and tolerance levels in the water samples analysed. Oms *et al.* (1995) found that copper (II) interfered in the reduction step and for it not to interfere, the copper

sulphate used for the copperised cadmium reductor should be less than 25 mg/ℓ, however, in this work the tolerance level is 20 mg/ℓ. Besides, in this work an acidified reactor was used in the place of the copperised one, thus minimising any interference that may arisedue to copper.

TABLE 7.11 Some of the ions present in the water samples, their ranges and tolerance levels in mg/ℓ when 2 mg/ℓ standard (nitrate + nitrite) was added.

Ion	Tolerance level	Range in samples
Phosphate as P	1	0.008 - 0.080
Chloride	800	10 - 400
Sulphate	300	0.018 - 66
Sodium	750	4 - 67
Potassium	700	0.3 - 8.3
Calcium	350	3 - 19
Magnesium	300	2 - 19
Copper	20	0.0011 - 0.057
Nickel	40	0.0043 - 0.79
Chromium	5	0.0084 - 0.14
Iron	20	11.4 - 14.2

7.4 Statistical comparison of techniques used

The comparison was done between the SIA and the standard method (Institute for Water Quality Studies) (Table 7.10). The comparison was done to establish whether the SIA system can be accepted as giving reliable results in the determination of oxidised nitrogen. The null hypothesis was used [41,42]. The t-test with multiple samples (paired by differences) was applied to

examined whether the two methods differed significantly at 95% confidence level. The null hypothesis is $H_o : \mu_d = 0$, against the alternative $H_t: \mu_d \neq 0$, where μ_d is the population paired difference.. The test is two tailed, as we are interested in both $\mu_d < 0$ and $\mu_d > 0$.

The mean, $\bar{x}_d$ standard deviation, s_d and $t_{calculated}$, $t_{calc.}$ can be determined from the following equations:

$$\bar{x}_d = \frac{\sum x_d}{N}$$

$$s_d = \sqrt{\frac{\sum (x_d - \bar{x}_d)^2}{N-1}}$$

and

$$t_{calc.} = \left|\bar{x}_d\right| x \frac{\sqrt{n}}{s_d}$$

From Table 7.10 we can deduce the following:

$$\sum x_d = 0.0339 \qquad \text{and} \qquad \sum x_d^2 = 0.065.$$

Substituting for the mean, standard deviation with N =10,. we get:

$$\bar{x}_d = 0.0034$$

$$S_d = 0.0848$$

and substituting for $t_{calculated}$ with n = 10 we get:

$$t_{calc.} = 0.1267$$

In the determinations we have 10 determinants (n=10), therefore $\upsilon = 9$ and at 95% confidence level $t_{0.05,9} = 2.36$. The critical t-values are therefore ± 2.36. Since the calculated value is less than the critical value, H_o cannot be rejected and it follows that there is no statistically significant difference between the two techniques.

7.5 Conclusions

The determination of the oxidised nitrogen (nitrate + nitrite as N) by SIA using a solid-phase reactor incorporated into the SIA manifold is an improvement on similar techniques which used FIA and semi-automated burettes. Furthermore, in the work an acidified cadmium reactor was

used which eliminated all possible interferences that may have been caused by copper or/and phosphate ions. In contrast to work already done, in this work the cadmium reactor was regenerated on-line without having to disconnect the system or replace it after regeneration. Thus, once more the SIA system was found to be time and reagent saving and suitable for the determination of oxidised nitrogen in water samples to a very low level.

7.6 References

1. WHO, **Nitrate, Nitrites and N-nitroso Compounds, Health Criterias, World Health Organisation,** Geneva, 1977.

2. J.F. van Staden, M.A. Makhafola and D. De WaaL, **Appl. Spectros., 50** (1996) 26.

3. W.J. Williams, **Handbook of Anion Determination, School of Chemistry,** University of Bath , Butterworth, 1979.

4. A. H. Goodman, **Potable water quality**: ***Development in water treatment - 2,*** Ed. W.W. Lewis , London, 1980.

5. M. Christy, J.R. Brown and G. E. Smith , **Nitrates in soils and plants. Science and Technology Guide**, Univ. of Missouri, Columbia Extension Division, 1973.

6. B.A.Schuster and K. Lee (1987), **J. Food Sci. 52** (1987) 1632.

7. J. J. Francis, **Pigments and other colorants** : ***Food chemistry*** Ed. O. K. Fennema, 62 New York, 1998.

8. S. S. Mirush, **J. Nat. Cancer Inst., 71** (1983) 629.

9. P. E. Hartman , **Nitrates and Nitrites**: ***Ingestion Pharmacopynamics*** **, vol (7)** Eds. F. J. De Serres and A. Hollaeuer, Plenum, 1982.

10. R. B. Gauntlet, **Removal of nitrogen compounds**: ***Development in water treatment - 2,*** Ed. W.W. Lewis, London, 1980.

11. N. Taylor, **Medical aspects of nitrate in drinking water:** ***Water Treat. Exam.,*** **24** (1975)194.

12. J. Bremmer and D. R. Keeney, **Anal. Chim. Acta, 32** (1965) 485.

13. J. Keay and P. M. A. Menage, **Analyst, 95** (1970) 379..

14. K. Takeda and K. Fujiwara, **Anal. Chim. Acta, 276** (1993) 25.

15. P. J. Rennie, A. M. Summerand and F. B. Basketter, **Analyst, 105** (1979) 837.

16. D. Huiro, J. Meigu and Z. Quing, **Anal. Lett., 24 (2)** (1991) 305.

17. K. E. Keeney, B. H. Byrnes and J. J. Genson, **Analyst, 95** (1970) 383.

18. R. S. Lambert and R. J. Dubois, **Anal. Chem., 43** (1971) 955.

19. W. Davidson and C. Woof, **Analyst, 104** (1978) 403.

20. M. F. Gine, H. F. Bergamin, E. A. G. Zagato and B. F. Reis, **Anal. Chim. Acta, 114** (1980)191.

21. C. A. Watson (1980) **Water analysis. Official and standardized methods of analysis, 3rd ed.** London,1980.

22. A. Chaube, A. K. Baveja and V. K. Gupta, **Anal. Chim. Acta, 143** (1982) 273.

23. S. Sunita and V. K. Gupta, **Int. J. Environ. Anal. Chem., 19** (1984)11.

24. W. A. Bashir and S. Flamez, **Talanta, 28** (1981) 697.

25. P. K. Daspupta, . **Anal. Lett., 17 (A10)** (1984)1005.

26. G. Norwitz and P. N. Kelliher, **Analyst, 110** (1985) 689.

27. P. K. Tarafder and D. P. S. Rathore, **Analyst, 113** (1988)1073.

28. H. P. S. Rathore and S. K. Tiwari, **Anal. Chim. Acta, 242** (1991) 225.

29. M. B. Shinn, **Ind. Eng. Anal. Ed., 13** (1941) 33.

30. E. A. G. Zagato, O. A. Jacintho, L. Mortatti and H. F. Bergamin, **Anal. Chim. Acta, 120** (1980) 399.

31. L. Anderson, **Anal. Chim. Acta, 110** (1980)123.

32. J .F. van Staden, **Anal. Chim. Acta, 138** (1982) 403.

33. T. McCormack, A.R.J. David, P. J. Worsfield and R. Howland, **Anal. Proc., 31**

(1994) 81.

34. J. F. van Staden and M. A. Makhafola, **Fresenius' J. Chem., 356** (1996) 70..

35. J. F. van Staden and M. A. Makhafola, **S. Afr. J. Chem., 52 (1)** (1999) 49.

36. M.T. Oms, A. Cerda, and V. Cerda, **Anal. Chim. Acta, 315** (1995) 321.

37. J. F. Van Staden and T. A. van der Merwe, **Microchim. Acta, 129** (1998) 33.

38. A. Cerda, M. T. Oms, R. Ferteza and V. Cerda, **Anal. Chim. Acta, 371** (1998) 63.

39. J. Růžička, G.D. Marshall and G. D. Christian, **Anal. Chem., 237** (1990) 329.

40. G. D. Marshall and J. F. van Staden, **Anal. Instrum., 20** (1992) 79.

41. D. McCormick and A Roach, **Measurement, Statistics and Computation. Analytical Chemistry by Open Learning**. Wiley & sons, London, 1995.

42. D. A. Skoog, D. M. West and F. J. Holler, **Fundamentals of Analytical Chemistry, 7th ed.** Saunders, USA, 1996.

CHAPTER 8

Determination of total chromium as chromate in electroplating and natural waters with a sequential injection analysis (SIA) system

8.1 Introduction

Chromium is a naturally occurring trace element found in rocks, plants, animals, soil, water and in volcanic dust and gases. It is very hard, is resistant to corrosion and takes a bright polish. The main ore of chromium is chromite, $FeO.Cr_2O_3$. Chromium is a white, hard, lustrous and brittle metal (mp. 1903 ± 10°C). It is extremely resistant to ordinary corrosive agents which accounts for its extensive use as an electroplated protective coating [1- 3].

The world industrial growth has brought in environmental pollution and has also increased the exposure of workers to several toxic substances. Toxicological studies have shown that some essential and non-essential elements become toxic at a certain level of concentration. It has been demonstrated that the degree of toxicity and negative effect of an element on health, depends on the chemical form on which the toxic agent is present and the oxidation state of the element [4, 5].

People are exposed when eating, drinking water, and inhaling air that may contain chromium. Dermal exposure may occur when using products that contain chromium. Occupational exposure occurs from chromate production, stainless steel production, chrome plating and the tanning industry [3].

Chromium is an essential element and is necessary for the maintenance of normal glucose, proteins and fat metabolism. Hexavalent chromium is believed to be toxic and it has been fed to animals in tests at a concentration of 25 mg/ℓ for over a year with no toxic effect in these animals. Studies have shown that hexavalent chromium can cause cancer of the respiratory tract when inhaled as a dust.

It is because of this association with a known hazard to health that a limit of 0.05 mg/ℓ as total chromium has been imposed in the US Interim Primary Drinking Water Standards. The same value appears in the WHO European Drinking Water Standards and in Japanese Standards, but relating to hexavalent chromium only.

The European Economic Community (EEC) Directives for Surface Water and for Drinking Water for Human Consumption both follow the American Standards and suggest 0.05 mg/ℓ as an imperative standard for total chromium. However, the Soviet Standard suggest 0.1 mg/ℓ of hexavalent chromium and 0.5 mg/ℓ for total chromium [7]. The reference dose (RfD) for hexavalent chromium is 0.005 mg/kg per day and the Rfd for trivalent chromium is 1 mg/kg per day. The US Environmental Protection Agency (EPA) estimates that consumption of these doses or less over a lifetime is unlikely to result in the occurrence of chronic non-carrier effects [8].

In water analysis, inorganic chromium is one of the pollutants that needs control. Trivalent and hexavalent chromium compounds are the major species of inorganic chromium in water. Their contamination sources are mainly waste-waters of metallic smelting, electroplating, mining, leather tanning, cement industry, dye stuff industry and corrosive paints [8, 9]. The chromium species most frequently found in water are chromates (CrO_4^{2-}), cations hydroxo complexes, $Cr(OH)^{2+}$ and $Cr(OH)_2^{+}$ and organically bound [10, 11] or colloidally sorbed Cr(III) [12]. The chemistry of hexavalent chromium will be briefly discussed as it will form the basis of our studies.

8.2 The chemistry of chromium (VI), d°

In basic solutions above pH 6, CrO_3 forms the tetrahedral yellow chromate ion, CrO_4^{2-}. Between pH 2 and pH 6, $HCrO_4^-$ and the orange-red dichromate ion $Cr_2O_7^{2-}$ are in equilibrium and at pH values below 1, the main species is H_2CrO_4. The equilibria are the following:

$$HCrO_4^- \rightleftharpoons CrO_4^{2-} + H^+$$

$$H_2CrO_4 \rightleftharpoons HCrO_4^- + H^+$$

$$Cr_2O_7^{2-} + H_2O \rightleftharpoons 2HCrO_4^-$$

In addition there are the base-hydrolysis equilibria :

$$Cr_2O_7^{2-} + OH^- \rightleftharpoons HCrO_4^- + CrO_4^{2-}$$

$$HCrO_4^- + OH^- \rightleftharpoons CrO_4^{2-} + H_2O$$

which have been studied kinetically for a variety of bases [1, 2]. The pH-dependent equilibria are quite labile, and on addition of cations that form insoluble chromates, (e.g. Ba^{2+}, Pb^{2+}, Ag^+) the chromates and not the dichromates are precipitated [1, 2].

8.3 Choice of analytical technique

From an analytical point of view, the determination of chromium is difficult since trace levels analyses are strongly affected by contamination. There are however, only a few analytical techniques available that have sufficient sensitivity and selectivity for the direct determination and speciation of trace levels of chromium in water [13]. The different pre-concentration methods used to determine low levels of individual chromium species are liquid-liquid extraction [14, 15], co-precipitation [11, 12, 16, 17], electroplating [18] and absorption [19].

Kingston *et al.* [20] developed a speciated isotope dilution mass spectrometry (SIDM). They described the applicability of their method to chromium. Bağ *et al.* [21] described the pre-concentration of Cr(III) from Cr(VI) and the determination of that chromium using AAS as detector.

Chromium occurs in the environment on two major valence states, trivalent chromium {Cr(III)} and hexavalent {Cr(VI)}.

Veilon [22] has shown that, so far graphite furnace atomic absorption spectrometry (GFAAS) is still one of the best alternative to determine trace levels of chromium. Even modern multi-element technique such as inductively coupled plasma mass spectrometry (ICPMS) do present limitations [23].

There are several flow injection analysis (FIA) methods used for chromium determination [24-30] with different detectors. But, very little using the sequential injection analysis (SIA) has been done. Luo *et al.* [31] demonstrated the use of organic wetting film extraction to enhance the sensitivity and selectivity in the SIA analysis of Cr(III) and Cr(VI) in natural waters. Oliviera and Masini [32] proposed an SIA method for the determination of Cr(VI) in residual waters from electroplating baths and steels.

From the above discussion, it is evident enough that much has to be done in the analysis of chromium. Therefore, some of the pre-requisites needed for an analyser in the determination of chromium, is that the system should be simple and robust, reliable with minimal needs for maintenance and re-calibration, low consumption of reagents and enhanced sensitivity. The SIA system seem to meet all these requirements. It is thus an ideal technique to use in the determination of chromium.

In this work, owing to the significance of Cr(III) monitoring in industrial electroplating processes and natural waters, the chemistry of chromium had to be revisited. A solid phase lead(IV) oxide is incorporated in the SIA manifold to enhance the selectivity and sensitivity of the chromate ion which is detected with a UV/VIS spectrophotometer in a basic medium. The proposed final reaction [33] is,

$$PbCrO_4 + 4OH^- \rightarrow [Pb(OH)_4]^{2-} + CrO_4^{2-}$$

SIA, launched in 1990 [34, 35] is a technique that has tremendous potential for on-line process measurements, due to its simplicity and convenience with witch sample manipulation can be automated. The versatility of the technique is centred around a selection valve, where each part of the valve allows a different operation to be performed [34-36].

8.4 Chromium determination

A modified version [24, 25], where Cr(III) is oxidised by Ce(VI) to Cr(VI) is investigated. A solid-phase lead(IV) oxide is incorporated into the SIA manifold to precipitate the chromate ion as lead chromate which subsequently releases the chromate ion in excess base to be detected with a UV/VIS spectrophotometer.

The following set of reactions are proposed from sample oxidation to detection:

$$6\ Ce\ (IV) + 2\ Cr\ (III) + 7\ H_2O \rightarrow 6\ Ce\ (III) + Cr_2O_7^{2-} + 14H^+ \text{----------(1)}$$

Reaction (1) occurs in hot acid medium. The Cr (VI) is expected to exist either as the chromate or dichromate[33]. After the pH was adjusted between 6.5 and 7.5, the Cr (VI) may be written as:

$$2CrO_4^{2-} + 2H^+ \Leftrightarrow 2HCrO_4^- \Leftrightarrow Cr_2O_7^{2-} + H_2O \text{----------(2)}$$

OR

$$2CrO_4^{2-} + 2H^+ \Leftrightarrow Cr_2O_7^{2-} + H_2O \text{ ----------(3)}$$

When the sample is propelled through the solid lead (IV) oxide the following occurs:

$$Pb^{2+} + CrO_4^{2-} \Rightarrow PbCrO_4 \text{ ----------(4)}$$

OR/AND

$$Pb^{2+} + CrO_4^{2-} + H_2O \Rightarrow PbCrO_4 + 2H^+ \text{ ----------(5)}$$

When the base is introduced the following reaction occurs:

$$PbCrO_4 + 2H^+ + OH^- \Rightarrow PbCrO_4 + H_2O\text{----------(6)}$$

An excess of the base (ammonium hydroxide) forms the soluble complex tetrahydroxoplumbate (II) ion. This suppresses the Pb^{2+} ion concentration to such an extent that the solubility product (1.8×10^{-14}) of lead chromate is no longer exceeded, and consequently the latter dissolves releasing chromate according to the following reaction:

$$PbCrO_4 + 4OH^- \Rightarrow [Pb(OH)_4]^{2-} + CrO_4^{2-} \text{ ----------(7)}$$

The chromate released in (7) is propelled towards the detector where it detected at 360 nm.

8.4.1 Experimental

8.4.1.1 Reagents and solutions

All reagents were prepared from analytical-reagent grade chemicals unless specified otherwise. All aqueous solutions were prepared from double de-ionised water. De-ionised water from Modulab system (Continental Water System, San Antonio, TX, USA) was used throughout.

8.4.1.1.1 Stock chromium (III) solution

A 5.1234 g of chromium (III)-chloride-6-hydrate (96% pure, Riedelhaën) was dissolved in 100 mℓ hydrochloric acid (1 mol/ℓ) solution and diluted to 1ℓ with water. Working standards in the range 0.01 to 10 mg/ℓ were prepared by appropriate dilutions of the stock solution with water.

8.4.1.1.2 Stock dichromate solution

A 2.8292 g of potassium dichromate (chemically pure, Protea Laboratory) was dissolved and diluted to 1ℓ with double de-ionised water. Working standards in the range of 0.01 to 10 mg/ℓ were prepared by appropriate dilution of the stock solution with water.

8.4.1.1.3 Stock chromate solution

A 3.7355 g of potassium chromate (pure analysis, SAARCHEM) was dissolved and diluted to 1ℓ with double de-ionised water. Working standards in the range 0.01 to 10 mg/ℓ were prepared by appropriate dilution of the stock solution with water.

8.4.1.1.4 Ammonium cerium (VI) sulphate solution

A 5.9635 g of ammonium cerium (IV) sulphate (BDH, Poole, England) was dissolved in 50 mℓ 2 mol/ℓ sulphuric acid (98%, H_2SO_4, Holpro analytics) solution and made up to 500mℓ.

8.4.1.1.5 Sodium nitrite solution

A 5.0076 g of sodium nitrite (pure analysis, Riedel de haën) was dissolved and diluted to 250 mℓ with water.

8.4.1.1.6 Ammonium hydroxide solution

A 18.7 mℓ of ammonia (25% NH_3, SAARCHEM) solution was diluted to 250 mℓ with water.

8.4.1.1.7 Sulphuric acid solution

A 55.6 mℓ of sulphuric acid (98%, H_2SO_4, chemically pure, Holpro analytics) solution was diluted to 500 mℓ with water.

8.4.1.2 Instrumentation

The sequential injection system depicted in Fig. 8.1 was constructed from the following components: a Gilson minipuls peristaltic pump (Model M312, Gilson, Villiers-Le Bel, France); a 10-port electrically actuated selection valve (Model ECSDIOP, Valco Instruments, Houston, Texas) and a Unicam 8625 UV-Visible spectrophotometer equipped with a 10-mm Hellma-type (Hellma GmbH and Co., Mulheim/Baden, Germany) flow-through cell (volume 80 $\mu\ell$) for absorbance measurements.

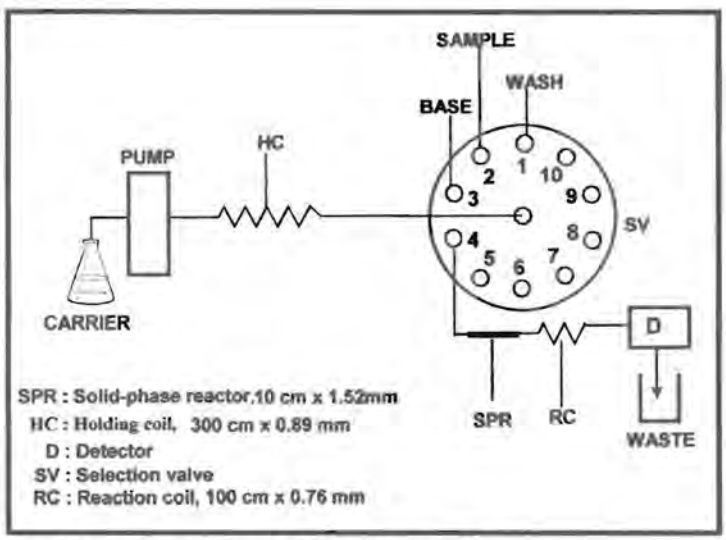

Fig. 8.1 A diagram for the SIA system used.

Data acquisition and device control was achieved using a PC30-B interface board (Eagle Electric, Cape Town) and an asssembled distribution board (Mintek, Randburg). The flowTEK [37] software package (obtainable from Mintek) for computer-aided flow analysis was used throughout for device control and data acquisition. All data given (mean peak height values) are the average of 10 replicates.

8.4.1.3 Solid-phase reactors

The solid-phase reactor (SPR) was constructed using PTFE tubing with an internal diameter of 1.52 mm (Fig.8.2). The reactor consisted of lead(IV)dioxide suspended on silica gel beads (35-70 mesh, 40 Å; Aldrich-Chemical Co. Gillingham-Dorset). The packing was prepared as described by Rüter and Neidhart [41], the only difference being the use of commercial sodium hypochlorite (3.5% m/V, sodium hypochlorite when packed) for supplying the sodium hypochlorite. The sodium hypochlorite oxidises the divalent lead acetate according to the following equation:

$$Pb(CH_3COO)_2 + NaOCl \rightarrow PbO_2 + 2CH_3COOH + NaCl$$

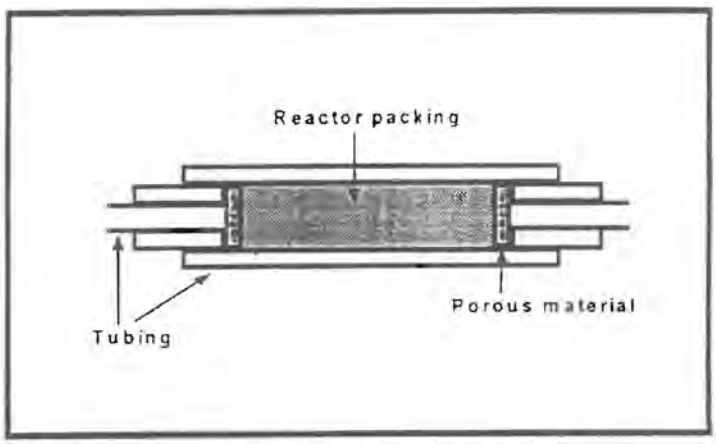

Fig. 8.2 Design of a tubular packed lead(IV) dioxide reactor

After packing each reactor had be conditioned (run in) for at least 60 minutes before use. Conditioning involved pumping de-ionised water through the reactor at a flow rate of 2.2 mℓ

/min for 45 minutes, then the carrier for 15 minutes at the same rate. This was to ensure that there were no air pockets and to ensure close packing of the beads. The lifetime of each reactor was established by comparing peak heights for the same standards from day to day. When the peak heights started to decrease systematically and drastically, the reactor had to be replaced. Another indication that the reactor was losing its conversion capacity was the colour of the packing itself. At the beginning of a new conditioned reactor the colour of the packing was dark brown which gave a greyish appearance inside the PTFE tubing. After the reactor was in use for several samples (400-500 experiments) and depending on the concentration of the chromate in the samples the colour of the packing at the front end of the reactor started to disappear. This meant that al of the led(IV)dioxide had stripped off the beads.

8.4.1.4 Sample preparation

The samples were obtained from the Institute for Water Quality Studies (Department of Water Affairs and Forestry) and Electroplating industries. The samples were collected from different localities (streams, rivers, dams, hydro plants, tunnels and effluent streams) at half a metre depth.

A 50 mℓ aliquot of each sample was transferred into a 100 mℓ Erlenmeyer flask. A 10 mℓ portion of a 2 mol/ℓ sulphuric acid solution was added into the sample. The Erlenmeyer flask and its contents were placed in a boiling water in a water bath. After 15 minutes a 10 mℓ aliquot of ammonium cerium (IV) sulphate solution was added into the hot solution to oxidise chromium(III) to chromium(VI). An excess amount of the cerium(IV) solution was added to ensure complete oxidation (having assumed that the amount of chromium may not exceed 5 mg/ℓ). The oxidised sample was removed from the boiling water after 45 minutes, the solution

was cooled to zero degree Celsius. A 5 mℓ portion of a 2% sodium nitrite solution was added to destroy any excess cerium (VI) solution that may be remaining. (Cerium(IV) may form the yellow cerium(IV)hydroxide which may interfere with the results).

The pH of the solution was adjusted to between 6.5 and 7.5 with ammonium hydroxide solution. The resulting solution was diluted to 100 mℓ with water and was now ready for chromium analyses with the proposed SIA system.

8.4.1.5 Operation of the system

A schematic diagram for the SIA system is depicted in Fig.8.1. The whole procedure, from sample injection to data processing and storage was computer controlled via the FlowTEK program. The whole SIA procedure involved designing a method which allows a single cycle of the experiment to be run. Fig. 8.3 and Table 8.1 shows the device sequence for one cycle.

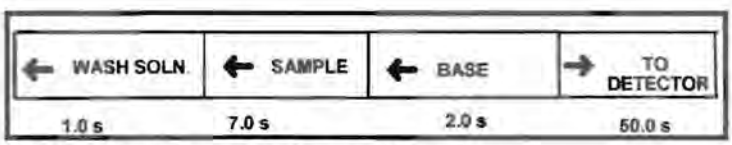

Fig. 8.3 Device sequence for one SIA cycle

The basic components of the system are a peristaltic pump with only one carrier stream, a single channel and a detector. The concept is based on the sequential injection of a wash solution, sample zone and reaction zone(s) into a channel [37-40]. In this way a stack of well defined zones adjacent to each other is obtained in a holding coil.

TABLE 8.1 Device sequence for one cycle of the SIA system

Time (s)	Pump	Valve	Description
0	Off	Position 1	Pump off. Select wash stream.
1	Reverse		Draw wash solution.
2	Off		Pump stop.
3	Off	Position 2	Select sample stream.
4	Reverse		Draw sample solution.
11	Off		Pump stop.
12	Off	Position 3	Select base stream.
13	Reverse		Draw base solution.
15	Off		Pump stop.
16	Off	Position 4	Select detector line.
17	Forward		Pump zones through SPR to detector.
60	Off	Position 1	Pump stop. Valve return home.

After the valve has been selected to the detector position, the flow in the carrier stream is reversed and the zones mutually disperse and penetrate each other as they passed through the reaction coil to the detector. The reversed flow, therefore creates a composite zone in which the sample and reagent zone penetrate each other due to combined axial and radial dispersion.

The sample and reagent zones were pumped through the solid lead(IV) oxide by the carrier stream (de-ionised water) to convert the dichromate to stable chromate. The total chromium as chromate was directed to the detector for measurement at 360 nm. The absorbance of the chromate at 360 nm was chosen after a scan of stock solutions (each diluted to a concentration of 2 mg/ℓ) for maximum absorbance over the 200 to 1100 nm range with a UV/VIS

spectrophotometer. The maximum absorbance was detected at 420, 430 and 360 nm for chromium (III), dichromate and chromate ions respectively. The data obtained was converted to a response time graph and was viewed on the monitor as a peak profile. The maximum peak height was automatically processed and stored on a computer via the FlowTEK program.

8.4.2 Method optimization

8.4.2.1 Chemical parameters

8.4.2.1.1 Chromium(III) concentration

The chromium(III) solution was treated exactly like the samples and its concentration was evaluated between 0.2 and 20 mg/ℓ and the 0.4 mg/ℓ was chosen as the optimum value for optimising the remaining parameters. The results of this optimisation is presented in Table 8.2 and Fig. 8.4. To verify efficiency of the oxidation by the cerium (IV) solution, a similar concentration of dichromate and chromate solutions, were analysed. The results were in agreement within 97% which can be considered acceptable. Table 8.3 gives these results.

TABLE 8.2 Effect of chromium concentration on response and precision

Conc. (mg/ℓ)	0.2	0.4	0.6	0.8	1	1.2
RPh	0.2	0.271	0.368	0.441	0.575	0.743
%RSD	0.81	0.37	1.07	1.02	1.1	0.66

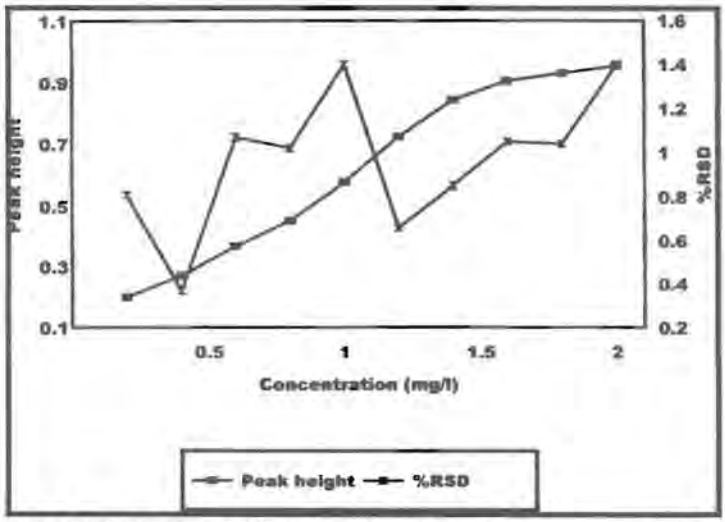

Fig. 8.4 Influence of chromium concentration on response and precision

TABLE 8.3 Comparison of response of oxidised Cr(III) to that of dichromate and chromate

Concentration (mg/ℓ)		0.2	0.4	0.6	0.8	1
Relative peak height	**Chromium (III)**	0.200	0.271	0.368	0.441	0.575
	Dichromate	0.206	0.28	0.379	0.456	0.59
	Chromate	0.208	0.287	0.383	0.461	0.594

8.4.2.2 Physical parameters

The contact time between the sample zone containing the oxidised chromium (III) solution and the solid phase lead (IV) oxide reactor is of utmost importance for total conversion of dichromate/chromate to chromate. This conversion is influenced by reactor length, flow rate, sample volume and base volume.

The performance of the SIA system depends on the efficiency of the solid lead (IV) oxide reactor to convert the chromate to the form in which it has to be detected. It thus form the heart of the manifold in the proposed SIA system.

8.4.2.2.1 Reactor length

The response and precision were studied by varying the length of the solid phase reactor between 6 and 14 cm with internal diameter fixed at 1.52 mm. The five reactors were compared for their conversion efficiency in Table 8.4a and Fig. 8.5.

TABLE 8.4a Effect of solid phase reactor length on response and precision

Length (cm)	6	8	10	12	14
RPh	0.38	0.389	0.421	0.422	0.421
%RSD	1.2	0.92	0.71	0.84	0.73

Furthermore, in order to verify whether the incorporation of the SPR reactor is justified at all, a stock chromium (III) solution was analysed (10 runs) with and without the SPR and the response compared. The incorporation of the SPR gave the best results (Table 8.4b).

TABLE 8.4b Influence of SPR on response and precision

Condition	**Relative peak height**	**%Relative standard deviation**
Without the SPR	0.325	1.46
With SPR	0.421	0.71

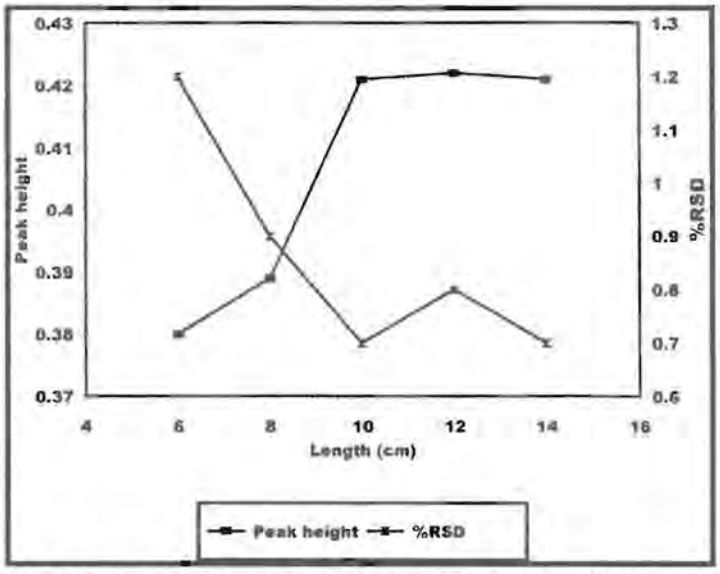

Fig. 8.5 Effect of reactor length on response and precision

From the results obtained it can be seen that there is a significant improvement in response as well as the precision with the incorporation of the SPR into the SIA manifold. This can only mean that although cerium oxidises Cr(III) to Cr(VI) the Cr(VI) is present both as the dichromate and chromate ions. The SPR reactor therefore ensures that all the Cr(VI) is present as chromate prior to detection (see proposed reactions 4, 5 and 6 page 237). Hence the presence of the SPR is important in the determination of chromium as chromate.

8.4.2.2.2 Flow rate

The conversion is also influenced by flow rate. Flow rates between 2.26 and 4.53 mℓ/min were evaluated. The optimum flow rate was found to be 3.96 mℓ/min. This is well presented in Fig. 8.6 and Table 8.5.

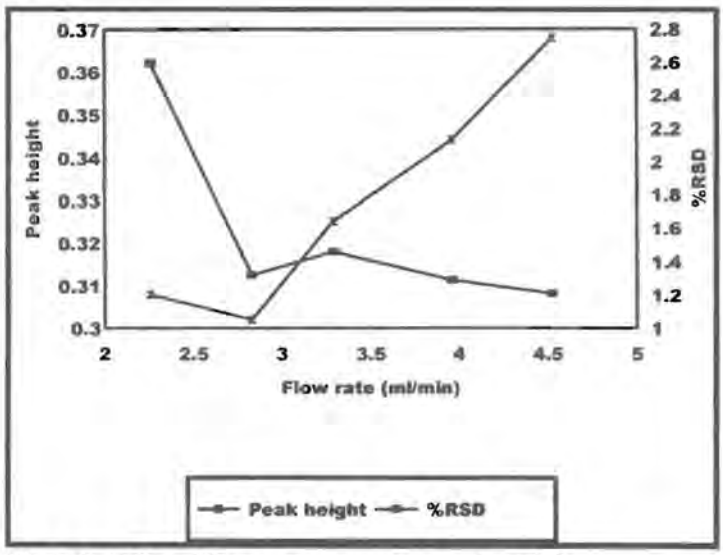

Fig. 8.6 Effect of flow rate on response and precision

TABLE 8.5 Effect of flow rate on response and precision

Rate (ml/min)	2.26	2.83	3.29	3.96	4.53
RPh	0.308	0.302	0.325	0.344	0.368
%RSD	2.6	1.3	1.46	1.29	1.2

8.4.2.2.3 Sample volume

The effect of sample and base were studied as well, and they were found to play a significant role. The sample volume was evaluated between 27.5 and 247.5 $\mu\ell$ and 137.5 $\mu\ell$ volume was found to be the best as shown in Table 8.6 and Fig. 8.7.

TABLE 8.6 Effect of sample volume on response and precision

Volume ($\mu\ell$)	27.5	82.5	137.5	192.5	247.5
RPh	0.232	0.312	0.393	0.454	0.505
%RSD	2.2	1.46	0.78	0.75	0.8

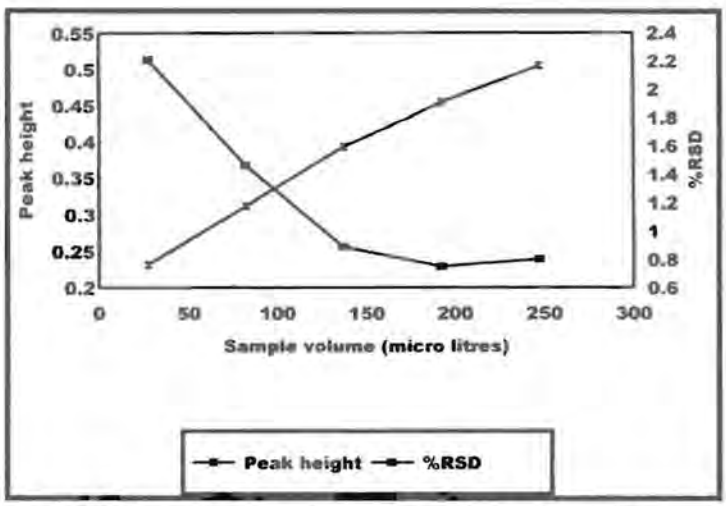

Fig. 8.7 Effect of sample volume on response and precision

8.4.2.2.4 Base volume

The base volume was evaluated between 27.5 and 137.5 $\mu\ell$. The 55 $\mu\ell$ gave the best results. Tables 8.7 and Fig. 8.8 gives the results.

TABLE 8.7 Effect of ammonium hydroxide on response and precision

Volume ($\mu\ell$)	27.5	55	82.5	110	137.5
RPh	0.421	0.393	0.418	0.423	0.416
%RSD	1.7	0.75	1	0.87	0.8

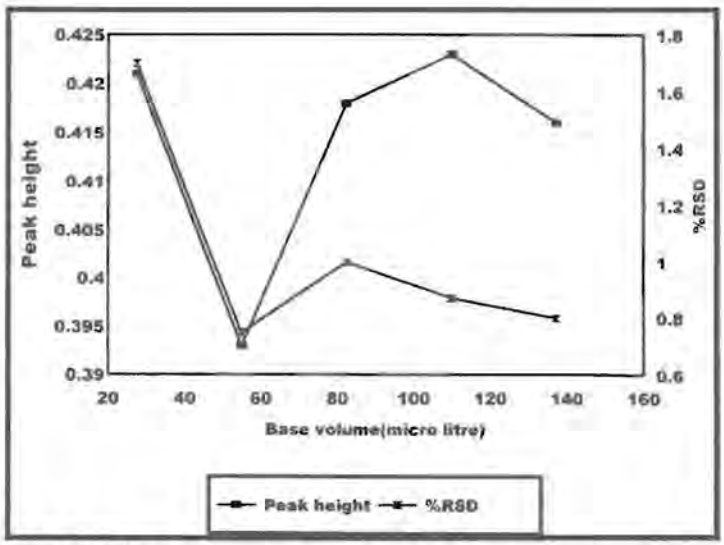

Fig. 8.8 Effect of ammonium hydroxide volume on response and precision

8.4.3 Method evaluation

8.4.3.1 Linearity

The linearity of the system was evaluated for analyte concentration between 0.01 and 5 mg/ℓ under optimum conditions Table 8.8. The system was found to be linear in the range of 0.01 to 1 mg/ℓ (Figure 8.9). The relationship obtained between response and concentration is given by the equation :

$$H = 4.8628x - 0.0495,\ r = 0.999,\ n = 8$$

where H is the relative peak height and x is the analyte concentration in mg/ℓ.

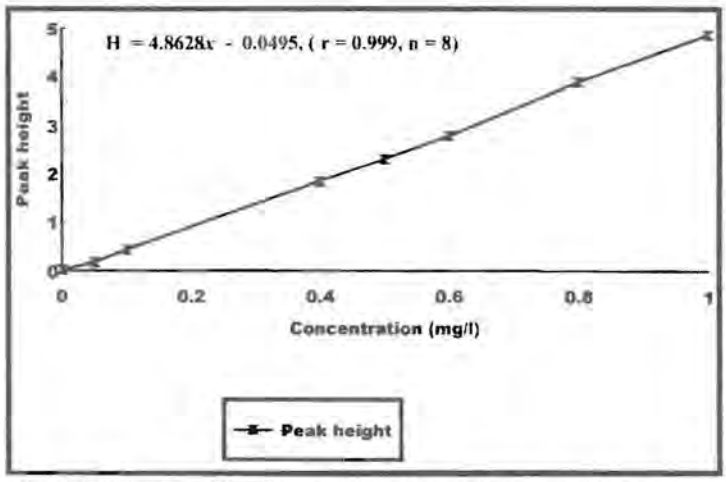

Fig. 8.9 A linear calibration graph under optimum conditions

TABLE 8.8 Optimum conditions

Parameter	Optimum value
Chromium concentration	0.4 mg/ℓ
Reactor length	10 cm
Flow rate	3.96 mℓ/min
Sample volume	137.5 $\mu\ell$
Base volume	55 $\mu\ell$

8.4.3.2 Accuracy

The accuracy was evaluated by comparing results obtained with the SIA system (Table 8.9) and the standard method (AAS) Table (8.10). The results obtained are a mean of 10 repetitive analysis of each sample.

TABLE 8.9 SIA results for samples analysed

Sample Id	Relative peak height	mg/ℓ Chromium
SE 1	3.395 (0.5%)	1.4164
SE 2	3.375 (0.5%)	1.4082
SE 3	0.148 (0.9%)	0.0812
SE 4	0.145 (0.9%)	0.0676
SE 5	6.959 (0.4%)	2.8821
SE 6	1.116 (0.8%)	0.4792
SE 7	3.802 (0.5%)	1.5838
Demiskanaal	0.57 (0.8%)	0.2546
GBR-mond	0.015 (1.0%)	0.0263
Hartebeeskuil dam	0.016 (1.0%)	0.0268
Chechasseur	0.099 (1.0%)	0.0611
Bree rivier	0.194 (0.6%)	0.1101
Mutshedzi dam	0.34 (0.9%)	0.1599
Driel barrage	0.57 (0.8%)	0.2546

TABLE 8.10 Standard AAS results for samples analysed

Sample	mg/ℓ Chromium
SE 1	1.4956
SE 2	1.4456
SE 3	0.0795
SE 4	0.0662
SE 5	2.8161
SE 6	0.4782
SE 7	1.4877
Demiskraal kanaal	0.2257

GBR-mond	0.0264
Hartebeeskuil dam	0.0264
Chechasseur	0.053
Bree Rivier	0.0928
Mutshedzi dam	0.146
Driel barrage	0.2257

8.4.3.3 Recovery

The recovery of the proposed system was determined by comparing results obtained, with the expected ones after addition of 0.05 mg/ℓ standard chromium solution to selected samples (Table 8.11). The recovery was calculated using the equation :

$$\% \text{ Recovery} = \frac{\text{obtained}}{\text{expected}} \times 100\%$$

The recovery ranged between 98.87 and 104.76%.

TABLE 8.11 Recovery results after addition of 0.5 mg of Cr(III) to selected samples

Sample	Expected	Recovered	% Recovery
SE 1	1.9164	1.9021	99.25
S6E	0.9792	0.9683	98.89
Mutshedzi dam	0.2099	0.2199	104.76
Demiskanaal dam	0.7546	0.7746	102.65
Bree rivier	0.6105	0.6305	103.27

8.4.3.4 Precision

The precision of the method was determined by 10 repetitive analysis of the standard solution (Fig. 8.9) as well as 10 repetitive analysis of the real samples (Table 8.9). All these were carried out under optimum conditions. The %RSD for the standard was 0.5% and for the real samples is less than 1.0%.

8.4.3.5 Detection limit

The detection limit was calculated using the formula:

$$\text{Detection limit} = \frac{[(3\sigma + k) - c]}{m}$$

where σ (0.002) is the standard deviation of the base line k (0.0415) and c(-0.04945) is the intercept and m(4.8628) is the slope of the calibration graph. The calculated limit of detection was found to be 0.02 mg/ℓ.

8.4.3.6 General problems

The problem encountered with this system was the reactor. It was discovered that when the packed reactor was left exposed to the atmosphere its effectiveness deteriorated compared to a freshly prepared reactor. This problem was overcome by storing the freshly prepared reactors in a dessicator until it was needed for use.

8.4.3.7 Interferences

The effect of the presence of other ions on the determination of chromium was investigated. For this purpose Ag^{+}, Fe^{3+}, Zn^{2+}, Cu^{2+}, Ni^{2+}, Mg^{2+}, Ca^{2+}, K^{+}, Na^{+}, SO_4^{2-}, Cl^{-}, NO_3^{-}, NO_2^{-} and PO_4^{3-} were added individually to a 100 mℓ solution containing 0.5 mg/ℓ chromium and the general procedure applied. As can be seen in Table 8.12, the tolerance levels and the ranges of the ions found in the samples are given. These ions did not significantly affect the determination of chromium in the various samples. The only ion that may interfere was the Ag^{+}, which was likely to form Ag_2CrO_4 precipitate, but this dissolves easily in the presence of ammonium hydroxide to release the chromate ion [33]. Furthermore, cations found were at very low concentrations to affect the results (Table 8.12). Anions were also found to be below the tolerance levels.

TABLE 8.12 Some of the ions present in the water samples, their ranges and tolerance levels in mg/ℓ when added to 0.5 mg/ℓ of chromium.

Ion	Tolerance level	Range in samples
Phosphate	4	0.008-0.080
Nitrate + Nitrite	10	0.47-1.68
Chloride	800	10-400
Sulphate	350	0.018-66
Sodium	800	4-67
Potassium	800	0.3-8.3
Calcium	450	3-19
Magnesium	350	2-19
Copper	30	0.0011-0.057
Nickel	35	0.0043-0.79
Zinc	50	0.005-14.8
Iron	40	11.4-14.2

Silver	50	0.005-15.9

8.5 Statistical comparison of techniques used

The comparison was done between the SIA and the AAS (Table 8.13) results to establish whether the SIA system can be accepted as giving reliable results in chromium determination. The null hypothesis was used [42, 43].

TABLE 8.13 Comparison of SIA and the standard AAS method results in mg/ℓ and paired differences

Sample	SIA method	Standard AAS	$x_d \times 10^{-4}$	$(x_d)^2 \times 10^{-8}$
SE 1	1.4164	1.4956	-792	627260
SE 2	1.4082	1.4456	-337	113569
SE 3	0.0812	0.0795	17	289
SE 4	0.0676	0.0662	13.6	185
SE 5	2.8821	2.8161	659	434300
SE 6	0.4792	0.4782	10	100
SE 7	1.5838	1.4877	961	923500
Demiskraal kanaal	0.2546	0.2257	289.5	83800
GBR-mond	0.0263	0.0264	-0.7	0.4
Hartebeeskuil dam	0.0268	0.0264	-0.7	0.4
Chechasseur	0.0611	0.053	-423.5	179350
Bree Rivier	0.1101	0.0928	173	29930
Mutshedzi dam	0.1599	0.146	139.5	19460
Driel barrage	0.2546	0.2257	289.5	83810

For the null hypothesis we assert that the two methods agree, that is the population mean

difference is zero, $H_0 : \mu_d = 0$. For the alternative hypothesis $\mu_d \neq 0$, where μ_d is the population (H_0) paired by difference. The t-test with multiple samples (paired by difference) was applied to examine whether two methods differed significantly at 95% and 99.9% level. The test is two tailed, as we are interested in both $\mu_d < 0$ and $\mu_d > 0$. From Table 8.13 the following is deduced:

$$\sum x_d = 0.396 \qquad \text{and} \qquad \sum x_d^2 = 0.02496$$

The mean $\bar{x}_d$, standard deviation, S_d and $t_{calculated}$, $t_{calc.}$ are determined from the following equations:

$$\bar{x}_d = \frac{\sum x_d}{N}$$

$$s_d = \sqrt{\frac{\sum (x_d - \bar{x}_d)^2}{N-1}}$$

and

$$t_{calc.} = \left|\bar{x}_d\right| \times \frac{\sqrt{n}}{s_d}$$

Substituting in the above equations with N = n =14, we get:

$$\bar{x}_d = 0.0283$$

$$S_d = 0.0846$$

and

$$t_{calc.} = 3.74$$

At 95% confidence level $t_{0.05,13} = 1.77$ and at 99.9% confidence level $t_{0.01,13} = 4.22$. Since the calculated value lies within the critical value at 99.9% level, it would imply that H_0 cannot be rejected and it follows that there is no significant difference between the two techniques at this level. However, at 95% level it may be rejected.

8.6 Conclusions

The proposed SIA method have shown that 97% of the chromium (III) can be detected. However, in the work already done [44, 45], the on-line oxidation of chromium (III) to chromium (VI) by Ce (IV) was reported incomplete. The incompleteness could have been caused by the reconversion of chromium (VI) back to chromium (III). The incorporation of the solid phase lead (VI) oxide and the basic media created when the chromium (VI) passed through the lead (IV) oxide, prevented the reconversion of chromium (VI) back to chromium (III). It has instead enhanced the production of chromium (VI) as chromate. The proposed SIA system was thus suitable for the determination of chromium in electroplating waters and natural waters. It is simple and robust, saving in reagents, reliable and sensitive as well as cost effective with a detection limit of 0.02 mg/ℓ. The standard AAS method has a detection limit of 0.03 mg/ℓ.

8.7 References

1. F. A. Cotton and G. Wilkinson, **Advanced inorganic chemistry: A comprehensive text, 4th ed.**, Interscience, USA. 1980.
2. W. L. Masterdom, E. J. Slowinski and C. L. Staniski, **Chemical principles with qualitative Analysis, 6th ed.**, Saunders, USA.
3. R. A. Anderson, **Clin. Physiol. Biochem., 4** (1980) 37.
4. P. L. Williams and J. L. Burson, **Industrial Toxicology,** van Norstand Reinhold, New York, 1983.
5. American Conference of Governmental Industrial Hygenists, **Supplemental documentation.** Cincinnati, OH, (1983) 98.
6. J. Versieck, R. Cornelis, **Trace elements in Human Plasma or Serum,** CRC Press, Boca Raton, FL,. 1989.
7. A. H. Goodman, **Potable Water Quality:** ***Developments in Water treatment***-1, Ed. By W. M. Lewis. Applied Science, London, 1980.
8. M. K. Donais, R. Henry and T. Rettberg. **Talanta, 49** (1999) 1045.
9. S. D ahbi, M. Azzi and M. de la Guardia, **Fresenius' J. Anal. Chem., 363** (1999) 404.
10. E. Nakayama, T. Kuwamoto, S. Tsurubo, H. Tokoro and H. Fujiwara. **Anal. Chim. Acta, 130** (1981) 289.
11. E. Nakayama, T. Kuwamoto, S. Tsurubo and T. Fujiwara. **Anal. Chim. Acta, 130** (1981) 401.
12. M. Hiraide, A. Mizuike, **Fresenius' J. Anal. Chem., 335** (1989) 924.
13. V. M. Rao and M. M. Sastri, **J. Sci. Ind. Res., 41** (1982) 607.

14. G. J. De Jong, U. A. T. Brinkman, **Anal. Chim. Acta, 98** (1978) 243.

15. K. S. Subramanian, **Anal. Chem., 60** (1988) 11.

16. T. C. Mullins, **Anal. Chim. Acta, 165** (1984) 97.

17. K. Takeda, C. Akamatsu and Y. Inoue, **Fresenius' J. Anal. Chem., 339** (1991) 50.

18. G. E. Battleu and J. P. Matousek, **Anal. Chem., 52** (1980) 1570.

19. B. Demirata, I. Tor, H. Filik and H. Afsar, **Fresenius' J. Anal. Chem., 356** (1996) 375.

20. H. M. "Skip" Kingston, D. Huo,Y. Lu and S. Challc, **Spectrochimica Acta Part B, 53** (1998) 297.

21. H. Bağ, A. R. Tűcker, M. Lale and A. Tunfeli, **Talanta, 51** (2000) 895.

22. C. Veilon, **Anal. Chem., 58** (1986) 85A.

23. A. Krilshevska, S. Waheed and J. A. Nóbrega, D. Amarisiriwardena, R. M. Barnes, **Appl. Spectrosc. 2** (1988) 205.

24. M. J. Whitaker, **Anal. Chim. Acta, 74** (1985) 375.

25. J. C. Andrade, J. C. Rocha and N. Baccana, **Analyst, 110** (1985) 197.

26. J. Ruz, A. Rios, M. D. Luque de Castro and M. Valcarcel, **Fresenius' J. Anal. Chem.,** (1988) 499.

27. L. Gizard and J. Hubert, **Talanta, 45** (1996) 1965.

28. T. P. Lynch, N. J. Fernoghan and J. N. Wilson, **Analyst, 109** (1984) 839.

29. J. E. T. Andersen, **Anal. Chim. Acta, 361** (1998) 125.

30. S. C. Nielsen, S. Stűrup, H. Spliid and E. H. Hansen, **Talanta, 49** (1999) 1027.

31. Y. Luo, B. Nakano, D. A. Holman, J. Růžička and G. D. Christian. **Talanta, 44** (1997) 1563.

32. P. C. C. Olivier and J. C. Masini, **Analyst, 123** (1998) 2085.

33. G. Svehla, **Vogel's Qualitative Inorganic Analysis 7th ed.**, Longman, London, 1996.

34. J. Růžička and G. D. Marshall, **Anal. Chim. Acta, 237** (1990) 329.

35. J. Růžička , G. D. Marshall and G. D. Christian, **Anal. Chem., 62** (1990) 1861.

36. G. D. Marshall, **Sequential injection analysis, Ph.D-thesis, University of Pretoria,** 1994.

37. G. D. Marshall and J. F. van Staden, **Anal. Instrum., 20** (1992) 79.

38. J. Růžička and T. Gübeli, **Anal. Chem., 63** (1991) 1680.

39. T. Gübeli, G. D. Christian and J. Růžička, **Anal. Chem., 63** (1991) 2407.

40. D. J. Tucker, B. Toivol, C. H. Pollema, J. Růžička and G. D. Christian, **Analyst, 119** (1994) 975.

41. J. Rüter and B. Neidhart, **Microchim. Acta, 18 (1984)** 271.

42. D. McCormick and A. Roach, **Measurement, Statistics and Computation. Analytical Chemistry by Open learning.** Wiley & sons, USA, 1995.

43. D. A. Skoog, D. M. West and F. J. Holler, **Fundamentals of Analytical Chemistry, 7th ed.**, Saunders, USA 1996.

44. B. P. Bubnis, M. R. Straka and G. E. Pacey, **Talanta, 30** (1983) 1669.

45. J. C. Andrade, J. C. Rocha and N. Baccan, **Analyst, 109** (1984) 645.

CHAPTER 9

Conclusions

The importance of manifold design in developing process analysis which are capable of on-line monitoring with high sample through put, minimum sample and reagent consumption, robust, reliable and requiring low frequency of maintenance has become very evident through the course of this work.

The introduction of super Serpentine reactors and solid - phase reactors into the SIA manifold was an attempt to make injection techniques more rugged for process control application. The SIA system contributes considerably to reducing reagent and sample as well as enhancing sensitivity which is one of its greatest attributes.

The simplicity by which the change from a homogeneous to a heterogeneous system was easily reached, is further evidence of the versatility of the SIA technique. Its simplicity is further attributed to the multiport selection valve by which the samples, reagents reactions lines and detectors are accessed. The system is computer controlled and can be configured to perform most operations of conventional flow injection analyses with no or minimal reconfiguration of the manifold.

It has become evident, that there are various parameters that influences the results that flow

systems deliver. The importance of controlling these parameters when developing a method is achieved by optimizing this parameters to obtain maximum response with the best precision.

In SIA high sensitivity is obtained by minimizing the dispersion in the flow manifold, however it is also important to achieve an adequate amount of dispersion so that, the sample can react effectively with the surrounding reagent. It has, though, been realised that for SIA, zone penetration plays an important role in the sample and reagent interaction.

The introduction of solid - phase reactors into the SIA manifold was to accommodate reagents and samples that are expensive , insoluble or partially soluble. The development of the SIA system is aimed at providing the industrial , agricultural, clinical and pharmaceutical fields with reliable , precise and cost effective instrumentation for performing, analysis they require.

The increasing awareness regarding environmental pollution and the regulation of the effluents that are released into the environment, particularly those affecting potable water sources , places an enormous responsibility on analysts to develop methods that can be effectively applied to determining the actual amount of polluting elements that are discharged.

In its study , theoretical aspects of SIA was done which was followed by a brief discussion of the reactor types used both in FIA and SIA this acted as a precursor to the introduction and evaluation of super Serpentine reactors.

A critical review of solid - phase reactors in FIA was made and its various applications to real systems. The SIA system incorporating solid-phase reactors was adapted from the existing FIA

system. Thus the application of the SIA system to real system further exposed its usefulness as a process analyser.

From the discussion of the reactor types, super Serpentine reactors were not previously studied and subsequently its study was undertaken. Super Serpentine reactors were evaluated with regard to its influence on response and precision. It was evaluated to give an in depth information regarding its effect on dispersion in the SIA system.

A comparative study achieved by overlaying peaks of different super Serpentine reactor types and length revealed that the simultaneous choice of reactor type and length play an important role with regard to response and precision and hence dispersion. The response and precision obtained for the various super Serpentine reactors may with proper choice of the reactor be of use in the analyses of trace elements. Dispersion in addition to zone penetration have an important effect on the amount of zone penetration attained.

For the application of solid-phase reactors to real systems, four elements were identified for analyses, namely manganese, iron, nitrogen and chromium. These elements were identified in relation to their potential toxicity to plants, animals as well as to human beings and how essential they are if present or taken in correct dosages in both water and supplements. The determination of these elements using solid-phase reactors in SIA had not been attempted previously and studies on these were subsequently undertaken.

A number of methods requiring laborious sample preparations, using large sample volumes and involving complicated procedures and expensive instruments have been used for the

determination of manganese. The determination of manganese in domestic waters and effluent streams using a solid lead (IV) dioxide reactor is an improvement on these methods as well as on FIA methods used. The manganese is oxidised to permanganate ion in which form it is determined. The proposed SIA system is found to be suitable for manganese determination in tap, domestic and effluent streams with a relative standard deviation of better than 3%.

In the determination of total iron as iron(II), an in depth research has been conducted using different techniques, however these techniques involved expensive instruments and are time consuming. The use of cadmium granules as solid-phase reactor is used in the determination of iron in pharmaceutical products and natural waters. The iron(III) in the samples is reduced to iron(II) and complexed with a colouring reagent to give a dye in which form the iron was determined. The cadmium reactor is regenerated on-line and this places the SIA system ahead in sample frequency and saving of samples and reagents. This developed system is thus suitable for the determination of total iron in pharmaceutical products and water samples within a wide range.

Many colorimetric methods have been used for the determination of nitrogen as nitrate or nitrite, however, most have been determined as nitrite. These determination are all based on the Griess' reaction. The determination of nitrogen involves the oxidation of nitrogen in water samples to nitrite which is diazotised to a red dye and determined as such. The reactor is regenerated on-line for consistency. Thus, the proposed system is found to be suitable for determination of oxidised nitrogen as nitrite in water samples from different sources.

There are several methods which are used for the determination of chromium, there are however,

a few that have sufficient sensitivity and selectivity for the direct determination of trace levels of chromium in water. Even multi-element techniques such as ICPMS do present limitations.

A method with a proposed reaction was developed for monitoring chromium in industrial electroplating processes and natural waters. This involves a solid-phase reactor incorporated into the SIA manifold. The reactor precipitates all the chromium present as lead chromate which is then released in excess base as the chromate ion in which form it is determined. The propose SIA system is suitable for monitoring chromium in industrial electroplating processes and natural waters.

All the above elements determinations were detected by means of a UV/VIS spectrophotometer as stated in the relevant Chapters. The SIA system in all the above is found to be easy to operate, versatile, robust and have the advantage of material saving.

A statistical comparison using the null hypothesis was used to assert that there is no statistical significant differences at 95% confidence level between the proposed SIA techniques and the different standard methods used. Finally, it may be concluded that the proposed SIA technique is suitable for on-line determination, is accurate, reagent saving and easily used even when reagents are expensive, partially soluble or insoluble.

ADDENDUM A

Method construction

Sequential injection analysis is dependent on precisely timed operations which takes place in a programmed sequence. The programming is done using the FlowTEK [1,2] program developed by Marshall [3]. The method used for the determination of total iron in multivitamin and water samples using a solid-phase reactor (Chapter 6) is used to explain the method construction and procedures in FlowTEK.

The analytical cycle used in the determination consisted of the following operations: aspiration of hydrochloric acid solution for reactor regeneration, the sample, the citrate buffer, the oxidation step itself, the complex formation of iron(II) and 1.10 Phenanthroline, the detection of the formed product (complex) and rinsing of the manifold (Fig. 6.1).

A Unicam 8625 UV-VIS spectrophotometere equipped with a 10-mm Hellma-type (Hellma GmbH and Co., Mülheim/Baden, Germany) flow-through cell for absorbance measurement was used as detector.

A FlowTEK [1,2] software package was used throughout for data acquisition and device control. This was achieved using a PC 30-B interface board (Eagle Electric, Cape Town) and an assembled distribution board (Mintek, Randburg). The FlowTEK was also used to send a signal

to the UV-VIS spectrophotometer when the product passed through the flow-through cell. Devices in the SIA system must be compatible with TTL or switch control signal [2] to be able to perform their functions. A device is defined as an analytial instrument or component which must be controlled by the software package. The first six device definitions are supplied with the software package. These devices can be viewed on the note pad menu (Table A1)

TABLE A1 Schematic representation of the FlowTEK notepad screen (page 1 for device description

Next Page Hard Copy RED Print MET Print PDR Print Quit

Board : PC30-B
Experiment time : 150
Zoom min time : 0.0
Zoom max time : 150
Start acquisition : 43
I/O port for GP : 1
I/O port for SV : 3
Save profile : Yes
Abridged profile : Yes
Regression on Height
Detector displ : Paged
Inject mode : Auto
Start up : (0)
Rescale Y-axis : Fixed
Min : 0.00 Max ; 10.0

F1 : Displ Analog input
F2 : Displ Digital input
F3 : 010000000000 (2)
F4 : 110000000000 (3)
F5 : 000000000000 (0)
F6 : 000000000000 (0)
F7 : 000000000000 (0)
F8 : 000000000000 (0)
F9 : 000000000000 (0)
F10 : Directory

Detector	1	2	3	4
A/D channel	1			
Transformation	None			
Auto Zero	None			
AZ time	0.0			
AZ offset	0.000			
Min Integ Lim	150.0			
Max Integ Lim	150.0			
Width Height	0.000			
Peak Time	@ Pk max			

Path : C:\ FLOWTEK \BOB\ IRON (II)
Main Procedure file : IRON (II).PDR
Method file : IRON (II).MET
Reduced data file : IRON(II).RED
Experimental Profile Root : Fe
Calibration file : DEFAULT.CAL

Name	AP	GP	IV	SV	AS	SW
Action	FWD REV OFF	FWD REV OFF	INJ LOAD	ADV HOME	NEXT	TRUE FALSE
Hotkey	F R O	F R O	I L	A H	N	T F
Output	01 (1) 10 (2) 00 (0)	10 (2) 11 (3) 00 (0)	01 (1) 10 (2)	10 (2) 01 (1) 00 (0)	1 (1) 0 (0)	1 (1) 0 (0)
Pulse	0.00	0.00	0.00	0.30	5.00	0.00

The function keys F1 to F10 are programmed to perform different functions. F1 is used to monitor and check analog inputs. When F1 is pressed one can adjust port on simulator and monitor reading on screen. The reading on the screen should be compared to a multimeter. F2 is used to check digital outputs. When F2 is pressed on the computer one uses jumpers to short out 0V to the digital inputs and monitor screen. To show that this is accomplished the inputs will go on and off. If all inputs on the screen are off, measure at the digital input on the 26 pin ribbon crimp connector for ±5V signal.

F3 - F9 are used to control the digital devices which are connected to one of the eight digital outputs on the distribution box. This setup is achieved on the setup menu page using the function key menu option. This digital outputs can be configured as switch. The voltage maybe set high (5V) or low (0V). In this work only F3 and F4 because only two devices were connected namely the SV and the GP. for example to programme F2 , 2 was typed which is equivalent ton 01 and for F3, 3 was typed which is equivalent to 11 (Table A1) F10 is used as directory to display or a list of defined procedures and methods.

The software package does however, provide for the configuration of another extra six devices as need may arise. These may further be viewed after typing the letter N to view the second page of the device configuration (Table A2).

TABLE A2 Schematic representation of the FlowTEK notepad screen (page 2 for device description)

Name Action	0	0	0	0	0	0
Hotkey						
Output						
Pulse	0.00	0.00	0.00	0.00	0.00	0.00

For the sequential injection analysis the device configuration data of the Gilson pump (GP) and the selection valve (SV), need not be programmed, since they are supplied with the software. From the main menu the letter **M** must be typed to obtain the method menu. The two devices needed can be selected using the option **Type (of) device**. The questions or commands which followed can be answered as follows:

Enter number of devices: **2**

Enter type device 1: **GP**

Enter digital point for GP: **1** (This represent the first position the device occupy on the interface board).

Enter digital point for SV: **3** (This represent the third position the device occupy on the interface board).

The screen is now divided into two panel, each containing a straight line in the middle of the panel. The position of these lines represent the 'OFF' position of each device. Programming of each device are now allowed. Device events are entered by choosing the option **Insert** in the

method menu. It is important to switch on **NUM LOCK** when using the **Insert** or **Delete** options. The programming for the different operations needed can be done as follows:

Insert

Device number:	**2**	(Selection valve)
Enter time of event:	**0**	
Hotkey (A H):	**H**	(Select HOME position-first port)

Insert

Device number:	**1**	(Gilson pump)
Enter time of event:	**1**	
Hotkey (F R O):	**R**	(Switch pump on in the reverse direction)

Insert

Device number:	**1**	(Gilson pump)
Enter time of event:	**6**	
Hotkey (F R O):	**O**	(Switch pump off)

Insert

Device number:	**2**	(Selection valve)
Enter time of event:	**11**	
Hotkey (A H):	**A**	(Select waste stream-second port)

Insert

Device number: **1** (Gilson pump)

Enter time of event: **12**

Hotkey (F R O): **F** (Switch pump on in the forward direction to waste)

Insert

Device number: **1** (Gilson pump)

Enter time of event: **23**

Hotkey (F R O): **O** (Switch pump off)

Insert

Device number: **2** (Selection valve)

Enter time of event: **24**

Hotkey (A H): **A** (Select sample stream-third port)

Insert

Device number: **1** (Gilson pump)

Enter time of event: **25**

Hotkey (F R O): **R** (Switch pump on in the reverse direction)

Insert

Device number: **1** (Gilson pump)

Enter time of event: **29**

Hotkey (F R O): **O** (Switch pump off)

Insert

Device number: **2** (Selection valve)

Enter time of event: **30**

Hotkey (A H): **A** (Select buffer stream-fourth port)

Insert

Device number: **1** (Gilson pump)

Enter time of event: **31**

Hotkey (F R O): **R** (Switch pump on in the reverse direction)

Insert

Device number: **1** (Gilson pump)

Enter time of event: **35**

Hotkey (F R O): **O** (Switch pump off)

Insert

Device number: **2** (Selection valve)

Enter time of event: **36**

Hotkey (A H): **A** (Select Orthophenanthroline stream-fifth port)

Insert

Device number: **1** (Gilson pump)

Enter time of event: **37**

Hotkey (F R O): **R** (Switch pump on in the reverse direction)

Insert

Device number: **1** (Gilson pump)

Enter time of event: **41**

Hotkey (F R O): **O** (Switch pump off)

Insert

Device number: **2** (Selection valve)

Enter time of event: **42**

Hotkey (A H): **A** (Select detector line-sixth port)

Insert

Device number: **1** (Gilson pump)

Enter time of event: **43**

Hotkey (F R O): **F** (Switch pump on in the forward direction to pump stack of zones through detector)

Insert

Device number: **1** (Gilson pump)

Enter time of event: **150**

Hotkey (F R O): **O** (Switch pump off-end of analytical cycle)

Insert

Device number: **2** (Selection valve)

Enter time of event: **150**

Hotkey (A H): **H** (Valve return home to first port)

To delete any existing event, the option **Delete** on the method menu must be used. The time of the event needed to be erased must be typed in when asked for. The procedure to delete an event is the same procedure needed to insert an event.

To avoid storing redundant data, data acquisition could be started only a few moments after the valve was switched to select the detector line. This will result in the collection of only peak profile and relevant data. To accomplish this the option **Exp time** on the method menu must be selected and the time to start data acquisition must be typed in. The final method is represented schematically in Table A3.

After the method is constructed it is saved using the option **File** on the method menu and typing **S** for save under appropriate name. The method file used for the iron determination was saved as **iron (II).met.** When the method must be repeated a fixed number of times it is best to write a procedure to carry out the repetitions. Ten repetitions of the method were used during the final evaluation of the SIA system.

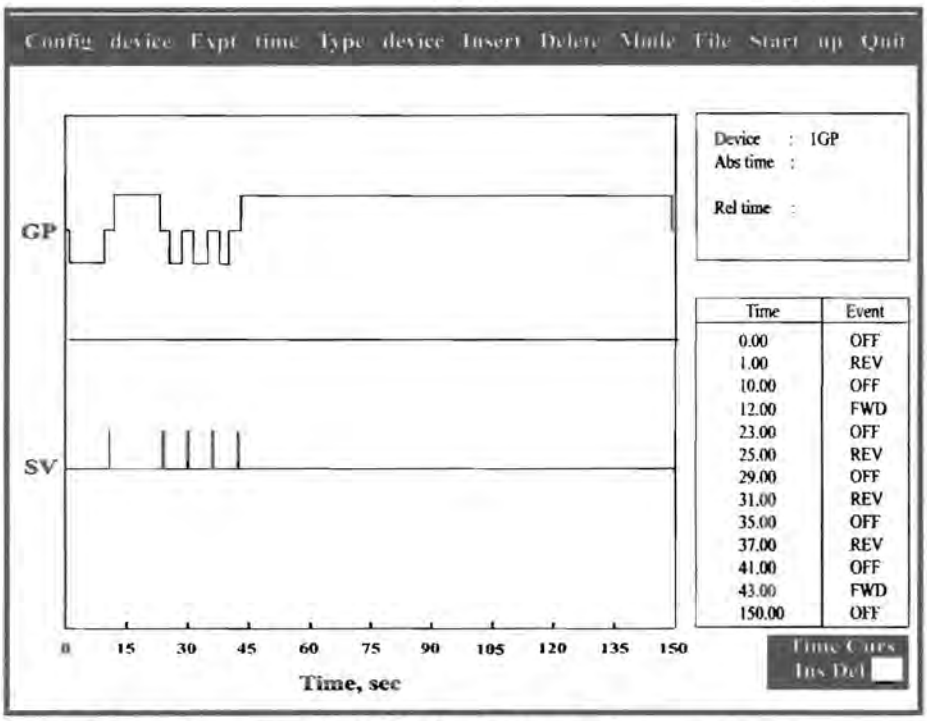

Fig.A1 Schematic representation of the flowTEK method screen.

To create a procedure, the option **Repeated** on the main menu must be selected. The option **Build Proc.** on the repeated menu is used to create a procedure. The procedure was named **iron (II). pdr**. It was necessary to specify whether a method file (.met) or another procedure file (.pdr) was used in this application. The following commands or questions must be answered:

Enter main procedure: **C:\ FLOWTEK\ BOB\Solid\iron(II).PDR**

Enter method or procedure file: **iron (II). MET.**

Enter number of repetitions: **10**

If more methods or procedures are to follow, the process must be repeated till all the methods together with their number of repetitions are listed. Otherwise **ESC** terminates the procedure definition. To use this main procedure file, the option **Main Proc** on the main procedure file must then be typed in.

The option **Red. Data file** on the **Repeated** menu selects a reduced data file for saving each experiment's peak parameter data and relative experiment identification information. The experiment number counter is reset to **1** when the reduced data file name is changed **or when the program was exited**. Every time the program is restarted a new reduced data file must be opened, otherwise the previous data would be lost. The option **Profile file** on the **Repeated menu** selects the file not name for storing the profile data. The file name extension gives the experiment number. If no profile root is chosen, profile files are not saved.

To execute the main procedure the option **GO!** on the **Repeated** menu must be chosen. The option **Once** on the Main menu is chosen if only one run is needed. The Main procedure can be aborted by pressing **ESC**.

Calibration can also be done using the FlowTEK program. Data used to calculate calibration constants are stored in a Calibration Response table. This table has 9 rows and 3 columns. The response for a p-articular calibration are stored on the rows of the table. Table A4 gives typical results for calibration from Chapter 6. Replicated values are placed in each column

the FlowTEK program keeps track of the number of replicates. When you measure more than

three replicates the oldest datum is replaced by the newest value. The regression is carried out on a simple arithmetic mean of the data for a particular concentration.

TABLE A3 A Response Calibration Table with some results of the calibration graph

Conc(ppm)	1st	2nd	3rd	Avg
1	0.3135	0.3079	0.3101	0.3165
10	1.1550	1.1501	1.1452	1.1501
20	2.2243	2.1779	2.1877	2.1960
30	3.2131	3.1618	3.2683	3.2000
40	4.3459	4.3190	4.3654	4.3434
50	5.4128	5.3298	5.2224	5.3216
60	6.1281	6.1745	6.2111	6.1711

Before a calibration calculation can be completed, you must specify the first and last standards in the calibration Response Table. This means that it is possible to store data for more than one calibration in the Calibration Response Table.

To calculate the regression constants for the first data, specify the first standard as 1 and last standard as 3. To calculate the regression constants for the second data specify the first standard as 4 and the last as 6. You can have any number of standards for a particular calibration set

References

1. G. D. Marshall, **Analytical Instrumentation, 20 (1)** (1992) 79.

2. **FlowTEK Reference Manual, Device Control and Data Acquisition software, ver. 1.1,** Mintek, 1993.

3. G. D. Marshall, **Sequential-Injection Analysis**, PhD-Thesis, University of Pretoria, 1994.

ADDENDUM B

Publications and Presentations

Publications

1. Determination of Manganese in tap water and effluent streams using a solid-phase Lead (IV) dioxide reactor in sequential injection systems.

   E. B. Naidoo and J. F. van Staden. **Fresenius J. Analytical Chemistry, 370 (6)** (2001) 776.

2. Super serpentine reactors - a comparative and precision study.

   E. B. Naidoo and J. F. van Staden. **Instrum. Sci. and Techn., 29 (2)** (2001) 77.

3. Determination of Iron as Fe(II) in multi-vitamins, Haematmics and effluent streams using a solid-phase (cadmium reductor) reactor incorporated in a sequential injection (SIA) system.

   J. F. van Staden and E. B. Naidoo. **South Africa J. Chemistry** (2001).

4. An improved technique for the determination of oxidised nitrogen in water using a solid-phase reactor with a sequential injection analysis (SIA) system.

   E. B. Naidoo and J. F. van Staden. **Waters SA, 27 (3)** (2001) 355.

5. An alternative enhanced method for the determination of chromium in electroplating and natural waters with a sequential injection analysis (SIA)

system.

E. B. Naidoo and J. F. van Staden. (submitted).

Presentations

1. The assay of S-enantiomers of enalapril, ramapril and trandolapril using an amperometric biosensor/sequential injection analysis system.

   J. F. van Staden, R. I. Stefan, H. Y. Aboul-Enein, E. B. Naidoo and L. V. Mulaudzi.

   ISCD 12, **The International Symposium on Chirality, Chamonix, Mount Blanc, France. 24-28 September 2000**

2. Determination of Manganese in tap water and effluent streams using a solid-phase Lead(IV) dioxide reactor in sequential injection systems.

   E. B. Naidoo and J. F. van Staden

   Euroanalysis XI. Working Party on Analytical Chemistry at the Federation of European Chemical Societies and the Portuguese Chemical Society, Lisbon, Portugal. 3-9 September 2000

3. Super Serpentine Reactors in SIA - a comparative response and precision study

   E. B. Naidoo and J. F. van Staden

   Euroanalysis XI. Working Party on Analytical Chemistry at the Federation of European Chemical Societies and the Portuguese Chemical Society. Lisbon, Portugal. 3-9 September 2000

4. Determination of S-Pentopril using an amperometric biosensor/SIA system.

R. I. Stefan, L. V. Mulaudzi, E. B. Naidoo, H. Y. Aboul-Enien and J. F. van Staden.

Flow Analysis VIII, Polish Academy of Science, Polish Chemical Society. Warsan, Poland. 25-29 June 2000

5. The assay of S-enalapril using an amperometric biosensor/SIA system.

J. F. van Staden, R. I. Stefan, E. B. Naidoo and H. Y. Aboul-Enein.

Flow Analysis VIII. Polish Academy of Science, Polish Chemical Society. Warsaw, Poland. 25-29 June 2000

6. Determination of Manganese in tap water and effluent streams using a solid-phase Lead (IV) dioxide reactor in sequential injection systems.

E. B. Naidoo, and J. F. van Staden.

Flow Analysis VIII. Polish Academy of Science, Polish Chemical Society. Warsaw, Poland. 25-29 June 2000

7. Super Serpentine Reactors in SIA - a comparative response and precision study.

E. B. Naidoo and J. F. van Staden.

Flow Analysis VIII. Polish Academy of Science, Polish Chemical Society. Warsaw, Poland. 25-29 June 2000.